

UNIVERSITY OF CINCINNATI

Date: November 26, 2007

I, Christopher Gulgas,

hereby submit this work as part of the requirements for the degree of:

Doctor of Philosophy

in:

Chemistry

It is entitled:

Synthesis of Macrocyclic Lanthanide Chelates for Anion Sensing and

Magnetic Resonance Imaging Applications

This work and its defense approved by:

Chair: Professor Theresa M. Reineke

Professor Michael Baldwin

Professor William Heineman

Professor William Connick

Synthesis of Macrocyclic Lanthanide Chelates for Anion Sensing and Magnetic Resonance Imaging Applications

A Dissertation submitted to the faculty of

University of Cincinnati in partial

fulfillment of the requirements

for the degree of

Doctor of Philosophy (Ph.D.)

in the Department of Chemistry

of the College of Arts and Sciences

By

Christopher G. Gulgas

Nov. 26, 2007

B.A. College of Wooster, Wooster, OH, 2001

Committee Chair: Professor Theresa M. Reineke

ABSTRACT

Novel Eu^{3+} -containing macrocyclic complexes were synthesized and studied as anion sensing probe molecules. Several of these macrocycles exhibited unique luminescence responses to hydrogen-bond accepting anions (fluoride, acetate, and dihydrogen phosphate) in DMSO, even in the presence of a chloride ion background. The first series of compounds highlighted a high-yielding synthetic route for highly functional macrocycles that incorporate a Eu^{3+} chelate, aromatic antennae, thiourea groups as anion-binding units, and a variable linker that tunes the size and rigidity of the pocket. These macrocycles exhibited Eu^{3+} luminescence where emission intensity ($\lambda_{\text{exc}} = 272 \text{ nm}$, $\lambda_{\text{em}} = 614 \text{ nm}$) was correlated to the linker length. Anion-induced changes in emission intensity were dependent on the basicity of the anion, and emission enhancements were observed up to 77% upon titration with fluoride in one case. Through luminescence lifetime studies of the Eu^{3+} macrocycles and the study of a newly synthesized series of organic model compounds, it was determined that the luminescence response to anions was the result of interaction with the thiourea moieties and no evidence was observed for anion coordination to Eu^{3+} . Additionally, two second-generation macrocycles were synthesized, incorporating an amine unit for stronger binding affinity. One of these macrocycles, featuring a pendant naphthalene antenna, responded to several anions in aqueous solution by means of a luminescence decrease of up to 30%. This general macrocyclic design shows promise for the development of Eu^{3+} -based anion sensors that function in competitive solvents.

In continuing work with lanthanide complexes, a new targeted Gd^{3+} -based magnetic resonance imaging contrast agent was designed and synthesized for specific binding to the dopamine receptor protein. A relaxivity of $7.1 \text{ mM}^{-1}\text{s}^{-1}$ was measured for this complex at 400

mHz and 310 K. A Eu^{3+} analogue was also synthesized and structurally characterized. Luminescence lifetime measurements revealed the presence of 2 coordinated water molecules in aqueous solution, consistent with the observed relaxivity of the Gd^{3+} complex. The synthetic scheme described herein can be extended to the synthesis of a series of targeted complexes for enhanced dopamine receptor binding and imaging studies.

ACKNOWLEDGMENT

I thank my advisor, Dr. Theresa Reineke, for giving me this great opportunity to learn and thrive as an independent scientist. Additionally, I thank my committee members Dr. William Heineman, Dr. William Connick, and Dr. Michael Baldwin for their support, questions, and countless insights.

I would like to thank my research group members for their support and discussion, especially Dr. Yemin Liu, Lisa Prevette, Josh Bryson, and Chen-Chang Lee.

I also thank my parents George and Barbara Gulgas, for their continuing support throughout my education.

Table of Contents

Table of Contents.....	1
List of Abbreviations	2
CHAPTER 1. Introduction: Lanthanide chelates for sensing and imaging applications.....	4
CHAPTER 2. Synthesis, characterization and luminescence properties of a new series of Eu ³⁺ - containing macrocycles.....	24
CHAPTER 3. Macrocyclic Eu ³⁺ chelates show selective luminescent responses to anions.....	49
CHAPTER 4. Synthesis and characterization of second-generation macrocyclic lanthanide chelates for anion recognition.....	84
CHAPTER 5. Synthesis, characterization and relaxivity of a new Gd ³⁺ chelate for imaging the dopamine transporter.....	105
CHAPTER 6. Conclusions	122

List of Abbreviations

CA	contrast agent
DCM	dichloromethane
DHP	dihydrogen phosphate
DMSO	dimethyl sulfoxide
DPA	dipicolinate dianion
DO2A	1,4,7,10-tetraazacyclododecane-1,7-diacetic acid
DO3A	1,4,7,10-tetraazacyclododecane-1,4,7-triacetic acid
DOTA	1,4,7,10-tetraazacyclododecane-1,4,7,10-tetraacetic acid
DTPA	diethylenetriaminepentaacetic acid
ESI-MS	electro-spray ionization – mass spectrometry
ET	energy transfer
IR	infrared
ISC	inter-system crossing
MeOH	methanol
MRI	magnetic resonance imaging
NMR	nuclear magnetic resonance

PET	photo-induced electron transfer
TBA	tetrabutylammonium
TBABr	tetrabutylammonium bromide
TBACl	tetrabutylammonium chloride
TBAF	tetrabutylammonium fluoride
TBAI	tetrabutylammonium iodide
TBAOAc	tetrabutylammonium acetate
TBAOBnz	tetrabutylammonium benzoate
TRF	time-resolved fluorescence
UV-Vis	ultraviolet-visible

Chapter 1. Introduction: Lanthanide Chelates for Sensing and Imaging Applications

Lanthanide metal ions have become increasingly more important for applications in the general fields of detection¹ and diagnosis.² The inherent photophysical properties of many of the lanthanide ions allow them to function as ideal signaling moieties in supramolecular devices due to their large Stokes shifts, long luminescent lifetimes (μs to ms range), and narrow emission bands in the visible to near-IR range.¹ One intrinsic drawback to the use of lanthanides is their low extinction coefficients resulting from Laporte forbidden f-f orbital transitions. However, population of the lanthanide excited state can easily be accomplished with the use of a nearby light harvesting antenna, most often an aromatic molecule.^{1,3} The paramagnetic nature of the lanthanide series also lends them to function well as nuclear magnetic resonance (NMR) shift reagents and, in the case of Gd^{3+} , as magnetic resonance imaging contrast agents (MRI-CA) for diverse medical applications *in vitro* and *in vivo*.² Much current research focuses on designing multidentate chelating ligands to accommodate the large coordination sphere and tailor the properties of the lanthanide metals for the desired purpose. Additionally, lanthanide ions can be highly toxic to biological systems as their respective aqua ions, and the chelate must be designed for high stability in the presence of other potential ligands to prevent their release.² For numerous applications aimed at studying biological systems and events, chelates based on the structures of diethylenetriaminepentaacetic acid (DTPA) and 1,4,7,10-tetraazacyclododecane-1,4,7,10-tetraacetic acid (DOTA) are common, attributed to the high stability and synthetic versatility provided by these ligand frameworks.² The structures of these ligands are shown in Figure 1.

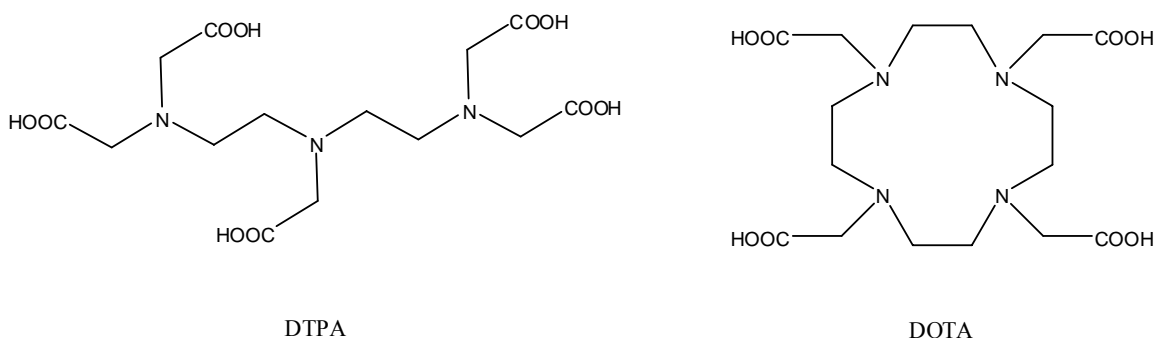


Figure 1. Structures of DTPA and DOTA ligands.

In this work, a series of large DTPA-based macrocyclic chelates for Eu^{3+} (that incorporate thiourea hydrogen bond donors) have been synthesized and characterized for function as selective anion sensors for fluoride, acetate, and dihydrogen phosphate (DHP) in DMSO. Additionally, a targeted MRI-CA based on the DOTA framework has been synthesized for binding and imaging the dopamine transporter protein using MRI. The full characterization of these new complexes relevant to their application including ^1H and ^{13}C -NMR, ESI-MS, UV-Vis absorbance, luminescence spectroscopy and model studies are reported within.

The Antenna Effect

The weak extinction coefficients ($\epsilon < 1 \text{ M}^{-1} \text{ cm}^{-1}$) of the lanthanide ions necessitate sensitization of the lanthanides' excited states through a coordinated or nearby absorbing chromophore, or antenna.¹ A general scheme for the mechanism of sensitization is depicted in Figure 2. Absorption of light by the aromatic antenna, Ar, results in a singlet excited antenna, ^1Ar , which can undergo inter-system crossing to the triplet excited state, ^3Ar .¹ The quantum yield for formation of ^3Ar can be reduced by ligand fluorescence, photo-induced electron transfer (eT) quenching of the singlet excited state, or through quenching by halide ions in solution, for example.¹ Energy transfer to the lanthanide is generally believed to occur from the

triplet excited state of the ligand and is maximized by a short lanthanide-antenna distance, a relatively small energy gap between ^3Ar and the excited lanthanide, Ln^* ($\text{Ln}^* = 17,200 \text{ cm}^{-1}$ for Eu^{3+}), and no competing back-energy transfer.^{1a} Back-energy transfer becomes significant when the ^3Ar and Ln^* states are close in energy and effectively extends the lifetime of ^3Ar which, for example, can allow significant triplet excited state quenching by O_2 to reduce the overall quantum yield of lanthanide luminescence.¹ The excited lanthanide ion may return to the ground state emissively, resulting in the luminescence characteristic of the particular ion, or may be subject to deactivation by the high-frequency vibrational modes of coordinated X-H oscillators (esp. when $\text{X} = \text{O}$ or N for Eu^{3+}).¹ Therefore, reducing the number of coordinated water molecules and nearby OH and NH bonds significantly augments the overall quantum yield of lanthanide emission.

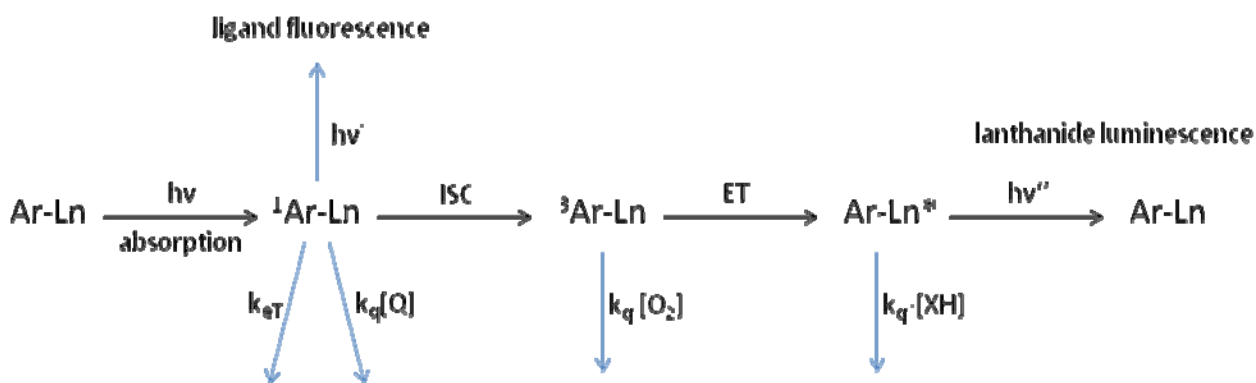


Figure 2. Mechanism of lanthanide luminescence through the antenna effect (adapted from Pandya et al.).^{1e}

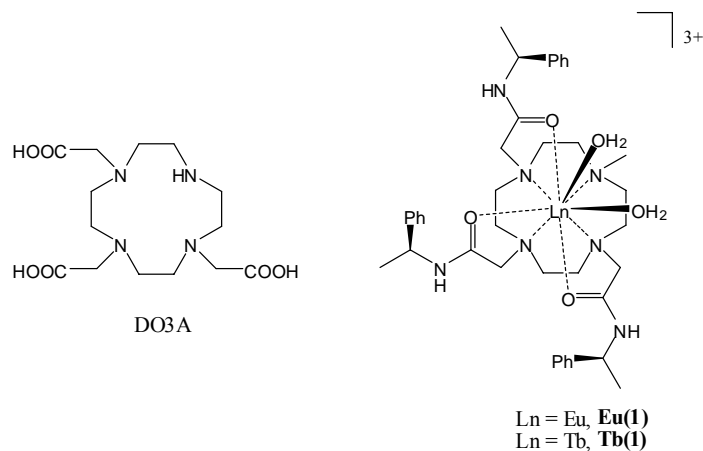


Figure 3. Structures of DO3A, **Eu(1)** and **Tb(1)**.³

Anion Sensing with Lanthanide Ions

Lanthanide ions have only recently been investigated for their anion sensing abilities. Pioneering work by Parker and co-workers^{1,3} led to the development of lanthanide chelates capable of signaling the binding of anions such as halides and simple oxoanions in aqueous solution through an increase in Eu³⁺ or Tb³⁺ luminescence. Water molecules are efficient quenchers of lanthanide excited states through vibrational energy transfer to the O-H oscillator. Typically, the ligands were designed to leave open sites for water molecules to coordinate to the metal, allowing displacement of water by anions to augment luminescence intensity and lifetime, providing a signal of the binding event. For example, triamide derivatives of 1,4,7,10-tetraazacyclododecane-1,4,7-triacetic acid (DO3A) were used to form stable lanthanide complexes, **Eu(1)** and **Tb(1)** shown in Figure 3, and binding constants (log K) for the formation of 1:1 complexes with acetate in water (pH = 7.4) were determined to be 2.4 and 3.5 for **Eu(1)** and **Tb(1)**, respectively.³ The same lanthanide complexes were studied for their affinity for monohydrogen phosphate (HPO₄²⁻) under the same conditions, and log K values greater than 4.7 were determined, which is consistent with the complexation of a more negatively charged anion.³

This type of approach was also utilized by Ziessel and co-workers in the development of Eu^{3+} chelates with 2,2'-bipyridine sensitizing antennae, yielding binding constants ($\log K$) of 5.2 for HPO_4^{2-} in TRIS buffer at pH 7.0.⁴ These studies demonstrated a great potential for lanthanides in the anion sensing field, but most complexes suffered from a lack of selectivity, whereby many different anions could displace coordinated water molecules, owing to the favorable electrostatic interactions, resulting in similar luminescent signals.

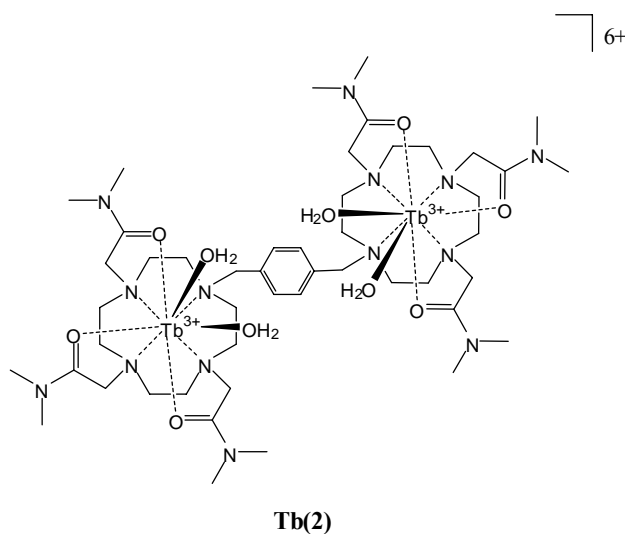


Figure 4. Structure of **Tb(2)**.^{5a}

Selectivity for *bis*-carboxylates was achieved using this approach through the development of a dinuclear Tb^{3+} chelate, **Tb(2)** (Figure 4), by Gunnlaugsson and co-workers capable of forming 1:1 complexes with terephthalate ($\log K = 5.42$) and pimelate ($\log K = 6.62$).^{5a} The binding constants and stoichiometries were determined through large increases in the Tb^{3+} emission upon displacement of coordinated waters, and were found to correlate with the spacer length and flexibility.^{5a} For example, when the spacer was too short to bridge the two metal centers, a 2:1 (anion: dinuclear metal complex) binding stoichiometry was determined. Additionally, the selective luminescence response of **Tb(2)** to terephthalate was greatly enhanced

by the dianion's ability to function as an antenna for Tb^{3+} , which also is beneficial for sensitivity in that responses can be observed at lower concentrations. Targeting anions that act as antennas for lanthanide luminescence has also been successful in work by Cable et al., where a complex of Tb^{3+} with 1,4,7,10-tetraazacyclododecane-1,7-diacetate (DO2A) having three open coordination sites (Figure 5) was found to be highly responsive to the tridentate dipicolinate dianion (DPA), an efficient sensitizer of Tb^{3+} and Eu^{3+} .^{5b-c} Remarkably, the binding constant in water ($\log K = 10.7$, $\text{pH} = 7.5$) for formation of the 1:1 complex (DPA: **Tb(3)**) was higher than that of DPA with the Tb^{3+} aqua ion.^{5b} More recent work by Parker has led to selective signaling of citrate anion binding ($\log K = 6.5$ in water) in the presence of HPO_4^{2-} , lactate, Cl^- , and HCO_3^- ($\text{pH} 7.4$) using a novel DO2A-based Eu^{3+} chelate (**Eu(4)**, Figure 5) where citrate coordination induces distinct changes in the individual emission bands of Eu^{3+} ($\Delta J = 0$, $\Delta J = 2$) allowing ratiometric detection.⁶ The observed ratiometric response is unique to the citrate anion and, due to its strong binding with **Eu(4)**, allows determination of citrate in the presence of potentially interfering, biologically relevant anions.

Although this field has grown immensely, the majority of sensors relying on direct association of the analyte with a lanthanide center to achieve selectivity are only effective in the cases of multidentate anions of interest or when targeting anions that function as antennas for the lanthanide luminescence. Multidentate anions such as di- and tricarboxylates may have binding affinities several orders of magnitude above those of interfering anions such as halides, phosphates and monocarboxylates, which allows the multidentate anions to compete effectively, and thus it is the binding event that is selective. The binding of anionic antennae to lanthanide ions can increase the luminescence response much greater than interfering anions that do not serve as antennae so that even if the binding affinities are similar, a selective response may be

observed for the anion that can harvest light energy for the lanthanide. However, when seeking to bind relatively small anions that do not function as antennae, such as fluoride, chloride, acetate or phosphates, achieving selectivity based on a lanthanide binding site alone has been a persistent challenge.

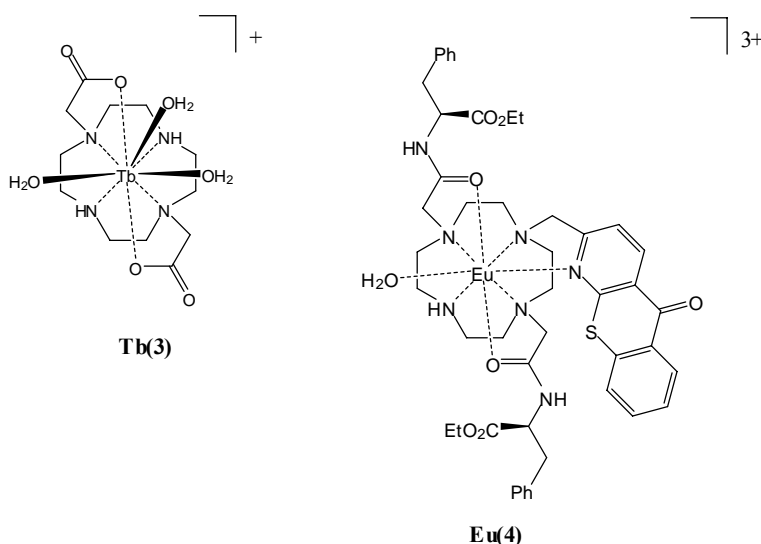


Figure 5. Structures of **Tb(3)** and **Eu(4)**.^{5b, 6}

Anion Sensing with Hydrogen Bond Donors

Hydrogen bond donating groups such as amides,⁷⁻⁸ pyrroles⁹ and (thio)ureas¹⁰ have been employed heavily in the design of neutral organic sensors for anions, primarily in CH₃CN and DMSO solutions. One advantage of working with these organic functional groups lies in their synthetic chemistries which are well-suited for constructing preorganized systems for selective binding. For example, macrocyclic pyrroles,^{9a, d-e} amides⁸ and (thio)ureas^{10h-i} have been synthesized and shown to have enhanced affinities for various anions by over an order of magnitude, relative to acyclic controls of similar functionality. Also, tripodal molecules with amides and (thio)ureas have also been applied to anion detection for the cooperative binding of

anions and stronger binding affinities.⁷⁻⁸ One example of a macrocyclic anion binding molecule utilizing amides as hydrogen bond donors was synthesized by Choi and Hamilton (compound **5**, Figure 6).^{8b,c} Compound **5** showed selectivity for tetrahedral anions in DMSO-*d*₆ with strong 1:1 binding of DHP (log K = 4.2 by ¹H-NMR) relative to halide and nitrate ions, possibly due to shape and size restrictions of the rigid macrocycle.^{8b,c}

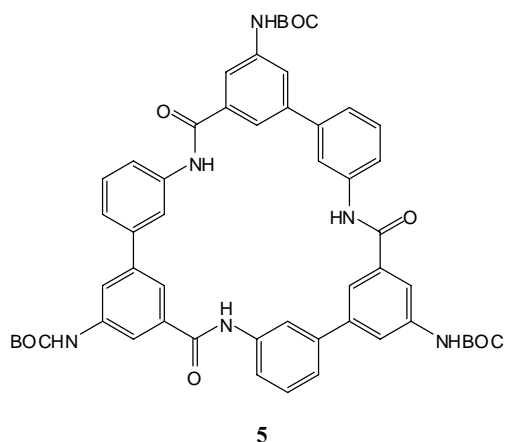


Figure 6. Structure of compound **5**.^{8c}

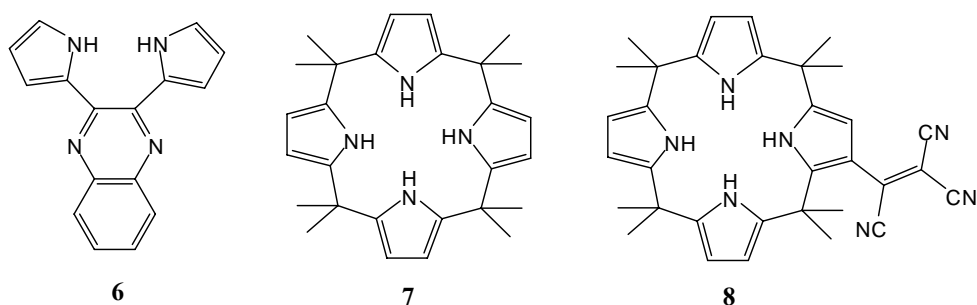


Figure 7. Structure of pyrrole-based molecules **6-8**.^{9d,e}

Another class of hydrogen bond donating anion binders is based on the pyrrole moiety. As shown in Figure 7, these structures can be acyclic or macrocyclic, but both are preorganized for cooperative anion binding between individual pyrrole units, leading to strong binding affinities for many different anions.⁹ Compound **6**, 2,3-di(1*H*-2-pyrrolyl)quinoxaline,

shows a strong preference for basic anions such as fluoride or pyrophosphate over other halides or DHP in CH₂Cl₂ or DMSO, but binding constants were not reported for DMSO.^{9d} Octamethylcalix[4]pyrrole, **7**, is the basic scaffold for a large number of anion binding and sensing supramolecular systems.⁹ The four pyrrole moieties are preorganized to form four hydrogen bonds to anionic guests. Binding constants for formation of 1:1 complexes of **7** and strong hydrogen bond accepting anions such as fluoride or acetate are moderate in DMSO (log K = 3.0 for fluoride⁹), but can be vastly augmented through the addition of electron-withdrawing dyes as in **8**.^{9e-g} Compound **8** binds fluoride more than 3 orders of magnitude stronger than **7** in DMSO (log K > 6), as determined by UV-Vis absorbance measurements, due to the electron-withdrawing tricyanoethylene moiety appended to one of the pyrrole units of the macrocycle.^{9e} However, compound **8** retains the selectivity common to the calix[4]pyrrole family for fluoride over other halides (log K = 3.1 for chloride).^{9e} Compound **8** is one example of several similar molecules based on this scaffold that exhibit remarkably strong binding of hard anions for neutral receptors in a competitive solvent like DMSO. Many of the compounds in this class are capable of sensing the presence of anions through colorimetric or fluorescence responses, by attaching appropriate chromophores and fluorophores to the basic calix[4]pyrrole scaffold, exemplified by compound **8**.⁹ Some examples of fluorescence signaling molecules are discussed below.

For application as sensing molecules, a chromophore capable of fluorescence or colorimetric signaling is typically incorporated into the design of supramolecular systems based on hydrogen bond donors. Early successful thiourea-based sensors (Figure 8) used photo-induced electron transfer (PET) to anthracene as a quenching mechanism for signaling the binding of anions.^{10a,c} Binding of the anion to the thiourea moiety results in a accumulation of

charge on the sulfur atom, causing an enhanced PET quenching of the anthracene excited state. Selectivity was observed with **9** for fluoride, acetate, and dihydrogen phosphate (DHP) over the other halides in DMSO with binding constants (log K) calculated from the anthracene fluorescence of 3.35, 2.33, and 2.05, respectively.^{10a} Sensor **10** had lower binding constants of 2.90, 2.15, and 1.82 for fluoride, acetate and DHP, respectively. The variation in structure of sensors **9** and **10** demonstrates the strengthening effect on anion binding of increasing the NH acidity of the thiourea proton through the use of electron-withdrawing substituents like the trifluoromethyl group. The observed selectivity pattern is typical of thiourea and urea groups, where strong binding is observed with harder anions.

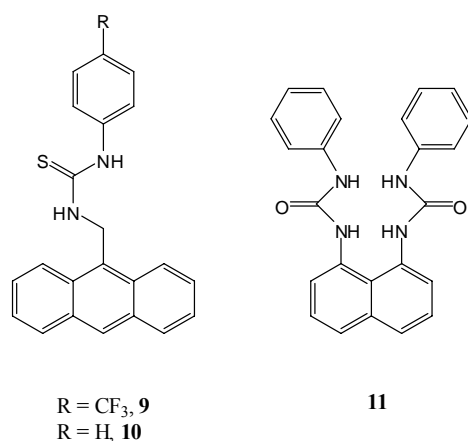


Figure 8. Structures of thiourea sensors **9** and **10** and *bis*-urea sensor **11**.^{10a, 10d}

Sensors employing *bis*-urea and *bis*-thiourea binding sites have been developed and show strong binding when operating cooperatively in a 1:1 (sensor: anion) fashion, where both (thio)ureas are hydrogen bonded to a single anion. A fluorescent *bis*-urea sensor, **11** (Figure 8) by Cho *et al.* showed high selectivity for fluoride over other halides with the distinct emergence of a new fluorescence band upon fluoride binding, most likely due to the basicity of the fluoride ion.^{10d} The binding constant (log K) for fluoride was determined to be 4.2 in CH₃CN-DMSO

(9:1), which was a forty-fold increase over chloride binding.^{10d} Additionally, a *bis*-thiourea colorimetric sensor based on a rigid [3]polynorbornane scaffold created by Gunnlaugsson and co-workers was selective for acetate and DHP in DMSO ($\log K = 3.5$ and 3.9 , respectively) but was deprotonated upon addition of excess fluoride ion and no longer bound the fluoride anion.^{10b} Deprotonation of (thio)urea-based sensors has been studied extensively by Fabbrizzi and co-workers, and has been shown to be the true cause of many colorimetric responses observed in those systems.¹¹ Although increasing the $-NH$ acidity of the thiourea group is directly related to increased anion binding affinities, the upper limit appears to be set by the tendency to deprotonate, resulting in dissociation of an authentic hydrogen-bonded complex. It is therefore important to increase binding affinity and selectivity through other means, such as the preorganization of multiple binding sites. Structural criteria for the placement of (thio)urea groups for shape selective binding of specific anions have been evaluated, and host preferences based on anion geometry have significant impacts on binding affinity.^{10j,k} For example, macrocyclic alkyl-substituted *bis*-thioureas (Figure 9) were designed and studied by Tobe and co-workers and showed a large increase in binding affinity for acetate in DMSO progressing from an acyclic molecule, **12**, ($\log K = 2.0$) to a macrocyclic molecule, **13**, ($\log K = 2.8$) to a macrocyclic molecule with a third, lariat-type thiourea site, **14** ($\log K = 3.9$).^{10h} This series of compounds clearly demonstrates the power of preorganization and multiple binding sites in designing molecules for anion binding applications, as binding affinity can be increased by orders of magnitude.

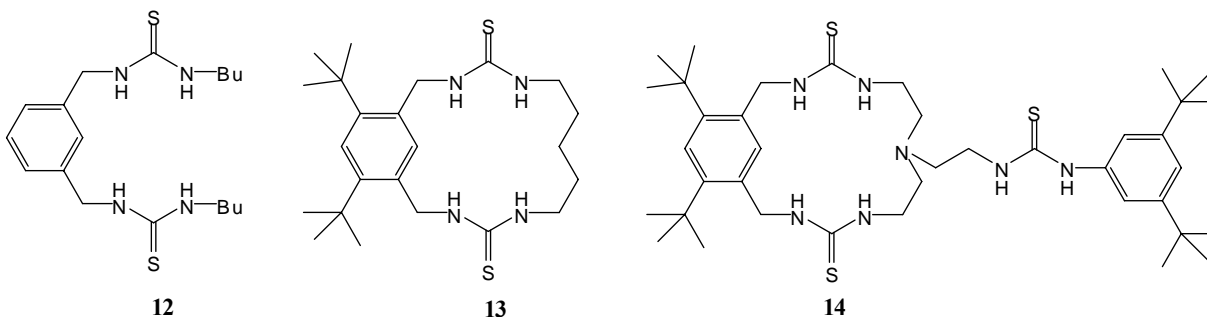


Figure 9. Structures of thiourea-containing macrocycles **12-14**.^{10h}

Until quite recently, there were no examples in the literature combining the selectivity of the thiourea group with the favorable photophysical characteristics of the lanthanide metal ions in the design of a molecule for anion sensing. One example, Tb³⁺ chelate **15** has emerged outside of our laboratory (Figure 10) and was found to be selective for acetate and DHP over other anions including fluoride, which is quite rare for urea-based systems.¹² In the presence of both DHP and acetate, a significant decrease in ligand fluorescence and Tb³⁺ luminescence was observed upon formation of a 1:1 complex, but a large increase in Tb³⁺ luminescence occurred only in the presence of excess DHP.¹² Unfortunately, the studies were performed in CH₃CN and the binding constants are not directly comparable to those performed herein. There is a strong literature precedent for systems employing either lanthanides or hydrogen bond donors in the development of anion sensing molecules. Our design principles (discussed in Chapters 2 and 3) seek to incorporate the photophysical properties of Eu³⁺ as a signal and hydrogen-bond donating thioureas as cooperative anion binding sites to create a responsive molecular probe for fluoride, acetate, and DHP in DMSO solution. Studies of the synthesis, photophysical properties and anion recognition mechanisms of this new series of molecular anion sensors are discussed herein.

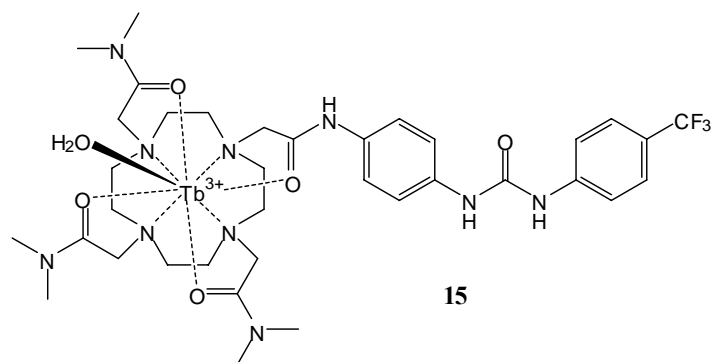


Figure 10. Structure of compound **15**.¹²

Targeted MR Imaging Agents

MRI has become one of the most common and important diagnostic tools in medicine due to its non-invasiveness, relatively high temporal and spatial resolution, and its deep tissue penetration.^{2,13-15} However, administration of a CA to combat the low sensitivity of the technique through enhancing contrast is also a fairly routine practice.^{2, 13} CAs function by catalytically reducing both the longitudinal relaxation time (T_1) and the transverse relaxation time (T_2) of bulk water protons in the body.² CAs that utilize the properties of the paramagnetic Gd^{3+} ion are typically referred to as T_1 agents because of their greater effect on the longitudinal relaxation rate ($1/T_1$). The efficiency of a CA in catalyzing the relaxation of bulk water protons (reducing T_1) is quantitated as its relaxivity, r_1 , where larger values imply higher contrast. There are three basic parameters to manipulate towards increasing r_1 values of Gd^{3+} -based MRI-CA: rotational correlation time (τ_r), water-exchange rate (τ_m) and the number of coordinated water molecules to Gd^{3+} (q).² CAs of larger molecular weight and size rotate more slowly in solution and have longer values of τ_r in general, which can increase the relaxivity of the CA. Large dendrimeric and polymeric CAs have taken advantage of long τ_r values for high relaxivities, finding application in blood pool imaging.¹³ Rates of water-exchange are impacted by the

functional groups incorporated into the Gd^{3+} chelate structure and differ greatly among known CAs, with τ_m particularly slowed by nearby amide (-NH) bonds.² Furthermore, increasing the hydration number, q , directly enhances the relaxivity through providing more sites for bulk water molecules to associate with the Gd^{3+} center. However, increasing q generally correlates to lower chelate stabilities among Gd^{3+} -containing CAs, which generates fears of Gd^{3+} ion release *in vivo*. Gd^{3+} is similar in size to Ca^{2+} and can be highly toxic to humans when stripped from its chelating ligand. Thus, typical CAs being developed for medical applications have either one or two coordinated water molecules ($q = 1$ or 2) to retain high chelate stabilities.

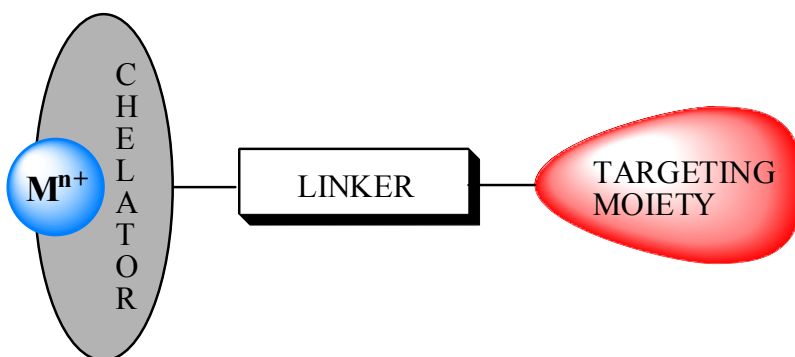


Figure 11. General structure of a targeted, metal-based imaging agent.¹⁶

Highly effective CAs have been developed by optimizing various parameters contributing to relaxivity.^{2,13-14} However, since MRI images water protons, one of the disadvantages in diagnosis lies in its limited specificity.^{2,13} Currently, opportunities abound for the design of novel, non-toxic Gd^{3+} chelates not only of high relaxivity but also specialized for specific studies and uses in a clinical setting. For targeted MRI a metal chelate is typically appended to a targeting biomolecule, such as an antibody or peptide, via a specially designed pharmacokinetic linker.^{2,16} The general scheme for target-specific metallopharmaceuticals is shown in Figure 11. Radiopharmaceuticals have been developed for targeted applications and have been successful in

tumor imaging¹⁶ and in imaging the brain.¹⁷ Extensions of this technology to MRI have been hampered by the large local concentrations of CA required to obtain quality images.^{2,13} However, high-payload carriers of CAs based on polymer, dendrimer, or micelle structures may be effective for targeted imaging at picomolar concentrations.^{15e} For example, blood pool CAs allow enhanced imaging of the cardiovascular system due to their large molecular weights, and hence, longer clearance times.¹³ The paramagnetic agents are bound to or incorporated within biocompatible macromolecules such as albumin, polymers, or lipids and thus, typically also have large relaxivities on a per particle basis.¹³ These characteristics allow enhanced imaging of blood vasculature when compared to that of small extracellular CAs such as Gd-DTPA.¹³

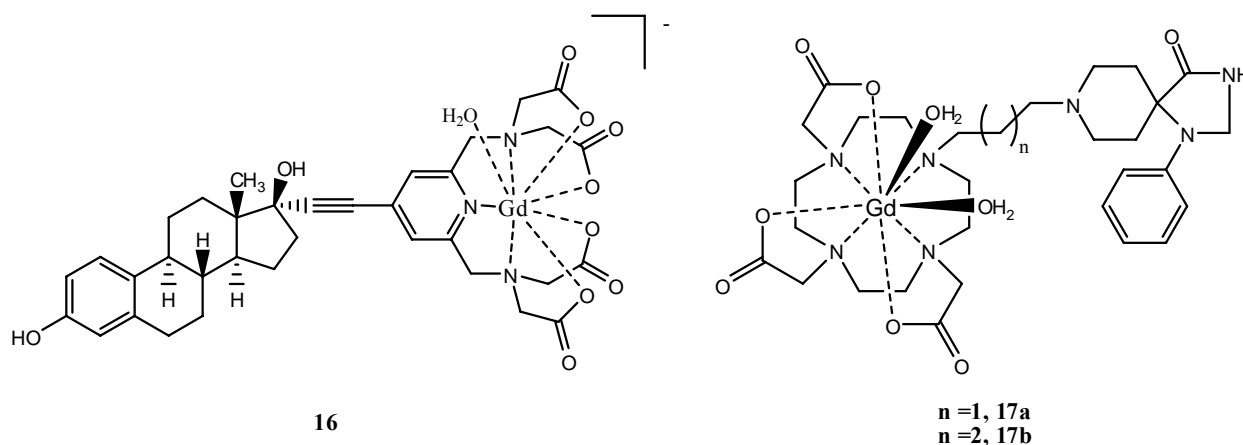


Figure 12. Structures of targeted MRI-CAs **16**, **17a**, and **17b**.^{15a,c}

The design of targeted MRI-CA is highly dependent on the specific application and focuses on new molecules with high molecular relaxivities and stabilities that retain the activity of the appended targeting group. One new Gd³⁺ CA for the imaging the nuclear estrogen receptors (ERs), **16**, is shown in Figure 12.^{15c} This chelate is appended to 17β-estradiol through an ethyne linker for specific targeting and assessment of the ER, with a molecular relaxivity (r_1) of $6.8 \text{ mM}^{-1} \text{ s}^{-1}$.^{15c} Although binding of **16** to the ER was measured to be three orders of

magnitude less than 17 β -estradiol itself, binding occurred within the micromolar range and induced a significant increase in the relaxivity (r_1) of the CA itself, which could be important in specifically signaling the ER binding event.^{15c} Additionally, one report has recently been published of two new CAs, **17a** and **17b** (Figure 12), for imaging the dopamine D2 receptor through a spiperone-based targeting moiety.^{15a} Inhibitory binding studies of [³H]-spiperone with either **17a** or **17b** to isolated mouse striatal membranes revealed significantly weaker binding of the CA to the receptor, but a degree of specificity was maintained.^{15a} The relaxivities (r_1) of **17a** and **17b** (5.94 and 8.31 mM⁻¹ s⁻¹, respectively) are in the range expected for Gd³⁺-based CAs at 400 MHz where $q = 2$.^{15a} The larger r_1 calculated for **17b** may be due to the longer linker length and formation of aggregates, which may slow τ_r .^{15a} These examples illustrate current trends in the development of MRI-CAs for target-specific applications. Maintaining the specificity and activity of the targeting moiety when incorporating a relatively large Gd³⁺ chelate is fundamental for success in this field.¹⁴⁻¹⁵ Future developments require modifications to enhance the relaxivities, binding affinities and *in vivo* stabilities of these prototype molecular systems.

REFERENCES

- (1) (a) Parker, D. *Coord. Chem. Rev.* **2000**, *205*, 109-130. (b) Parker, D. *Chem. Soc. Rev.* **2004**, *33*, 156-165. (c) Bünzli, J.-C. G.; Piguet, C. *Chem. Soc. Rev.* **2005**, *34*, 1048-1077. (d) Bünzli, J.-C. G.; Piguet, C. *Chem. Rev.* **2002**, *102*, 1897-1928. (e) Pandya, S.; Yu, J.; Parker, D. *Dalton Trans.* **2006**, 2757-2766. (f) Døssing, A. *Eur. J. Inorg. Chem.* **2005**, 1425-1434. (g) de Sá, G.F.; Malta, O.L.; Donegá, C. de M.; Simas, A.M.; Longo, R.L.; Santa-Cruz, P.A.; Da Silva Jr., E.F. *Coord. Chem. Rev.* **2000**, *196*, 165-195.
- (2) (a) Caravan, P.; Ellison, J.J.; McMurry, T.J.; Lauffer, R.B. *Chem. Rev.* **1999**, *99*, 2293-2352. (b) Caravan, P. *Chem. Soc. Rev.* **2006**, *35*, 512-523.
- (3) Bruce, J.I.; Dickins, R.S.; Govenlock, L.J.; Gunnlaugsson, T.; Lopinski, S.; Lowe, M.P.; Parker, D.; Peacock, R.D.; Perry, J.J.B.; Aime, S.; Botta, M. *J. Am. Chem. Soc.* **2000**, *122*, 9674-9684.
- (4) Charbonnière, L.J.; Schurhammer, R.; Mameri, S.; Wipff, G.; Ziessel, R. F. *Inorg. Chem.* **2005**, *44*, 7151-7160.
- (5) (a) Harte, A.J.; Jensen, P.; Plush, S.E.; Kruger, P.E.; Gunnlaugsson, T. *Inorg. Chem.* **2006**, *45*, 9465-9474. (b) Cable, M.L.; Kirby, J.P.; Sorasaene, K.; Gray, H.B.; Ponce, A. *J. Am. Chem. Soc.* **2007**, *129*, 1474-1475. (c) Zhang, X.; Young, M.A.; Lyandres, O.; Van Duyne, R.P. *J. Am. Chem. Soc.* **2005**, *127*, 4484-4489.
- (6) Parker, D.; Yu, J. *Chem. Commun.* **2005**, 3141-3143.
- (7) (a) Martínez-Máñez, R.; Sancenón, F. *Chem. Rev.* **2003**, *103*, 4419-4476. (b) Martínez-Máñez, R.; Sancenón, F. *J. Fluoresc.* **2005**, *15*, 267-285.

(8) (a) Bondy, C.R.; Loeb, S.J. *Coord. Chem. Rev.* **2003**, *240*, 77-99. (b) Choi, K.; Hamilton, A.D. *Coord. Chem. Rev.* **2003**, *240*, 101-110. (c) Choi, K.; Hamilton, A.D. *J. Am. Chem. Soc.* **2001**, *123*, 2456-2457.

(9) (a) Camiolo, S.; Gale, P. A. *Chem. Commun.* **2000**, 1129-1130. (b) Gale, P.A.; Anzenbacher Jr., P.; Sessler, J.L. *Coord. Chem. Rev.* **2001**, *222*, 57-102. (c) Aldakov, D.; Anzenbacher Jr., P. *Chem. Commun.* **2003**, 1394-1395. (d) Pohl, R.; Aldakov, D.; Kubát, P.; Jursíková, K.; Marquez, M.; Anzenbacher Jr., P. *Chem. Commun.* **2004**, 1282-1283. (e) Nishiyabu, R.; Anzenbacher Jr., P. *J. Am. Chem. Soc.* **2005**, *127*, 8270-8271. (f) Palacios, M.A.; Nishiyabu, R.; Marquez, M.; Anzenbacher Jr. P. *J. Am. Chem. Soc.* **2007**, *129*, 7538-7544. (g) Nishiyabu, R.; Anzenbacher Jr., P. *Org. Lett.* **2006**, *8*, 359-362.

(10) (a) Gunnlaugsson, T.; Davis, A.P.; Hussey, G.M.; Tierney, J.; Glynn, M. *Org. Biomol. Chem.* **2004**, *2*, 1856-1863. (b) Pfeffer, F.M.; Gunnlaugsson, T.; Jensen, P.; Kruger, P.E. *Org. Lett.* **2005**, *7*, 5357-5360. (c) Gunnlaugsson, T.; Glynn, M.; Tocci, G.M.; Kruger, P.E.; Pfeffer, F.M. *Coord. Chem. Rev.* **2006**, *250*, 3094-3117. (d) Cho, E.J.; Moon, J.W.; Ko, S.W.; Lee, J.Y.; Kim, S.K.; Yoon, J.; Nam, K.C. *J. Am. Chem. Soc.* **2003**, *125*, 12376-12377. (e) Cho, E.J.; Ryu, B.J.; Lee, Y.J.; Nam, K.C. *Org. Lett.* **2005**, *7*, 2607-2609. (f) Jose, D.A.; Kumar, D.K.; Ganguly, B.; Das, A. *Org. Lett.* **2004**, *6*, 3445-3448. (g) Gunnlaugsson, T.; Davis, A.P.; O'Brien, J. E.; Glynn, M. *Org. Biomol. Chem.* **2005**, *3*, 48-56. (h) Sasaki, S.; Mizuno, M.; Naemura, K.; Tobe, Y. *J. Org. Chem.* **2000**, *65*, 275-283. (i) Hisaki, I.; Sasaki, S.; Hirose, K.; Tobe, Y. *Eur. J. Org. Chem.* **2007**, 607-615. (j) Hay, B.P.; Firman, T.K.; Moyer, B.A. *J. Am. Chem. Soc.* **2005**, *127*, 1810-1819. (k) Jose, D.A.; Singh, A.; Das, A.; Ganguly, B. *Tetrahedron Lett.* **2007**, *48*, 3695-3698.

- (11) (a) Esteban-Gómez, D.; Fabbriizzi, L.; Licchelli, M.; Monzani, E. *Org. Biomol. Chem.* **2005**, *3*, 1495-1500. (b) Esteban-Gómez, D.; Fabbriizzi, L.; Licchelli, M. *J. Org. Chem.* **2005**, *70*, 5717-5720. (c) Boiocchi, M.; Del Boca, L.; Esteban-Gómez, D.; Fabbriizzi, L.; Licchelli, M.; Monzani, E. *Chem. Eur. J.* **2005**, *11*, 3097-3104. (d) Amendola, V.; Esteban-Gómez, D.; Fabbriizzi, L.; Licchelli, M. *Acc. Chem. Res.* **2006**, *39*, 343-353. (e) Evans, L.S.; Gale, P.A.; Light, M.E.; Quesada, R. *Chem. Commun.* **2006**, 965-967.
- (12) dos Santos, C.M.G.; Fernández, P.B.; Plush, S.E.; Leonard, J.P.; Gunnlaugsson, T. *Chem. Commun.*, **2007**, 3389-3391.
- (13) (a) Clarkson, R.B. *Top. Curr. Chem.* **2002**, *221*, 201-235. (b) Saeed, M.; Wendland, M.F.; Higgins, C.B. *J. Magn. Reson. Imaging* **2000**, *12*, 890-898. (c) Kroft, L.J.M.; de Roos, A. *J. Magn. Reson. Imaging* **1999**, *10*, 395-403.
- (14) (a) Lewin, M.; Clément, O.; Belguise-Valladier, P.; Tran, L.; Cuénod, C.; Siauve, N.; Frija, G. *Invest. Radiol.* **2001**, *36*, 9-14. (b) Mahfouz, A.E.; Hamm, B.; Taupitz, M. *Eur. Radiol.* **1997**, *7*, 507-513. (c) Yan, G.; Liu, M.; Li, L. *Radiography* **2005**, *11*, 117-122.
- (15) (a) Zigelboim, I.; Offen, D.; Melamed, E.; Panet, H.; Rehavi, M.; Cohen, Y. *J. Incl. Phenom. Macro.* **2007**, *59*, 323-329. (b) Artemov, D. *J. Cell. Biochem.* **2003**, *90*, 518-524. (c) Gunanathan, C.; Pais, A.; Furman-Haran, E.; Seger, D.; Eyal, E.; Mukhopadhyay, S.; Yehoshua, B.; Leituss, G.; Cohen, H.; Vilan, A.; Degani, H.; Milstein, D. *Bioconjugate Chem.* **2007**, *18*, 1361-1365. (d) Barrett, T.; Brechbiel, M.; Bernardo, M.; Choyke, P.L. *J. Magn. Reson. Imaging* **2007**, *26*, 235-249. (e) Morawski, A.M.; Winter, P.M.; Crowder, K.C.; Caruthers, S.D.; Fuhrhop, R.W.; Scott, M.J.; Robertson, J.D.; Abendschein, D.R.; Lanza, G.M.; Wickline, S.A. *Magn. Reson. Med.* **2004**, *51*, 280-286. (f) Sosnovik, D.E.; Weissleder, R. *Curr. Opin. Biotech.*

2007, *18*, 4-10. (g) Morawski, A.M.; Lanza, G.A.; Wickline, S.A. *Curr. Opin. Biotech.* **2005**, *16*, 89-92.

(16) Liu, S.; Edwards, S. *Bioconjugate Chem.* **2001**, *12*, 7-34.

(17) (a) Meltzer, P.C.; Blundell, P.; Jones, A.G.; Mahmood, A.; Garada, B.; Zimmerman, R.E.; Davison, A.; Holman, B.L.; Madras, B.K. *J. Med. Chem.* **1997**, *40*, 1835-1844. (b) Meltzer, P.C.; Blundell, P.; Zona, T.; Yang, L.; Huang, H.; Bonab, A.A.; Livni, E.; Fischman, A.; Madras, B.K. *J. Med. Chem.* **2003**, *46*, 3483-3496.

Chapter 2. Synthesis, Characterization and Luminescence Properties of a New Series of Eu³⁺ - Containing Macrocycles

Based on: Gulgas, C.G.; Reineke, T.M. *Inorg. Chem.* **2005**, *44*, 9829-9836.

ABSTRACT: The synthesis and structural characterization of a series of neutral Eu³⁺-containing macrocyclic complexes, **Eu(4)-Eu(7)**, are reported. The synthetic pathway herein allows for the size and functionality of the macrocycle to be tailored in one step from a common precursor (N,N''-Bis(*p*-isothiocyanatobenzylcarbamoylemethyl)diethylenetriamine-N,N'N''-triacetic acid, **3**) in high yield. The macrocyclic ligands **4-7** have within their structure a bis-amide derivative of diethylenetriaminepentaacetic acid (DTPA) functioning as the europium chelate that is bridged through thiourea groups by either a butyl (**4**), hexyl (**5**), octyl (**6**) or *m*-benzyl (**7**) linker. The two thiourea groups were designed into the host macrocycle to serve as hydrogen bond donors to potential guest molecules that may alter the luminescence properties of the parent macrocycle. Characterization of the luminescence of **Eu(4)-Eu(7)** reveals an antenna effect from the ligand and the luminescence lifetime data reveals the presence of one coordinated water molecule in aqueous solution.

Introduction

Anions play essential roles in biological and environmental systems. For example, DNA, amino acids, and a majority of enzyme substrates are anionic or have anionic components.¹⁻² Anions are present in detergents and fertilizers and as additives in foods and drinking water. The ability to detect various quantities of specific anions in different media is important for

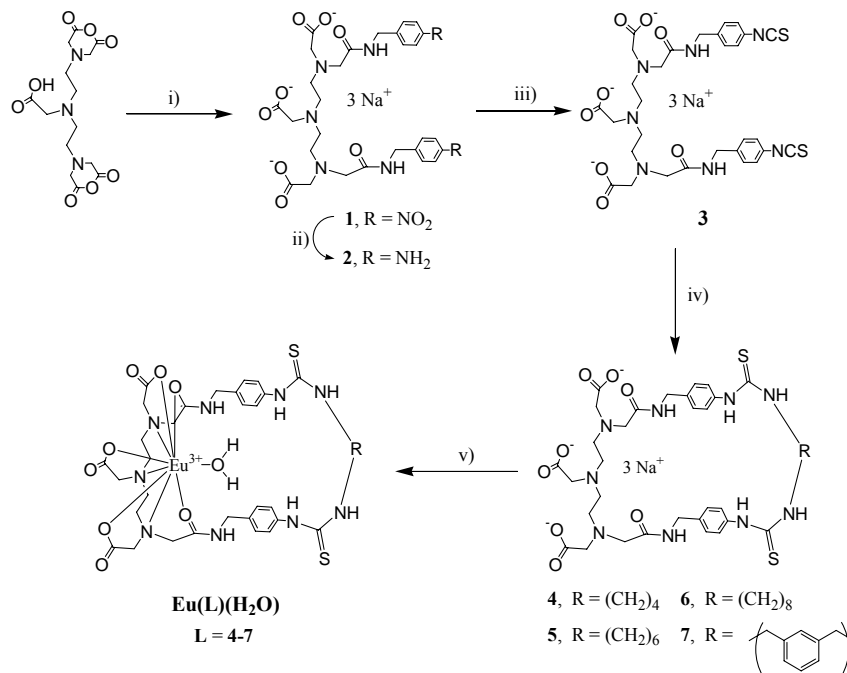
monitoring pollutant levels and studying biological processes. For this reason, a large area of interest in the field of supramolecular chemistry has evolved to include studies of anion binding, transport, and recognition.¹ Designing molecules with the potential to selectively identify a specific anion is a current challenge within this field. In recent years, several articles have appeared in the literature, summarizing and highlighting the diverse approaches toward anion complexation and sensing.²⁻⁶ Many groups have employed a variety of potential binding sites (metals, organic cations, hydrogen bond donors), yielding a growing number of systems, many of which take advantage of a fluorophore as the signaling unit.⁴⁻⁶ Fluorescence signaling, including lanthanide luminescence, has been widely applied to cation recognition as well, mainly due to its potential for “on/off” switching and high sensitivities.⁷⁻⁹

Numerous ion sensing systems exploit photo-induced electron transfer (PET) to an aromatic moiety or a metal ion as a luminescence quenching mechanism.⁵⁻¹⁰ A number of anion sensors use a thiourea group as the binding site and PET donor.¹⁰ Thioureas are neutral hydrogen bond donors that, based on the design of the receptor, can selectively bind anions such as acetate,^{11a} fluoride,^{11b} dihydrogen phosphate,^{12b} or bis-carboxylates.^{10a-b} Upon anion binding, the signal is typically a change in fluorescence intensity,¹⁰ absorption wavelength,¹¹ or ¹H-NMR chemical shift of the receptor.¹² In addition, a few macrocyclic thioureas have been developed, with the intention of improving selectivity through preorganization.¹²

Our design strategy is to integrate several components of successful anion sensing systems into a new series of macrocycles featuring lanthanide luminescence as the signal and thioureas as the binding sites. Previously studied thiourea-based systems have utilized simple organic fluorophores such as anthracene^{10a-c} or pyrene^{10d-e}. Lanthanide luminescence allows for time-resolved fluorescence measurements to be obtained, which is important to eliminate the

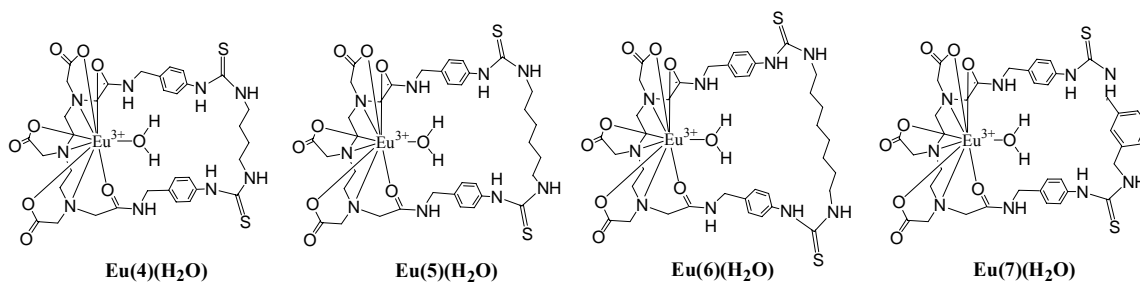
fluorescent background possible in biological samples.^{6-7,13} To the best of our knowledge, this is the first examination of a lanthanide-based macrocycle to incorporate thiourea groups for potential application in anion sensing. Also, we have chosen a chelate (N, N''-bis-amide derivative of diethylenetriaminepentaacetic acid, DTPA) that is responsible for binding the lanthanide moiety to provide the signaling event. DTPA-based macrocycles and their lanthanide complexes have been previously studied.¹⁴ However, as shown in Scheme 1, the synthetic pathway chosen to create our systems allows for both the size and functionality of the pocket to be tailored easily through altering the diamine used in the cyclization step. Here, we report the synthesis and characterization of a series of lanthanide-containing macrocycles, **Eu(4)-Eu(7)** (Scheme 1). These macrocycles will serve as models to study energy transfer phenomena with lanthanide ions upon specific binding events and have potential to be utilized for anion recognition applications.

Scheme 1. Synthesis of macrocyclic ligands **4-7** as trisodium salts.^a



^a (i) 4-nitrobenzylamine, N(et)₃, DMF; (ii) 10% Pd/C, H₂, MeOH; (iii) CSCl₂, CHCl₃, H₂O, NaHCO₃; (iv) H₂NRNH₂, Na₂CO₃, MeOH/H₂O (high dil); (v) Eu(NO₃)₃ · 6H₂O, H₂O.

Chart 1. Macrocyclic Eu³⁺ chelates, **Eu(4)-Eu(7)**.



Experimental

General. All reagents used in the synthesis, if not specified, were obtained from Aldrich Chemical Co. (Milwaukee, WI) and were used without further purification. The mass spectra were obtained from an IonSpec HiResESI mass spectrometer in positive ion mode. NMR spectra were collected on a Bruker AC-250 MHz or a Bruker AV-400 MHz spectrometer. All NMR samples prepared in D₂O were adjusted to pD = 10 with Na₂CO₃. ¹H-NMR samples were standardized relative to sodium 3-(trimethylsilyl)propionate ($\delta = 0.0$ ppm). ¹³C-NMR samples in D₂O were standardized relative to DMSO, which was assigned at $\delta = 39.5$ ppm. Elemental analysis of **3** was performed by the University of Illinois Microanalytical Laboratory and elemental analyses of **4-7** and **Eu(4)-Eu(7)** were performed by Midwest Microlab, LLC. Determination of the %Eu content was performed using a Perkin-Elmer ELAN 6000 Inductively-Coupled Plasma Mass Spectrometer. Ultraviolet absorption data was obtained using a Varian Cary 50 UV-Visible Spectrophotometer. Luminescence studies were performed using a Varian Cary Eclipse Fluorescence Spectrophotometer. Thin-layer chromatography (TLC) was performed using TLC plastic sheets (silica gel 60 F₂₅₄) from Merck (Darmstadt, Germany). The TLC solvent system for determination of all retention factors (R_f) was 2:1:1 (acetonitrile: methanol: water). Dialysis membranes [500 molecular weight-cutoff (MCWO)] were manufactured by Spectrum Laboratories, Inc. (Rancho Dominguez, CA).

Synthesis.

Trisodium N,N''-Bis(*p*-nitrobenzylcarbamoylmethyl)diethylenetriamine-N,N'N''-triacetate (1). *p*-Nitrobenzylamine (1.73 g, 11.3 mmol) was generated from its hydrochloride salt in an aqueous solution of NaOH at pH = 12, and extracted using ether, which was promptly removed

by evaporation. This yellow solid was dissolved in anhydrous DMF (15 mL), affording a yellow solution. Anhydrous triethylamine (5 mL) was then added to the solution of *p*-nitrobenzylamine via syringe. This solution was then added via syringe to a mixture containing diethylenetriaminepentaacetic acid *bis*-anhydride (DTPA-BA) (1.50 g, 4.2 mmol), and anhydrous DMF (15 mL) under N₂ (g). This solution was then stirred for 30 hours, and the resulting mixture turned deep yellow in color. Upon removal of solvent, a thick yellow oil remained and H₂O (35 mL) was added to give a cloudy yellow mixture. Aqueous NaOH (1M) was then added (to pH = 10), and this aqueous solution was washed with ether (5 x 25 mL) to remove unreacted amine. Upon removal of water and drying under vacuum overnight, the title compound was obtained as a yellow crystalline solid. Yield: 2.63 g, 77.6%. ESI-MS: *m/z* 728.1895 [**1**H⁺]. Anal. Calcd for C₂₈H₃₃N₇O₁₂Na₂ · 6H₂O: C, 41.33; H, 5.57; N, 12.05. Found: C, 41.37; H, 5.42; N, 11.85. R_f 0.39. ¹H-NMR (400 MHz, D₂O): δ_H (ppm) 8.17 (d, 4H, *ArH*), 7.48 (d, 4H, *ArH*), 4.51 (s, 4H), 3.32 (s, 4H), 3.21 (s, 4H), 3.15 (s, 2H), 2.74 (br s, 8H). ¹³C-NMR (100 MHz, CD₃OD): δ_C (ppm) 179.1, 174.2, 148.4, 148.1, 129.6, 124.6, 61.3, 60.6, 60.0, 55.6, 55.3, 43.4.

Trisodium N,N''-Bis(*p*-aminobenzylcarbamoylmethyl)diethylenetriamine-N,N'N''-triacetate (2). Compound **1** (1.01 g, 1.39 mmol) and 10% Pd/C (0.807 g) were placed in a flask and methanol was added (70 mL), dissolving **1** and forming a black, turbid solution upon stirring. This solution was degassed by bubbling N₂ through the solution for 1 hr. H₂ was then bubbled into the mixture using a needle outlet. After 35 min. the outlet was removed, and the solution stirred under H₂. After 2 hrs, the reaction appeared complete by TLC, however, the mixture was allowed to stir for a total of 5 hrs to ensure complete conversion. The solution was then vacuum filtered through celite, the solvent removed, and vacuum dried yielding the desired

compound as a white powder. Yield: 0.863 g, 93.0%. ESI-MS: m/z 668 [$2H^+$]. Anal. Calcd for $C_{28}H_{36}N_7O_8Na_3 \cdot 2.5H_2O$: C, 47.19; H, 5.80; N, 13.76. Found: C, 47.47; H, 5.93; N, 13.58. R_f 0.11. 1H -NMR (400 MHz, D_2O): δ_H (ppm) 7.11 (d, 4H, *ArH*), 6.82 (d, 4H, *ArH*), 4.28 (s, 4H), 3.19 (s, 4H), 3.13 (s, 4H), 2.97 (s, 2H), 2.52 (br s, 8H). ^{13}C -NMR (100 MHz, CD_3OD): δ_C (ppm) 179.1, 173.4, 147.9, 129.9, 129.5, 116.7, 61.1, 59.9, 55.0, 54.9, 43.8.

***N,N'*-Bis(*p*-isothiocyanatobenzylcarbamoylmethyl)diethylenetriamine-*N,N'*-triacetic acid (**3**).** Compound **2** (0.500 g, 0.749 mmol) and $NaHCO_3$ (0.300 g, 3.57 mmol) were dissolved in 165 mL H_2O . This solution was then carefully added dropwise to a solution of thiophosgene ($CSCl_2$, CAUTION!) (1.08 g, 9.40 mmol) in 165 mL $CHCl_3$ over 65 min with vigorous stirring. The reaction stirred for 5 hrs and the layers were allowed to separate. The aqueous layer was removed and the organic layer was then washed with H_2O (2 x 100 mL). The aqueous portions were combined and then washed with $CHCl_3$ (3 x 150 mL) to remove unreacted thiophosgene. It should be noted that all steps were performed in a closed hood due to the toxic nature of this reaction. Hydrochloric acid (1M) was then slowly added until a white precipitate formed. The solution was then filtered to isolate the precipitated product (**3**), which was then dried under vacuum. Yield: 0.350 g, 61.0%. ESI-MS: m/z 686.1727 [$3H^+$]. Anal. Calcd for $C_{30}H_{33}N_7O_8S_2Na_2 \cdot 2H_2O$: C, 47.05; H, 4.87; N, 12.80; S, 8.37. Found: C, 46.92; H, 4.97; N, 12.66; S, 8.31. R_f = 0.42. 1H -NMR (400 MHz, D_2O): δ_H (ppm) 7.30 (d, 4H, *ArH*), 7.28 (d, 4H, *ArH*), 4.39 (s, 4H), 3.28 (s, 4H), 3.18 (s, 4H), 3.05 (s, 2H), 2.70 (br s, 8H). ^{13}C -NMR (100 MHz, 9:1 $CD_3OD:D_2O$): δ_C (ppm) 179.2, 174.3, 139.8, 136.3 (SCN), 131.0, 130.1, 126.9, 60.5, 60.3, 55.1, 54.2, 51.9, 43.4.

General Procedure for Macrocyclic Synthesis.

Butyl Macrocyclic (4). Compound **3** (0.167 g, 0.218 mmol) and Na₂CO₃ (0.060 g, 0.566 mmol) were dissolved in 20 mL of 1:1 MeOH/H₂O. A solution of 1,4-diaminobutane (0.023 g, 0.260 mmol) was prepared in 20 mL of MeOH. The two solutions were then added dropwise to a vigorously-stirred solution of MeOH (20 mL) in equal amounts by pipet to a three-neck reaction flask over 1 hr. The reaction was left to stir for 20 hrs, after which the solvent was evaporated down to ~5 mL. Hydrochloric acid (0.5 M) was then slowly added until pH = 3, where a white precipitate had formed. The solution was then filtered and dried under vacuum to isolate the precipitate, **4**, as a monosodium salt. Yield: 0.123 g, 72.8 %. ESI-MS: *m/z* 796.28 [4Na⁺]. IR (KBr): cm⁻¹ 3280 (br), 3055, 2934, 1720, 1643 (s), 1539 (s), 1512, 1385, 1344, 1314, 1237, 1092 (w), 1018 (w). Anal. Calcd for C₃₄H₄₆N₉O₈S₂Na · 2H₂O: C, 49.09; H, 6.06; N, 15.15. Found: C, 49.59; H, 6.16; N, 14.97. R_f = 0.33. ¹H-NMR (400 MHz, D₂O): δ_H (ppm) 7.39 (d, 4H, ArH), 7.23 (br s, 4H, ArH), 4.40 (s, 4H), 3.54 (br s, 4H), 3.25 (s, 4H), 3.16 (s, 4H), 3.02 (s, 2H), 2.63 (br s, 8H), 1.58 (br s). ¹³C-NMR (100 MHz, D₂O): δ_C (ppm) 180.0, 179.8, 175.2, 162.6 (CS), 138.2, 136.5, 129.9, 127.3, 59.6, 59.5, 53.1, 52.3, 45.3, 43.4, 26.9.

Hexyl Macrocyclic (5). Compound **3** (0.167 g, 0.218 mmol), Na₂CO₃ (0.060 g, 0.566 mmol), and 1,6-diaminohexane (0.030 g, 0.258 mmol) were reacted as described above for compound **4**. Compound **5** was isolated as a monosodium salt. Yield: 0.115 g, 65.7%. ESI-MS: *m/z* 824.25 [5Na⁺]. IR (KBr): cm⁻¹ 3302 (br), 3070, 2923, 1720, 1643 (s), 1539 (s), 1514, 1388, 1344, 1314, 1241, 1092 (w), 1018 (w). Anal. Calcd for C₃₆H₅₁N₉O₈S₂Na · 2H₂O: C, 50.28; H, 6.33; N, 14.66. Found: C, 50.72; H, 6.49; N, 14.59. R_f = 0.30. ¹H-NMR (400 MHz, D₂O): δ_H (ppm) 7.39 (d, 4H, ArH), 7.22 (br s, 4H, ArH), 4.41 (s, 4H), 3.54 (br s, 4H), 3.25 (s, 4H), 3.18 (s, 4H), 3.04 (s, 2H), 2.62 (br s, 8H), 1.59 (br s, 4H), 1.33 (br s, 4H). ¹³C-NMR (100 MHz, D₂O): δ_C

(ppm) 179.8, 179.5, 175.0, 162.6 (CS), 137.8, 136.3, 129.5, 126.8, 59.6, 59.4, 53.0, 52.3, 45.5, 43.1, 28.8, 26.4.

Octyl Macrocycle (6). Compound **3** (0.167 g, 0.218 mmol), Na₂CO₃ (0.060 g, 0.566 mmol), and 1,8-diaminooctane (0.037 g, 0.256 mmol) were reacted as described above for **4**. Compound **6** was isolated as a monosodium salt. Yield: 0.147 g, 81.2%. ESI-MS: *m/z* 852.34 [6Na⁺]. IR (KBr): cm⁻¹ 3286 (br), 3059, 2929, 1722, 1640 (s), 1540 (s), 1512, 1385, 1316, 1236, 1100 (w), 1020 (w). Anal. Calcd for C₃₈H₅₅N₉O₈S₂Na · H₂O: C, 52.46; H, 6.49; N, 14.49. Found: C, 53.02; H, 6.54; N, 14.56. R_f = 0.35. ¹H-NMR (400 MHz, D₂O): δ_H (ppm) 7.32 (d, 4H, ArH), 7.16 (br s, 4H, ArH), 4.39 (s, 4H), 3.53 (br s, 4H), 3.22 (s, 4H), 3.16 (s, 4H), 3.02 (s, 2H), 2.56 (br s, 8H), 1.58 (br s, 4H), 1.31 (br s, 8H). ¹³C-NMR (100 MHz, D₂O): δ_C (ppm) 179.8, 179.6, 174.8, 163.4 (CS), 137.4, 136.6, 129.5, 126.3, 59.6, 59.2, 53.0, 52.5, 45.6, 43.1, 28.8, 28.7, 26.5

***m*-Benzyl Macrocycle (7).** Compound **3** (0.167 g, 0.218 mmol), Na₂CO₃ (0.060 g, 0.566 mmol), and *m*-xylylenediamine (0.035 g, 0.254 mmol) were reacted as described above for **4**. Compound **7** was isolated as a monosodium salt. Yield: 0.098 g, 85.5%. ESI-MS: *m/z* 843.82 [7Na⁺]. IR (KBr): cm⁻¹ 3332 (br), 3049, 2923, 1730, 1642 (s), 1540 (s), 1514, 1394, 1343, 1314, 1232, 1092 (w), 1018 (w). Anal. Calcd for C₃₈H₄₇N₉O₈S₂Na · H₂O: C, 52.95; H, 5.61; N, 14.62. Found: C, 52.91; H, 5.51; N, 14.07. R_f = 0.38. ¹H-NMR (400 MHz, D₂O): δ_H (ppm) 7.31 (d, 4H, ArH), 7.20 (m, 8H, ArH), 4.8 (s, 4H, hidden under HOD resonance), 4.34 (s, 4H), 3.22 (s, 4H), 3.16 (s, 4H), 2.94 (s, 2H), 2.57 (br d, 8H). ¹³C-NMR (100 MHz, D₂O): δ_C (ppm) 180.3, 179.8, 174.9, 163.2 (CS), 139.4, 137.6, 136.2, 129.5, 126.9, 126.5, 124.0, 59.6, 59.2, 52.9, 52.4, 48.4, 43.0.

General procedure for Eu complex formation with macrocycles.

Eu(4). Macrocycle **4** (0.050 g, 0.063 mmol) was dissolved in an aqueous NaOH solution (10 mL; 2.7×10^{-2} M) and $\text{Eu}(\text{Cl})_3$ (0.017 g, 0.066 mmol) in H_2O (10 mL) was added dropwise over 45 minutes. This mixture was stirred at 45 °C for 5 hours. The solution was evaporated down to ~5 mL under reduced pressure and then transferred into a 500 MWCO cellulose membrane for dialysis (24 hours; 3 x 4L H_2O exchange). The water was evaporated and the remaining solid dried under vacuum to yield an off-white powder. Yield: 0.057 g, 95%. ESI-MS: m/z 924.20 [**Eu(4)** H^+]. UV-vis (DMSO) $\lambda_{\text{max}}/\text{nm}$ ($\epsilon/\text{M}^{-1} \text{cm}^{-1}$): 274 (19800). IR (KBr): cm^{-1} 3418 (br), 3264, 3088, 2929, 1621 (s), 1539, 1514, 1399, 1314, 1257, 1095 (w), 1021 (w), 927 (w). Anal. Calcd for $\text{C}_{34}\text{H}_{44}\text{N}_9\text{O}_8\text{S}_2\text{Eu}_{0.9} \cdot 5\text{H}_2\text{O} \cdot 3\text{NaCl}$: C, 34.81; H, 4.64; N, 10.75; Eu, 11.66. Found: C, 34.11; H, 4.22; N, 9.63; Eu, 10.67.

Eu(5). Macrocycle **5** (0.052 g, 0.065 mmol) and $\text{Eu}(\text{Cl})_3$ (0.017 g, 0.066 mmol) were reacted as described above for **Eu(4)**, yielding an off-white powder. Yield: 0.058 g, 94%. ESI-MS: m/z 951.98 [**Eu(5)** H^+]. UV-vis (DMSO) $\lambda_{\text{max}}/\text{nm}$ ($\epsilon/\text{M}^{-1} \text{cm}^{-1}$): 273 (22000). IR (KBr): cm^{-1} 3434 (br), 3264, 3088, 2929, 1621 (s), 1542, 1514, 1399, 1314, 1257, 1095 (w), 1018 (w), 927 (w). Anal. Calcd for $\text{C}_{36}\text{H}_{48}\text{N}_9\text{O}_8\text{S}_2\text{Eu} \cdot 5\text{H}_2\text{O} \cdot 3\text{NaCl}$: C, 35.55; H, 4.81; N, 10.36; Eu, 12.49. Found: C, 34.28; H, 4.59; N, 9.54; Eu, 11.53.

Eu(6). Macrocycle **6** (0.054g, 0.065 mmol) and $\text{Eu}(\text{Cl})_3$ (0.017 g, 0.066 mmol) were reacted as described above for **Eu(4)**, yielding an off-white powder. Yield: 0.062 g, 97%. ESI-MS: m/z 980.04 [**Eu(6)** H^+]. UV-vis (DMSO) $\lambda_{\text{max}}/\text{nm}$ ($\epsilon/\text{M}^{-1} \text{cm}^{-1}$): 274 (23200). IR (KBr): cm^{-1} 3429 (br), 3088, 2929, 1616 (s), 1553, 1512, 1402, 1314, 1257, 1095 (w), 1021 (w), 927 (w).

Anal. Calcd for $C_{38}H_{52}N_9O_8S_2Eu \cdot 5H_2O \cdot 2NaCl$: C, 38.49; H, 5.27; N, 10.63; Eu, 12.81.

Found: C, 38.85; H, 5.15; N, 10.11; Eu, 12.08.

Eu(7). Macrocyclic **7** (0.053 g, 0.065 mmol) and $Eu(Cl)_3$ (0.017 g, 0.066 mmol) were reacted as described above for **Eu(4)**, yielding an off-white powder. Yield: 0.058 g, 92%. ESI-MS: m/z 972.46 [**Eu(7)**H⁺]. UV-vis (DMSO) λ_{max}/nm ($\epsilon/M^{-1} cm^{-1}$): 275 (23000). IR (KBr): cm^{-1} 3418 (br), 3093, 2918, 1608 (s), 1539, 1512, 1399, 1317, 1257, 1095 (w), 1018 (w), 927 (w). Anal. Calcd for $C_{38}H_{44}N_9O_8S_2Eu \cdot 4H_2O \cdot 2NaCl$: C, 39.35; H, 4.52; N, 10.87; Eu, 13.10. Found: C, 39.72; H, 4.49; N, 10.34; Eu, 13.20.

Luminescence Studies.

Excitation and emission spectra of **Eu(4)-Eu(7)** (DMSO, 2.0×10^{-5} M) were obtained in phosphorescence mode with a total decay time of 0.02 s, a delay time of 0.10 ms, and a gate time of 5.0 ms. Excitation and emission slit widths were both set at 10 nm. The excitation wavelengths (λ_{exc}) used in the emission studies were either 274 nm or 395 nm. The emission wavelength (λ_{em}) for the excitation studies was 615 nm. Determination of the luminescence lifetime (τ) of **Eu(4)-Eu(7)** was performed in both H₂O and D₂O (3.5×10^{-5} M) with a delay time of 0.05 ms, a gate time of 0.1 ms, $\lambda_{exc} = 272$ nm, and $\lambda_{em} = 615$ nm. Excitation and emission slit widths were 10 nm. Calculations of q used the equation $q = 1.11[k_{H_2O} - k_{D_2O} - 0.31 + 0.075n_{O=CNH}]$ where k is the rate of luminescence decay and $n_{O=CNH}$ is the number of amide N-H oscillators in which the amide carbonyl oxygen is coordinated to Eu^{3+} .¹⁵

Results

Macrocyclic Synthesis and Characterization. The syntheses of macrocyclic ligands **4-7** are shown in Scheme 1. The first step involves opening the bis-anhydride of DTPA (DTPA-BA)

with two equivalents of p-nitrobenzylamine to yield the bis-amide, **1**. The $^1\text{H-NMR}$ spectrum of **1** indicates high conversion. The ESI-MS data support this conclusion with major peaks occurring at 662, 684, 706, 728 and 750 m/z. The peak at 662 is identified as **1** with each carboxylate protonated and ionized with an additional proton, denoted $\mathbf{1H}_4^+$. Each successive peak in the series is due to replacement of one proton with a sodium ion (684 m/z = $\mathbf{1H}_3\text{Na}^+$, 706 m/z = $\mathbf{1H}_2\text{Na}_2^+$, 728 m/z = $\mathbf{1HNa}_3^+$, 750 m/z = $\mathbf{1Na}_4^+$).

Compound **2** is generated by catalytic hydrogenation of the nitro group in **1**. TLC analysis during the course of this reaction shows complete disappearance of **1** after 2 hours with concurrent appearance of **2**. The $^1\text{H-NMR}$ spectrum of **2** lacks resonances from the nitrobenzyl precursor, and a large upfield shift of the aromatic resonances occurs (consistent with formation of an electron-donating amino group as a substituent). In the ESI mass spectrum of **2**, peaks at 624, 646, 668, and 690 are obtained, where the peak at 624 is due to the monosodium species, $\mathbf{2H}_3\text{Na}^+$, and each successive peak thereafter is the result of the replacement of a proton with a sodium ion (646 m/z = $\mathbf{2H}_2\text{Na}_2^+$, 668 m/z = $\mathbf{2HNa}_3^+$, 690 m/z = $\mathbf{2Na}_4^+$) similar to the result obtained with **1**. The next step in the synthetic route requires reaction of **2** with excess thiophosgene (CSCl_2) in a two-phase reaction to generate the bis-isothiocyanate **3**.¹⁶ Full caution (closed hood, lab coat and gloves) must be taken when working with thiophosgene due to its high toxicity and volatility. The desired product (**3**) is obtained in an efficient manner and isolated by precipitation with acid, which effectively removes trace impurities resulting from addition of only one equivalent of p-nitrobenzylamine to DTPA-BA in the first step of the reaction sequence. The mono-substituted impurities are retained in the aqueous layer due to the presence of four carboxylic acid groups and only one aromatic ring. The $^1\text{H-NMR}$ spectrum of **3** reveals two resonances in the aromatic region ($\delta = 7.28$ and 7.30 ppm) consistent with

conversion to the isothiocyanate-substituted benzene rings. Elemental analysis of this compound indicates a formula of $C_{30}H_{33}N_7O_8S_2Na_2 \cdot 2H_2O$, consistent with the proposed structure, where two waters of hydration persist after drying under vacuum. Two major peaks occur in the ESI mass spectrum corresponding to $3H_4^+$ and $3H_3Na^+$ at 686 m/z and 708 m/z, respectively. Macrocyclic, oligomeric, and all trace solvents are not detected at this stage. The first three steps in this synthesis yield **3** in a highly pure form and thus, purification via chromatography is deemed unnecessary for any of these precursor molecules.

Compound **3** is the synthetic precursor to forming macrocycles **4-7**. The key step in the synthesis of these systems is the cyclization step, where, for example, 1,4-diaminobutane is reacted with **3** under highly diluted conditions to generate **4** in high yield. NMR data indicate the formation of a single product in this reaction, characterized by a few large changes. For example, 1H -NMR resonances appear in the aliphatic region of the spectrum ($\delta = 3.54$ and 1.58 ppm), corresponding to two sets of four equivalent methylene protons, which represents linking of the aliphatic chain to form the macrocycle. In the ^{13}C -NMR spectrum of **4** the resonance near 136.3 ppm (characteristic of the isothiocyanate group) is absent, however a new peak appears at 162.6 ppm, indicative of the newly-formed thiourea functionality. In addition, new resonances appear in the aliphatic region at 45.3 and 26.9 ppm, ascribed to the carbons linking the thiourea moieties together. Similar spectral changes are also observed in the NMR spectra of **5-7**, indicating complete conversion of the starting material to the desired products.

The ESI-MS of **4** has a major peak at 796 m/z which corresponds to the neutral ligand ionized with a sodium ion, $4H_3Na^+$. In addition, similar to the pattern observed in compounds **1** and **2**, there are significant peaks at 774 [$4H_4$] $^+$, 818 ($4H_2Na_2$), 840 ($4HNa_3$), and 862 ($4Na_4$) m/z. These results indicate this product to be the [1:1] macrocycle, where [1:1] denotes the ratio

of DTPA precursor and the diamine that form the final product, as shown in Chart 1. The ESI-MS data for **4-7** are similar with respect to the formation of exclusively the [1:1] product. In addition, a small peak at 708 m/z is observed as a fragmentation product in the mass spectra for **4-7** and is most likely not due to the presence of unreacted **3**, which has the same m/z ratio. Small peaks are also found in the region of the MS where [2:2] macrocyclic products would appear (1547-1701 m/z for **4**). However, an ESI-MS-MS experiment using **6** as a model revealed that these peaks are due to proton or sodium ion-bound dimers that decompose at low energy into the monomer. The NMR and elemental analysis data support this conclusion that the [1:1] products of **4-7** are obtained in a pure form.

The DTPA unit of these macrocycles is an octadentate ligand for lanthanide metals. Addition of $\text{Eu}(\text{Cl})_3$ to aqueous solutions of **4-7** gives the final macrocyclic products **Eu(4)-Eu(7)**. The products are purified by dialyzing each compound in ultrapure H_2O using a 500 MWCO membrane to remove salts and any excess reactants. The infrared spectra of **Eu(4)-Eu(7)** show intense bands at $\sim 1610\text{ cm}^{-1}$, which is a lower stretching frequency than expected for amide or carboxylate $\text{C}=\text{O}$'s, and is consistent with coordination of these groups to Eu^{3+} . In addition, complexation with Eu^{3+} simplifies the ESI mass spectra of **4-7**, and in the spectrum of **Eu(4)**, for example, the major peaks occur at 924 and 946 m/z corresponding to the $[\text{Eu}(\mathbf{4})]\text{H}^+$ and $[\text{Eu}(\mathbf{4})]\text{Na}^+$ ionized species, respectively. In the case of **Eu(5)**, **Eu(6)**, and **Eu(7)**, peaks for the proton-ionized species occur at 952, 980, and 972 m/z, respectively. The isotopic distribution pattern for $[\text{Eu}(\mathbf{7})]\text{H}^+$ is shown in Figure 1. The highest peak at 972.1992 is due to the complex with the major isotope, ^{153}Eu , whereas the peak at 970.1854 is attributed to the complex with ^{151}Eu .

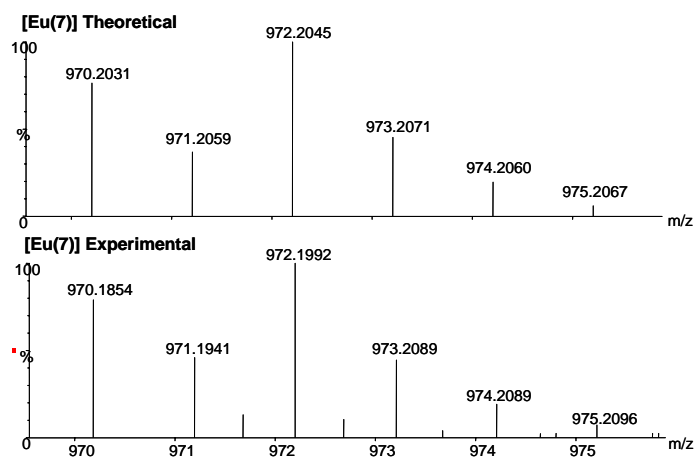


Figure 1. ESI isotopic distribution pattern for $[\text{Eu}(7)]\text{H}^+$. Top: theoretical distribution. Bottom: actual.

Luminescence Studies. All the complexes studied have similar excitation and emission spectra, and the luminescence spectra of **Eu(4)**, shown in Figure 2, are representative of the spectra observed for products **Eu(5)-Eu(7)**. The excitation spectrum of **Eu(4)** (Figure 2a, emission at 615 nm) is dominated by a broad band at 250-325 nm with a maximum at 276 nm. This large band is primarily due to the absorbance of the benzene sensitizers present in the macrocycle structures. However, significant bands arising from direct excitation of Eu^{3+} are also observed in the region from 310-480 nm. The most intense band, at 395 nm, is characteristic of Eu^{3+} absorption. The general UV-VIS absorption spectrum of **Eu(4)** shows only a broad band at 250-305 nm that is much more symmetrical in shape than the broad band in the excitation spectrum ($\lambda_{\text{em}} = 615 \text{ nm}$) and is attributed to absorption from the aryl portion of the ligand.

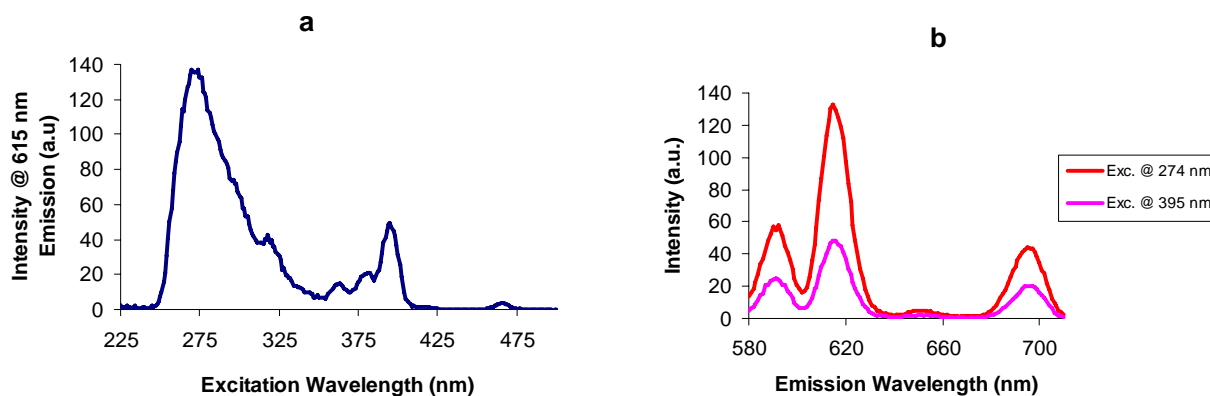


Figure 2. Excitation (a) and emission (b) spectra of **Eu(4)** in DMSO (2.0×10^{-5} M).

The emission spectra taken at excitation wavelengths of 274 and 395 nm of complex **Eu(4)** are shown in Figure 2b. Again, similar emission spectra to that shown in Figure 2b are observed for all products **Eu(4)**-**Eu(7)**. At a 274 nm excitation wavelength, the emission intensity for the three main emission bands [$^5D_0 \rightarrow ^7F_1$ ($\lambda_{\max} = 592$ nm), $^5D_0 \rightarrow ^7F_2$ ($\lambda_{\max} = 615$ nm), $^5D_0 \rightarrow ^7F_4$ ($\lambda_{\max} = 695$ nm)] is approximately 2.5 times more intense than when excited at 395 nm (the wavelength used for direct excitation of Eu^{3+}). The degree of luminescence enhancement via energy transfer from the ligand for complexes **Eu(4)**-**Eu(7)** is very similar, even though **Eu(7)** contains a *m*-xylene linker.

Luminescence lifetime data also have been obtained for the complexes **Eu(4)**-**Eu(7)** to determine q , the number of coordinated water molecules in aqueous solution. Experimental lifetime data from the study of **Eu(4)** is shown in Figure 3, and the summarized results from studies of all the complexes are shown in Table 1. The luminescence lifetime, τ , has been determined in both H_2O and D_2O .¹⁵ Calculations of q were performed using the equation $q = 1.11[k_{\text{H}_2\text{O}} - k_{\text{D}_2\text{O}} - 0.31 + 0.075n_{\text{O}=\text{CNH}}]$ where k is the rate of luminescence decay ($k = 1/\tau$) and $n_{\text{O}=\text{CNH}}$ is the number of amide N-H oscillators in which the amide carbonyl oxygen is

coordinated to Eu^{3+} .¹⁵ For the Eu^{3+} complexes studied, $n_{\text{O}=\text{CNH}} = 2$ and $q \approx 1$ in all cases. The octadentate macrocyclic ligand in **Eu(4-7)** allows for one vacant coordination site on the metal to be filled by solvent, resulting in the preferred nine-coordinate complex.^{14a}

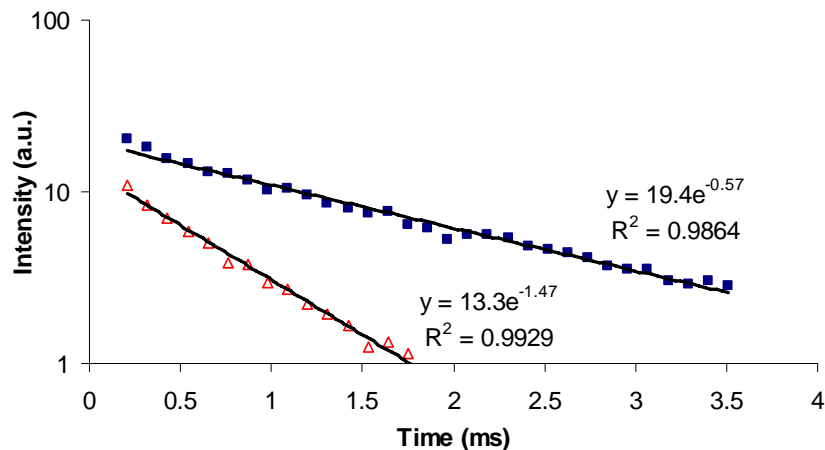


Figure 3. Decay of the luminescence emission ($\lambda_{\text{exc}} = 272$ nm; $\lambda_{\text{em}} = 615$ nm) of a 3.5×10^{-5} M solution of **Eu(4)** in H_2O (open triangle) and D_2O (closed square).

Table 1. Summarized luminescence lifetime data of **Eu(4)-Eu(7)**.

Compound	$\tau_{\text{H}_2\text{O}}$ (ms)	$\tau_{\text{D}_2\text{O}}$ (ms)	q^a
Eu(4)	0.68	1.74	0.82
Eu(5)	0.71	1.63	0.69
Eu(6)	0.79	2.04	0.68
Eu(7)	0.75	2.08	0.78

^a Values for q were calculated using the method from Horrocks et al.¹⁵

Discussion

The design principles behind this new series of macrocycles, **Eu(4)-Eu(7)**, require three components: i) a lanthanide chelate complex that serves as the signaling unit, ii) an aromatic moiety that functions both as a spacer and a light harvesting unit (antenna), and iii) thiourea groups that function as the anion binding pocket. This pocket can be tailored by substitution of the functional group between the two opposing thioureas, which may potentially allow for increased selectivity based on anion shape recognition through incorporation of additional binding sites.¹⁷ Applying these systems for anion sensing depends on excitation of the organic chromophore on the macrocyclic ligand, which transfers energy to the Eu^{3+} center, resulting in luminescence.⁶⁻⁷ Our working hypothesis is that hydrogen bonding interactions between the thiourea hydrogens and bound anionic acceptors could affect the energy transfer between chromophore and Eu^{3+} , therefore resulting in a detectable change in luminescence intensity. Gaining an understanding of this process and mechanism is the goal of this research and has driven the design of these new macrocycles. These first models were created to study the efficiency of the synthetic pathway, which incorporates simple substituted benzene groups as the antenna with differing hydrocarbons linking the functional thiourea groups together. Here, we have developed a versatile route that allows for a systematic variation in the final structure through choice of an appropriate diamine moiety to form a variety of macrocycles. The cyclization step, which results in formation of two thiourea functionalities in the cyclic binding pocket, proceeds in high yield and with minimal byproducts for a number of diamines of different lengths. This result demonstrates the versatility and promise for future models to study anion sensing and energy transfer mechanisms involving lanthanide metals.

The first three synthetic steps en route to macrocycles **4-7** (Scheme 1) are high yielding with minimal purification required, resulting in an overall yield of 44.0% for **3** from DTPA-BA. In particular, column chromatography is not needed to isolate **3** in high purity. The synthesis of macrocycles **4-7** from **3** can be compared to previous one-step syntheses, where reaction of the bis-anhydride of DTPA with various diamines resulted in a vast array of macrocyclic ligands for lanthanide ions.¹⁴ Dilute conditions (20-40 mM) with either DMF^{14b-c}, DMSO^{14e-f}, or MeOH^{14d} are used to avoid formation of oligomers and post-purification yields ranged from 10-45%.¹⁴ In the synthesis of **4-7**, a bicarbonate-buffered H₂O/MeOH solvent system is used at high dilution (2 mM), with yields between **70-80%**. The bis-isothiocyanate **3** is stable in the presence of H₂O under these conditions, and the reaction proceeds in good yield. Previous syntheses of macrocyclic thioureas (that lack a metal chelating group) through the reaction of bis-isothiocyanates with diamines under high dilution (2 mM in CHCl₃) have resulted in similar yields, 70-79%.^{12b} In the current work, the synthetic scheme producing **4-7** maintains the higher yields particular to the isothiocyanate reaction, while also producing a DTPA-containing macrocycle.

Ligands **4-7** were dissolved using aqueous NaOH solution and subsequently reacted with EuCl₃ to yield **Eu(4)-Eu(7)**, respectively. Yields ranged from 92-97%. ESI-MS data indicate the formation of **Eu(4)-Eu(7)** and intense peaks are observed for both the H⁺ and Na⁺ ionized species. The IR spectra of the four complexes are similar, with the most intense band occurring between 1608 and 1621 cm⁻¹. This relatively low frequency reflects the weakening of the C=O of amide and carboxylate functionalities upon Eu³⁺ coordination. Elemental analyses of **Eu(4)-Eu(7)** reveals the presence of NaCl in the bulk sample, despite dialysis of the complexes. In

addition, the %Eu found in the **Eu(4)** sample is slightly low, possibly due to the more tightly restricted macrocyclic ligand.

Due to the weak absorption capabilities of Eu^{3+} , organic chromophores are often used to increase ion emission through energy transfer processes.³⁻⁴ A relatively intense emission is important for practical applications involving induced changes in the luminescent signal. Also, enhancing the emission allows low concentrations to be used. In the case of ligands **4-7**, only the disubstituted benzenes are possible sensitizers for the Eu^{3+} emission, and insight into the efficiency of the sensitization can be gained through analysis of the absorption, excitation, and emission spectra of these complexes. The excitation and emission spectra of **Eu(4)-Eu(7)** (Figure 2) are typical in that a large ligand-based excitation band ($\lambda_{\text{max}}=274$ nm) as well as a Eu^{3+} -based band ($\lambda_{\text{max}}=395$ nm) are present, with both excitations giving rise to Eu^{3+} emissions at 592, 615 and 700 nm.

The mass spectra of **Eu(4)-Eu(7)** indicate that a coordinated solvent molecule is not present in the isolated and dried product. However, it is important to determine if a solvent molecule is coordinated to the Eu^{3+} center in solution because the availability of an open coordination site on the metal could disrupt potential interaction of an anion with the hydrogen-bond donating thioureas of the macrocycle, complicating future studies. In H_2O and D_2O , luminescence lifetime measurements indicate that one water molecule is coordinated in **Eu(4)-Eu(7)**. Previous crystal structure determinations of DTPA bis-amide macrocyclic Ln^{3+} complexes have shown that a water molecule occupies a capping position in a distorted tricapped trigonal prism (TTP) geometry.^{14a-c} This capping position is not oriented toward the cavity of the macrocycle. Currently, it is unknown as to whether or not this ninth site is accessible in DMSO

solution, but this possibility would allow Eu^{3+} to act as an additional anion binding site in macrocycles of this series.

Our hypothesis of the possible anion sensing capabilities in macrocycles such as **Eu(4)-Eu(7)** depends on changing the intensity of the lanthanide emission upon anion binding to the thiourea groups via hydrogen bonding. It has been reported that anion binding to thiourea lowers the oxidation potential of the sulfur atom, in effect, making it a better donor to suitable acceptors nearby.^{10a-c} In PET mechanisms, the fluorescence of an aromatic group can be quenched by such a process, where typically there is a methylene spacer between the fluorophore and the thiourea group.^{10a-c} In **Eu(4)-Eu(7)**, the thiourea moiety is directly attached to the benzene chromophore and anion binding may alter the chromophore's photophysical properties, potentially resulting in a change in Eu^{3+} luminescence. For example, significant changes in absorption spectra have occurred with simple thioureas directly covalently attached to aromatic units.¹¹ However, without suitable models for comparison, potential changes in the luminescence upon anion binding to **Eu(4)-Eu(7)** are difficult to predict. Preliminary studies in DMSO have shown that the luminescence of **Eu(4)-Eu(7)** increases up to ~100% in the presence of up to 8 equivalents of the tetrabutyl ammonium salts of dihydrogen phosphate and benzoate, but no change is observed in the presence of tetrabutyl ammonium iodide. These results show that a response to anions is achieved by our current system, but it is not by a PET quenching mechanism.

Studying the effects of anion binding requires that the antenna is excited and then proceeds to transfer energy to the Eu^{3+} center. As shown in Figure 2b, the benzene spacer in **Eu(4)-Eu(7)** appears to function as a weak antenna, evidenced by the enhancement of Eu^{3+} luminescence when the complex is excited at 274 nm compared to 395 nm, where Eu^{3+} is excited directly. This feature is also reflected in the excitation spectra of **Eu(4)-Eu(7)**, which show

significant bands assigned as direct excitations of Eu^{3+} ($\lambda_{\text{max}} = 319$ and 395 nm, for example), roughly one-third the intensity of the band from 250-305 where the ligand absorbs. In designing future systems analogous to **Eu(4)-Eu(7)**, incorporation of more efficient antenna moieties will be necessary. The *m*-xylylene linker in **Eu(7)** did not appear to have any effect on enhancing the luminescence of the complex, as compared with **Eu(4)-Eu(6)**. This is most likely due to a larger distance between this group and the Eu^{3+} center.

Conclusion

The synthesis, characterization, excitation-emission spectra, and luminescence lifetime data for a new series of lanthanide and thiourea-containing macrocycles [**Eu(4)-Eu(7)**] are presented. These systems represent a new series of complexes synthesized by a clean, versatile process that potentially allows for functional variability for future macrocycles. Excitation-emission spectra reveal that these complexes luminesce, and luminescence lifetime studies reveal that one water molecule is coordinated to the Eu^{3+} center in aqueous solution. Current studies are focused on designing similar macrocycles with improved sensitizers that will further enhance the antenna effect to create highly luminescent complexes. Also, studies on the anion-binding ability and response of **Eu(4)-Eu(7)** are underway, to study the inclusion chemistry of this new macrocyclic system. A solid understanding of the structure of the complex, energy transfer properties of the ligand, and its interaction with various anions is necessary for developing more responsive and selective macrocyclic systems for specific anion recognition.

REFERENCES.

- (1) (a) Bianchi, A.; Bowman-James, K.; García-España, E., Eds. *Supramolecular Chemistry of Anions*, Wiley-VCH: New York, 1997. (b) Anzenbacher, P.; Jursikova, K.; Aldakov, D.; Marquez, M.; Pohl, R. *Tetrahedron* **2004**, *60*, 11163. (c) Nishiyabu, R.; Anzenbacher, P. *J. Am. Chem. Soc.* **2005**, *127*, 8270. (d) Kim, T.; Swager, T. *Angew. Chem. Int. Ed.* **2003**, *42*, 4803.
- (2) Beer, P.D.; Gale, P.A. *Angew. Chem. Int. Ed.* **2001**, *40*, 486-516.
- (3) Gale, P.A. *Coord. Chem. Rev.* **2003**, *240*, 191-221.
- (4) Keefe, M.H.; Benkstein, K.D.; Hupp, J.T. *Coord. Chem. Rev.* **2000**, *205*, 201-228.
- (5) (a) Martínez-Mañez, R.; Sancenón, F. *Chem. Rev.* **2003**, *103*, 4419-4476. (b) Suslick, K.; Rakow, N.; Sen, A. *Tetrahedron* **2004**, *60*, 11133. (c) Gale, P.; Anzenbacher, P.; Sessler, J. *Coord. Chem. Rev.* **2001**, *222*, 57. (d) Anzenbacher, P.; Jursikova, K.; Sessler, J. *J. Am. Chem. Soc.* **2000**, *122*, 9350.
- (6) Parker, D. *Coord. Chem. Rev.* **2000**, *205*, 109-130.
- (7) (a) de Silva, A.P.; Gunaratne, H.Q.N.; Gunnlauugsson, T.; Huxley, A.J.M.; McCoy, C.P.; Rademacher, J.T.; Rice, T.E. *Chem. Rev.* **1997**, *97*, 1515-1566. (b) de Silva, A.P.; Fox, D.B.; Huxley, A.J.M.; Moody, T.S. *Coord. Chem. Rev.* **2000**, *205*, 41-57.
- (8) (a) Swager, T. *Acc. Chem. Res.* **1998**, *31*, 201. (b) Kim, J.; McQuade, T.; McHugh, S.; Swager, T. *Angew. Chem. Int. Ed.* **2000**, *39*, 3868.

(9) (a) Gunnlaugsson, T. *Tetrahedron Lett.* **2001**, *42*, 8901-8905. (b) Gunnlaugsson, T.; Leonard, J.P.; Sénéchal, K.; Harte, A.J. *J. Am. Chem. Soc.* **2003**, *125*, 12062-12063. (c) Gunnlaugsson, T.; Mac Dónaill, D.A.; Parker, D. *J. Am. Chem. Soc.* **2001**, *123*, 12866-12876. (d) Holliday, B.; Farrell, J.; Mirkin, C. *J. Am. Chem. Soc.* **1999**, *121*, 6316. (e) Lee, S.; Luman, C.; Castellano, F.; Lin, W. *Chem. Commun.* **2003**, 2124.

(10) (a) Gunnlaugsson, T.; Davis, A.P.; O'Brien, J. E.; Glynn, M. *Org. Lett.* **2002**, *4*, 2449-2452. (b) Gunnlaugsson, T.; Davis, A.P.; O'Brien, J. E.; Glynn, M. *Org. Biomol. Chem.* **2005**, *3*, 48-56. (c) Gunnlaugsson, T.; Davis, A.P.; Hussey, G.M.; Tierney, J.; Glynn, M. *Org. Biomol. Chem.* **2004**, *2*, 1856-1863. (d) Sasaki, S.; Citterio, D.; Ozawa, S.; Suzuki, K. *J. Chem. Soc., Perkin Trans. 2*, **2001**, 2309-2313. (e) Nishizawa, S.; Kaneda, H.; Uchida, T.; Teramae, N. *J. Chem. Soc., Perkin Trans. 2*. **1998**, 2325-2327.

(11) (a) Kato, R.; Nishizawa, S.; Hayashita, T.; Teramae, N. *Tetrahedron Lett.* **2001**, *42*, 5053-5056. (b) Jose, D.A.; Kumar, K.; Ganguly, B. Das, A. *Org. Lett.* **2004**, *6*, 3445-3448.

(12) (a) Choi, K.; Hamilton, A.D. *Coord. Chem. Rev.* **2003**, *240*, 101-110. (b) Sasaki, S.; Mizuno, M.; Naemura, K.; Tobe, Y. *J. Org. Chem.* **2000**, *65*, 275-283. (c) Lee, K.H.; Hong, J. *Tetrahedron Lett.* **2000**, *41*, 6083-6087. (d) Snellink-Ruël, B.H.M.; Antonisse, M.M.G.; Engbersen, J.F.J.; Timmerman, P.; Reinhoudt, D.N. *Eur. J. Org. Chem.*, **2000**, 165-170.

(13) (a) Mayer, A.; Neuenhofer, S. *Angew. Chem. Int. Ed. Engl.* **1994**, *33*, 1044-1072. (b) Hanaoka, K.; Kikuchi, K.; Kojima, H.; Urano, Y.; Nagano, T. *J. Am. Chem. Soc.* **2004**, *126*, 12470-12476.

(14) (a) Caravan, P.; Ellison, J.J.; McMurry, T.J.; Lauffer, R.B. *Chem. Rev.* **1999**, *99*, 2293-2352. (b) Inoue, M.B.; Santacruz, H.; Inoue, M.; Fernando, Q. *Inorg. Chem.* **1999**, *38*, 1596-

1602. (c) Inoue, M.B.; Navarro, R.S.; Inoue, M.; Fernando, Q. *Inorg. Chem.* **1995**, *34*, 6074-6079. (d) Franklin, S.J.; Raymond, K.N. *Inorg. Chem.* **1994**, *33*, 5794-5804. (e) Carvalho, J.F.; Kim, S.; Chang, C.A. *Inorg. Chem.* **1992**, *31*, 4065-4068. (f) Brunet, E.; Juanes, O.; Sedano, R.; Rodríguez-Ubis, J. *Org. Lett.* **2002**, *4*, 213-216.

(15) Supkowski, R. M. Horrocks, Jr., W. D. *Inorg. Chim. Acta* **2002**, *340*, 44-48.

(16) Brechbiel, M.W.; Gansow, O.A.; Atcher, R.W.; Schlom, J.; Esteban, J.; Simpson, D.E.; Colcher, D. *Inorg. Chem.* **1986**, *25*, 2772-2781.

(17) Hay, B.P.; Firman, T.K.; Moyer, B.A. *J. Am. Chem. Soc.* **2005**, *127*, 1810-1819.

Chapter 3. Macrocyclic Eu³⁺ Chelates Show Selective Luminescent Responses to Anions

Based on: Gulgas, C.G.; Reineke, T.M. *Inorg. Chem.* **2007**, *submitted*.

ABSTRACT: A series of lanthanide-containing macrocycles, **Eu(2)-Eu(5)**, exhibited unique luminescent responses in the presence of strong hydrogen bond-accepting anions (F⁻, CH₃COO⁻, H₂PO₄⁻) in DMSO. The macrocycles examined herein were designed to include a lanthanide chelate, aromatic spacers that function as antennae, thiourea groups as anion binding units, and an alkyl or aryl linker between the thioureas that tailors the size and rigidity of the macrocycle. The anion-induced change in emission intensity ($\lambda_{\text{exc}} = 272 \text{ nm}$, $\lambda_{\text{em}} = 614 \text{ nm}$) varied across the series of macrocycles and was dependent on the basicity of the anion. The largest luminescent response was observed in **Eu(2)**, whereby the emission increased 77% upon addition of 8 equivalents of fluoride. A change in luminescence was not observed when exciting Eu³⁺ directly ($\lambda_{\text{exc}} = 395 \text{ nm}$) over the course of anion titration experiments with all of the anions studied. These macrocycles contain only slight variations in structure, and insights into the mechanism of the anion interaction have been gained through monitoring anion titrations via luminescence, absorbance, and luminescence lifetime measurements. In addition, model compounds (**2-5**) lacking the Eu³⁺ moiety were synthesized to study the binding pockets of **Eu(2)-Eu(5)** using absorbance and ¹H-NMR spectroscopy. These studies indicate that the anions interact with the thiourea moiety of **Eu(2)-Eu(5)**, and the luminescent response is controlled by changes in the binding pocket of the macrocycle.

Introduction

Due to the importance of anions in industrial and environmental applications, as well as their essential physiological roles, there has recently been an increased demand for selective anion sensors.¹ For example, the recent elevated consumption of fluoridated water has increased public concerns with the detrimental health effects of fluoride on the development of conditions such as dental and skeletal fluorosis.² Although efforts to discriminate fluoride from the other halides have been successful with a variety of designed receptors,³⁻⁴ the selectivity in the presence of other common anions remains a challenge. In addition, the important role of carboxylates in many ligand binding interactions with proteins¹ motivates fundamental studies of carboxylate recognition and sensing, ranging from the simple acetate anion⁵ to more biologically relevant amino acids and di- and tricarboxylates.⁶⁻⁷ Also, metabolic pathways driven by the hydrolysis of adenosine triphosphate (ATP) involve release of orthophosphate and pyrophosphate, and synthetic receptors selective for these anions have also been the objective of numerous studies.⁸ Hence, the development of molecular systems combining both anion recognition components and signaling units for use as anion sensors is of high interest for probing biological systems.

In general, anions are large and carry a more diffuse charge relative to cations, which challenges chemists to design novel preorganized receptors to effectively compete with solvent molecules for anion binding of high affinity.¹ A variety of routes have been employed to design novel materials endowed with anion recognition properties. Many of the receptors used in recognition of the aforementioned anions employ neutral hydrogen bond donating groups such as amides, ureas, thioureas, and pyrroles. Thioureas are often used in receptor design because they offer directional hydrogen bond donors (-NH) and the acidity of these moieties can be modulated

by changing the electron-withdrawing nature of adjacent functional groups.^{1h,4} Because it is common for hydrogen bond accepting anions (i.e. F^- , OAc^- , $H_2PO_4^-$) to elicit a similar receptor affinity or sensor response with only moderate selectivities, research is generally focused on structurally tailoring many previous receptors to improve selectivity for the anion of interest.^{1,3,5-}
⁸ Toward this end, thiourea binding groups have been coupled with organic fluorescence signaling molecules where photo-induced electron transfer (PET) occurs from the sulfur atoms upon an anion binding event, resulting in highly sensitive fluorescence quenching.^{1,6b-c}

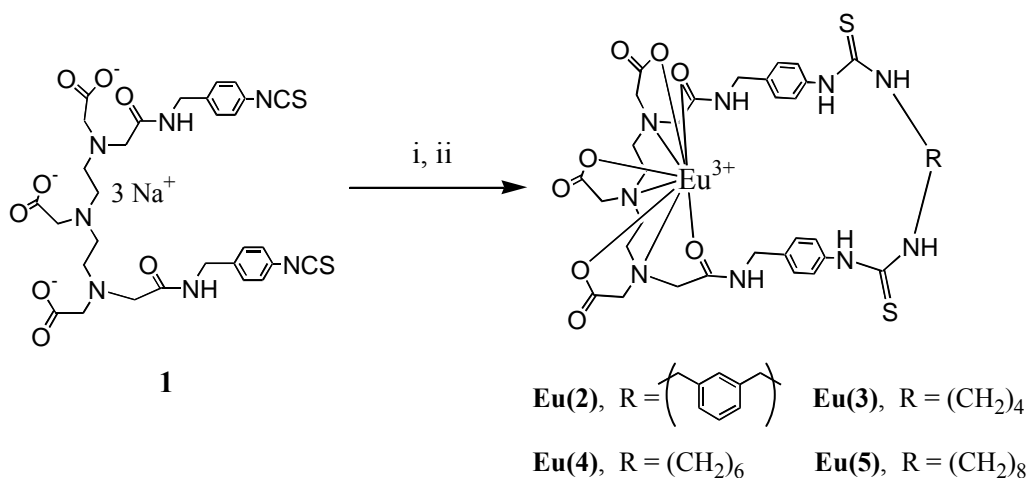
In designing molecular systems for potential sensors in biological samples, it is important to anticipate the possibility of background fluorescence, which could interfere with measurements of target analytes. Lanthanides have found application in this area as signaling units due to their long luminescence lifetimes, which allow for time-resolved fluorescence (TRF) measurements to be obtained, which is particularly useful for biological systems with high auto-fluorescence.⁹ Lanthanides have also been examined previously for anion sensing, however, direct coordination of the anion to the lanthanide is typically required, where in aqueous solution, displacement of water molecules results in enhanced luminescence intensity and longer luminescence lifetimes.^{7,10} Inspired by the properties of both systems, we have reported the synthesis of four macrocyclic systems, denoted **Eu(2)**-**Eu(5)** (Scheme 1).¹¹ These macrocycles were the first example of receptors that incorporate two opposing thiourea groups that possibly serve as preorganized anion binding sites and contain an N, N''-bis-amide derivative of diethylenetriaminepentaacetic acid (DTPA) to chelate Eu^{3+} as a signaling unit.¹¹ This general motif has been designed to allow for the size, flexibility, and functionality of the macrocycle pocket to be synthetically varied with relative ease and to tune the system for enhanced selectivity. In addition, this series was designed to examine how structural changes affect anion

response behavior. Our systems include functionalized aromatics to act as spacers between the binding and signaling moieties and serve as antennae to enhance the lanthanide emission intensity through energy transfer.⁹ These macrocycles were designed with biological sensing in mind due to the possibility of performing time-resolved measurements.

Herein, we report the luminescence, anion recognition/sensing properties, and signaling mechanism studies of these novel macromolecules [**Eu(2)-Eu(5)**], and their responses are compared as a function of the linker moiety. It was generally found that the luminescent response to fluoride and acetate varies widely across the series of macrocycles studied, and that the luminescence intensity changes observed during the anion titrations were not found to be correlated to changes in the absorption spectrum of the macrocycle in the solvent studied (DMSO). We have discovered that a particular system, **Eu(2)**, which contains a *m*-xylyl linker, shows a selective luminescent response to fluoride as compared to the other halide anions and is also selective for acetate over dihydrogen phosphate and nitrate in DMSO. To further examine this phenomenon, organic bis-thiourea sensors **2-5** were synthesized and characterized as a model system to elucidate the sensing response of **Eu(2)-Eu(5)** to acetate and fluoride using absorption spectroscopy and ¹H-NMR. These model studies, coupled with luminescence lifetime studies of Eu³⁺ emission in the original macrocycles, support our theory that thiourea-based (and not Eu³⁺) anion binding is responsible for the recognition event with these materials. To the best of our knowledge, this is one of the first examples of lanthanide-based anion sensors that does not require direct coordination of anions to the metal.^{8j,10} These macrocycles appear to exploit a unique signaling mechanism related to the efficiency of energy transfer and distance of the ligand antennae to the lanthanide moiety.¹⁰ Additionally, we reveal that **Eu(2)-Eu(5)** reversibly bind various anions and remain responsive to fluoride and acetate in DMSO solutions containing

a high background of chloride ions. Due to the millisecond lifetimes of europium emission and our findings that anions do not directly coordinate to Eu^{3+} , these macrocycles show promise to be further developed as unique receptors that exploit the ratio in emission intensity at the two different wavelengths of excitation [Emission Intensity at $\lambda_{\text{ex}}=272$ (antennae) / Emission Intensity at $\lambda_{\text{ex}}=395$ (Eu^{3+})] for absolute concentration measurements. These findings are important scientific steps toward designing selective, specific, and time-resolved sensors for analysis of biological samples where the physiological NaCl concentration can interfere with the measurement of target anions.

Scheme 1. Synthesis of **Eu(2)-Eu(5)**.¹¹



(i) NH_2RNH_2 , MeOH/ H_2O (high dil); (ii) $\text{Eu}(\text{Cl})_3$, H_2O .

Experimental

General. All reagents used in the synthesis, if not specified, were obtained from either Aldrich Chemical Co. (Milwaukee, WI) or Acros Organics (Morris Plains, NJ) and were used without further purification. **Eu(2)-Eu(5)** were prepared as previously reported by our group, according

to Scheme 1.¹¹ The mass spectra were obtained from an IonSpec HiResESI mass spectrometer in positive ion mode. NMR spectra were collected on a Bruker AV-400 MHz spectrometer.

Titration experiments monitored via ¹H-NMR were conducted according to the method of Snellink-Rüel et al.^{8g} Ultraviolet absorption data was obtained using a Varian Cary 50 UV-visible spectrophotometer. Luminescence studies were performed using a Varian Cary Eclipse Fluorescence Spectrophotometer. Dimethyl sulfoxide (DMSO) used in the absorption and luminescence experiments was spectrophotometric grade, and CH₃CN was distilled over CaH₂ before use.

General Procedure for Model Receptor Syntheses. α,α' -Bis(N'-*p*-tolylthioureylene)-*m*-

xylene (2). *p*-Tolyl isothiocyanate (0.983 g, 6.60 mmol) was dissolved in CH₂Cl₂ (7 mL) and *m*-xylylenediamine (0.449 g, 0.330 mmol) in CH₂Cl₂ (3 mL) was added dropwise over 5 minutes.

This mixture was stirred at RT for 14 hours, during which a white solid precipitate formed. The precipitate was filtered, washed with CH₂Cl₂ (3 x 3 mL), and dried *in vacuo* yielding a white solid. Yield: 1.22 g, 85.3%. ESI-MS: Calculated *m/z*: 435.168 [(2)H⁺]. Found *m/z*: 435.158.

UV-Vis (DMSO) $\lambda_{\text{max}}/\text{nm}$ ($\epsilon/\text{M}^{-1}\text{cm}^{-1}$): 272 (24700); (CH₃CN) $\lambda_{\text{max}}/\text{nm}$ ($\epsilon/\text{M}^{-1}\text{cm}^{-1}$): 260 (26900).

¹H-NMR (400 MHz, DMSO- *d*₆): δ 9.54 (s, 2H, *NHar*), 8.07 (s, 2H, *NHCH*₂*ar*), 7.29 – 7.12 (m, 12H, *Har*), 4.73 (s, 4H, *CH*₂), 2.26 (s, 6H, *CH*₃). ¹³C-NMR (100 MHz, DMSO-*d*₆): δ 181.3 (CS), 139.7, 136.9, 134.1, 129.6, 128.7, 126.8, 126.4, 124.3, 47.7, 21.0.

1,4-Bis(N'-*p*-tolylthioureylene)-butane (3). *p*-Tolyl isothiocyanate (0.527 g, 3.54 mmol) and 1,4-diaminobutane (0.155 g, 1.76 mmol) were reacted as described above for **2**. Compound **3**

was isolated as a white powder. Yield: 0.601 g, 88.5%. ESI-MS: Calculated *m/z*: 387.168

[(3)H⁺]. Found *m/z*: 387.169. ¹H-NMR (400 MHz, DMSO- *d*₆): δ 9.38 (s, 2H, *NHar*), 7.63 (s, 2H, *NHCH*₂), 7.23 (d, 4H, *Har*), 7.14 (d, 4H, *Har*), 3.47 (s, 4H, *CH*₂*NH*), 2.27 (s, 6H, *CH*₃), 1.54

(s, 4H, CH_2CH_2NH). ^{13}C -NMR (100 MHz, DMSO- d_6): δ 180.8 (CS), 136.9, 133.9, 129.6, 124.0, 44.1, 26.6, 20.9.

1,6-Bis(N'-*p*-tolylthioureylene)-hexane (4). *p*-Tolyl isothiocyanate (0.527 g, 3.54 mmol) and 1,6-diaminohexane (0.204 g, 1.76 mmol) were reacted as described above for **2**. Compound **4** was isolated as a white powder. Yield: 0.560 g, 76.8%. ESI-MS: Calculated m/z : 415.199 [(**4**)H $^+$]. Found m/z : 415.201. 1H -NMR (400 MHz, DMSO- d_6): δ 9.34 (s, 2H, *N*Har), 7.61 (s, 2H, *NHCH* $_2$), 7.25 (d, 4H, *Har*), 7.13 (d, 4H, *Har*), 3.44 (s, 4H, CH_2NH), 2.27 (s, 6H, CH_3), 1.53 (s, 4H, CH_2CH_2NH), 1.31 (s, 4H, $CH_2CH_2CH_2NH$). ^{13}C -NMR (100 MHz, DMSO- d_6): δ 180.8 (CS), 136.9, 133.8, 129.5, 123.9, 44.3, 29.0, 26.7, 20.9.

1,8-Bis(N'-*p*-tolylthioureylene)-octane (5). *p*-Tolyl isothiocyanate (0.523 g, 3.51 mmol) and 1,8-diaminooctane (0.250 g, 1.74 mmol) were reacted as described above for **2**. Compound **5** was isolated as a white powder. Yield: 0.605 g, 78.7%. ESI-MS: Calculated m/z : 443.230 [(**5**)H $^+$]. Found m/z : 443.228. 1H -NMR (400 MHz, DMSO- d_6): δ 9.33 (s, 2H, *N*Har), 7.59 (s, 2H, *NHCH* $_2$), 7.23 (d, 4H, *Har*), 7.13 (d, 4H, *Har*), 3.43 (s, 4H, CH_2NH), 2.27 (s, 6H, CH_3), 1.52 (s, 4H, CH_2CH_2NH) 1.29 (s, 8H, $CH_2CH_2CH_2NH$ and $CH_2CH_2CH_2CH_2NH$). ^{13}C -NMR (100 MHz, DMSO- d_6): δ 180.8 (CS), 137.1, 133.8, 129.5, 124.0, 44.3, 29.2, 29.0, 26.8, 20.9.

Luminescence Studies. Excitation and emission spectra of **Eu(2)-Eu(5)** (DMSO, 1.0×10^{-5} M) were obtained in phosphorescence mode with a total decay time of 0.01 s, a delay time of 0.10 ms, and a gate time of 5.0 ms. Excitation and emission slit widths were set at 5 and 10 nm, respectively. The excitation wavelengths (λ_{exc}) used in the emission studies were either 272 nm or 395 nm. The emission wavelength (λ_{em}) for the excitation studies was 614 nm. The anion titration studies were performed at the above instrument settings and each aliquot of anion

solution was made such that $10.0 \mu\text{L} = 1$ equivalent (eq) of anion, where “one equivalent” of anion means that the anion and receptor are present in equal molar amounts (1:1 molar ratio). The aliquots were added to a cuvette originally containing 3.00 mL of macrocycle solution in DMSO ($1.0 \times 10^{-5} \text{ M}$). Each data point was the average of three measurements, and the titrations were performed in duplicate (maximum error $< 5\%$). All anions were used as their tetrabutylammonium (TBA) salts. The stock solution of TBAOH was prepared using a 40% (w/w) TBAOH solution in water. The luminescence lifetime titrations of **Eu(2)**-**Eu(5)** were performed in DMSO ($1.0 \times 10^{-5} \text{ M}$) with a delay time of 0.05 ms , a gate time of 0.2 ms , $\lambda_{\text{exc}} = 272 \text{ nm}$ or 395 nm , and $\lambda_{\text{em}} = 614 \text{ nm}$. Excitation and emission slit widths were 10 nm , and each data point was the average of five measurements.

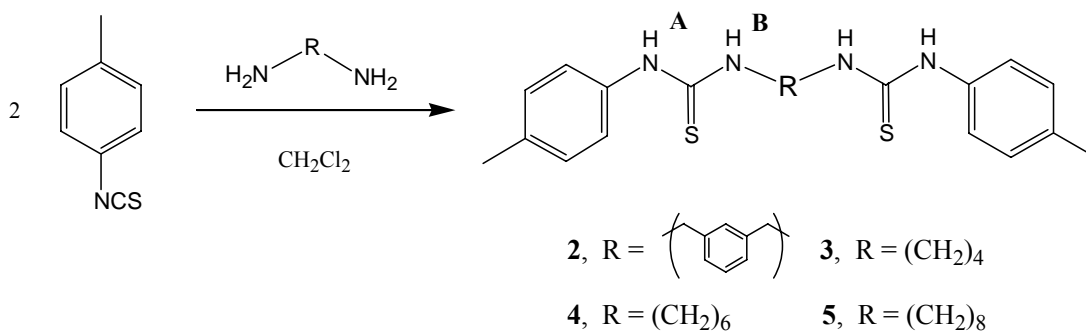
Binding Constant Determinations. Binding constants were calculated from the $^1\text{H-NMR}$ chemical shift data of the titration of **2-5** with TBAOAc ($\text{DMSO-}d_6$) using WinEQNMR software.¹² This software requires initial guesses for stability constants and chemical shifts of intermediate complexes and, through a series of non-linear least squares refinements, calculates the concentrations of all free and complexed species through a “best-fit” convergence method. Binding constants for complexation of **Eu(2)** and **Eu(5)** with either acetate or DHP in DMSO were determined from the luminescence data using the method of Fery-Forgues et al.¹³

Results and Discussion

Synthesis. In an effort to design anion-selective sensors, previously, we reported the synthesis of compound **1**, along with **Eu(2)**-**Eu(5)** (Scheme 1).¹¹ These receptors were originally developed to include *i*) a luminescent signal at the Eu^{3+} center, *ii*) functionalized benzene spacers to act as antennae to enhance the Eu^{3+} emission, *iii*) thiourea groups for anion binding, and *iv*) a

linker that connects the opposing thioureas and allows variation of the flexibility and size of the macrocycle cavity. This series of macrocycles was also developed to gain insight into how the size and flexibility of the macrocycle pocket, especially near the hydrogen bond-donating thiourea moieties, affects anion binding and selectivity. As shown in Scheme 1, the macrocycles can be readily synthesized by reaction of the *bis*-isothiocyanate precursor, **1**, with an alkyl or xylyl diamine in dilute aqueous methanol. This synthetic pathway is advantageous in that a variety of macrocycles can be generated from one precursor, allowing for tailoring of the macrocycle pocket by the selection of the diamine used in this cyclization step. It should be noted that a slightly modified method of isolation and purification of the final ligands was utilized, involving precipitation of the macrocyclic ligand out of aqueous solution using dilute HCl to remove bicarbonate impurities, prior to addition of EuCl₃. In the present study, we sought to examine how the various structural changes within the series **Eu(2)-Eu(5)** affect the recognition and signaling properties in the presence of various anions through absorbance, luminescence and ¹H-NMR experiments.

Scheme 2. Synthesis of compounds **2-5**, where the thiourea protons are denoted H_A and H_B.



To accompany the macrocycle-based studies, organic model compound, **2-5**, similar in structure to **Eu(2)-Eu(5)** but lacking the DTPA-lanthanide unit, were synthesized to examine the

role of the thiourea moiety in anion binding. Anion binding to these model compounds was monitored via absorbance and $^1\text{H-NMR}$ to support our hypothesis that the lanthanide in the macrocycle is not involved in anion binding. This study was important because the Eu^{3+} -functionalized macrocycles cannot be structurally examined via NMR due to their paramagnetic nature and poor solubility properties, and also crystallization has been unsuccessful. It is assumed that the acidity of the thiourea protons in the model compounds **2-5** and their macrocyclic analogs **Eu(2)-Eu(5)** should be similar. Compounds **2-5** were synthesized from *p*-tolyl isothiocyanate and the respective diamine in CH_2Cl_2 (Scheme 2), to model the binding pockets of **Eu(2)-Eu(5)**. During the course of each reaction, **2-5** precipitated as white solids and did not require further purification, prior to characterization via ESI-MS, ^1H and $^{13}\text{C-NMR}$. For compound **2**, resonances appeared at 8.07 and 9.54 ppm in the $^1\text{H-NMR}$ spectrum, as well as at 181.3 ppm in the $^{13}\text{C-NMR}$ spectrum, indicative of the thiourea protons and carbon atom, respectively. Similar resonances were observed in the spectra of **3-5**. In addition, the UV-VIS absorbance profile was obtained for **2** ($\lambda_{\text{max}} = 272 \text{ nm}$; $\epsilon = 24700 \text{ M}^{-1} \text{ cm}^{-1}$) and was quite similar to the spectrum previously reported for **Eu(2)** ($\lambda_{\text{max}} = 275 \text{ nm}$; $\epsilon = 23000 \text{ M}^{-1} \text{ cm}^{-1}$).¹¹ These model compounds allowed for anion titration experiments to be performed and monitored via $^1\text{H-NMR}$ ($\text{DMSO-}d_6$) and UV-VIS (CH_3CN), providing insight into the binding mechanism of fluoride and acetate with **Eu(2)-Eu(5)** (*vide infra*). It should be noted that a family of bis-thioureas, structurally related to our model compound **2**, have been previously reported for use as anion binders.¹⁴

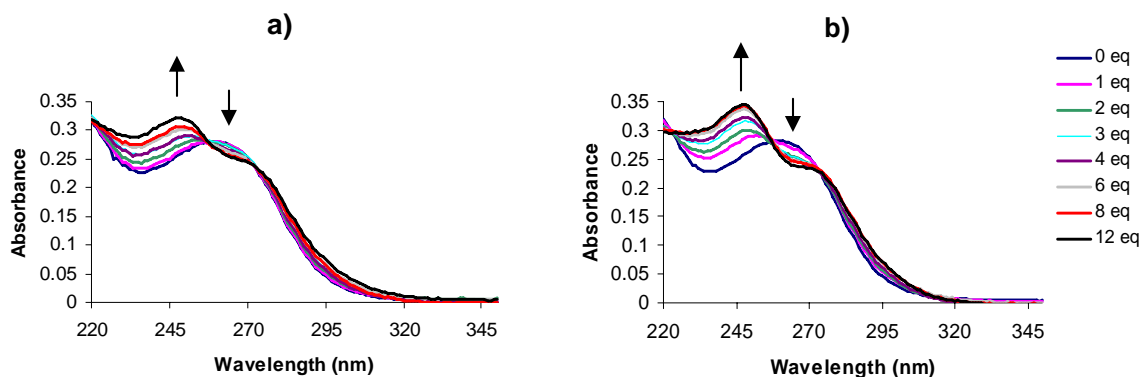


Figure 1. Absorbance titrations of the model compound **2** with (a) TBAF and (b) TBAOAc in CH_3CN (1.0×10^{-5} M).

Model Studies. UV-Vis absorbance was measured during titrations of **2** with either fluoride or acetate in both DMSO and CH_3CN (Figure 1). In DMSO, where there was a heavy solvent absorbance in the region of interest, the spectral changes were minimal (similar to those obtained for **Eu(2)**). However, in CH_3CN , where no interference from the solvent was present in the region of interest, a small decrease and red shift of the band at 260 nm was observed and was concurrent with the emergence and ensuing increase of a band at 248 nm (λ_{max}) over the course of fluoride or acetate addition (Figure 1). Isosbestic points were present at 258 nm and 272 nm. The changes observed in the absorbance spectra were consistent with hydrogen-bond donation and/or deprotonation of the thiourea upon anion addition, affecting the nature of the benzene chromophore.^{3f-g, 4}

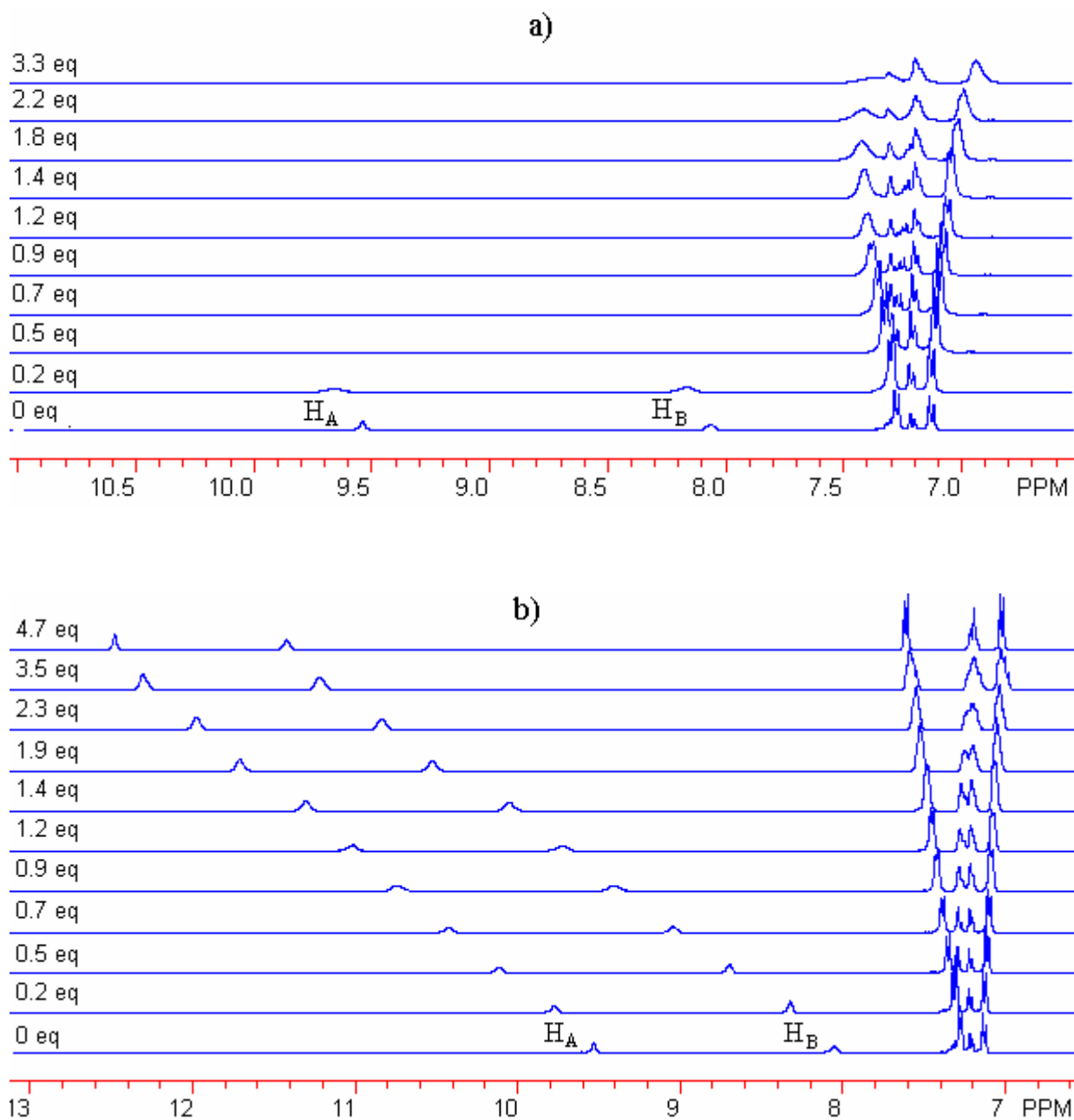


Figure 2. $^1\text{H-NMR}$ of **2** upon titration with (a) TBAF and (b) TBAOAc in $\text{DMSO-}d_6$ (2.8×10^{-2} M).

$^1\text{H-NMR}$ was used to more precisely study the interaction between the model compound thiourea protons and the anions by monitoring the change in chemical shift of the thiourea proton resonances of **2** during the titration experiments (Figure 2). Titration of **2** with fluoride in

DMSO- d_6 (2.8×10^{-2} M) resulted in a downfield shift and broadening of both thiourea resonances, followed by disappearance of the resonances entirely at 1.4 equivalents. At 2.2 equivalents of fluoride, a triplet appeared at 16.1 ppm, characteristic of $[\text{HF}_2]^-$, indicating that deprotonation of the thiourea had occurred. Studies employing thiourea-based systems report similar findings upon titration with fluoride.^{3d,4,8h} Titration of **2** with acetate yielded different results. The thiourea resonances were shifted downfield by 2.94 and 3.37 ppm (H_A and H_B , respectively) upon addition of up to 4.7 equivalents of acetate, and minimal broadening occurred, indicating the formation of a hydrogen bonded $[\mathbf{2} \cdot \text{OAc}]^-$ complex. As shown in Figure 3, the binding stoichiometry was determined using the Job's plot method to be 1:2 (receptor: anion).^{8g} However, the binding stoichiometry of the acyclic model **2** does not necessarily translate to **Eu(2)**, where there is a higher preorganization of the opposing thioureas. Job's plot analyses and anion titrations of **3-5** monitored using $^1\text{H-NMR}$ were also performed and yielded quite similar results to those obtained with **2** for both acetate and fluoride. WinEQNMR¹² was then used to determine the association constants of compounds **2-5** with acetate, displayed in Table 1. The strongest association for 1:1 complex formation was observed for the most rigid and preorganized receptor, **2**, containing the xylyl spacer. In 1:1 complexes formed with receptors **3-5**, association was weaker as the spacer length increased. The formation of 1:2 (receptor: anion) complexes with acetate exhibited the opposite trend, as K_{12} was largest with **5**, where the thioureas are separated by the octyl chain. Under the assumption that each acetate anion is bound to only one thiourea group in the 1:2 complexes, the trend observed for K_{12} can be attributed to charge repulsion. As the spacer length increases, binding of a second acetate anion is facilitated. Overall, these binding constants are weak compared to similar receptors that employ electron-withdrawn thioureas³ but are in the expected numerical range due to the relative

electron-rich nature of the aromatic rings directly bonded to the thiourea in compound **2-5**, which has a large effect on the -NH acidity.^{1h,4} Weaker binding from individual thiourea units due to lower -NH acidity may be advantageous in producing a reversible sensor molecule that does not irreversibly deprotonate. Strong binding may then be achieved through the preorganization of a number of anion-binding sites, as demonstrated in the enhanced binding affinities for acetate of macrocycles **Eu(2)** and **Eu(5)** (*vide infra*). The model studies with **2-5** suggest that deprotonation does not likely occur in the titration of macrocycles **Eu(2)-Eu(5)** with acetate, but could possibly occur in the case of fluoride. In either case, however, there is a favorable interaction between the thioureas and anion(s) that affects the chromophoric benzene antennae as revealed by the UV-Vis absorption studies.

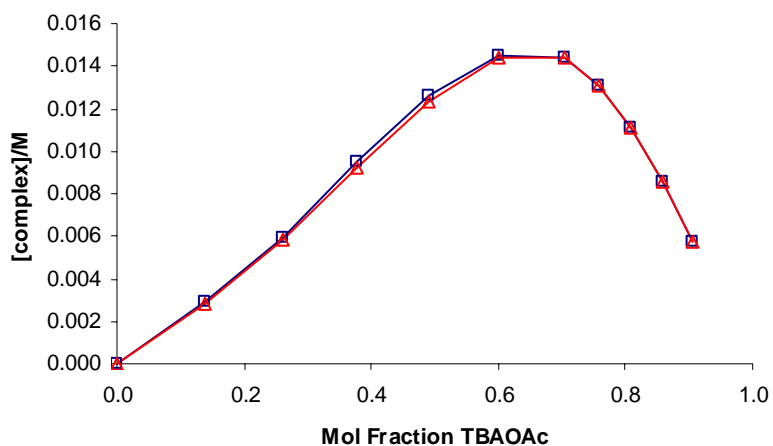


Figure 3. ^1H -NMR Job's plot of **2** with TBAOAc in $\text{DMSO-}d_6$ using $\Delta\delta$ of H_A (blue squares) and H_B (red triangles).^{8g}

Table 1. Association constants of compounds **2-5** (1.0×10^{-2} M, DMSO- d_6) with acetate anion.¹²

Compound	Log K_{11}	Log K_{12}
6	3.33 ± 0.02	1.81 ± 0.03
7	3.29 ± 0.04	1.97 ± 0.05
8	3.21 ± 0.02	2.15 ± 0.03
9	3.19 ± 0.03	2.17 ± 0.04

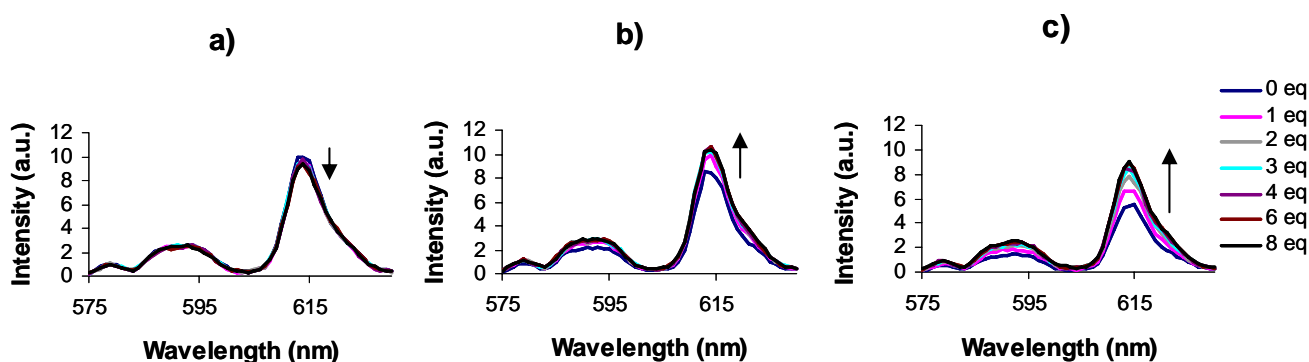


Figure 4. Titration of (a) **Eu(3)**, (b) **Eu(4)**, and (c) **Eu(5)** with TBAF in DMSO (1.0×10^{-5} M) as monitored via luminescence ($\lambda_{\text{exc}} = 272$ nm).

Anion Response of Eu^{3+} Macrocycles. All spectroscopic studies of **Eu(2)-Eu(5)** were carried out in DMSO due to a lack of solubility of these complexes in other organic solvents. The titration of **Eu(3)-Eu(5)** with increasing amounts of fluoride anion was monitored via Eu^{3+} luminescence at $\lambda_{\text{exc}} = 272$ nm (Figure 4). This wavelength was chosen for the most efficient sensitization of the Eu^{3+} luminescence through the antenna effect of the macrocyclic ligand (*vide infra*). In these experiments, the “anion equivalent” denotes the molar ratio of anion titrated into a fixed molar amount of dissolved macrocycle. Thus, “one equivalent of anion” means that the

anion and receptor are present in equal molar amounts (1:1 molar ratio). It was observed that **Eu(3)** exhibits a slight *decrease* in the intensity of the emission at 614 nm ($^5D_0 \rightarrow ^7F_2$) by up to 9% as F^- is added, whereas **Eu(4)** and **Eu(5)** show a maximum *increase* in emission intensity of about 24% and 65%, respectively. The other emission bands ($^5D_0 \rightarrow ^7F_0$, $^5D_0 \rightarrow ^7F_1$, and $^5D_0 \rightarrow ^7F_4$) are affected similarly by the addition of fluoride (the changes in luminescence are not f-f transition specific). These effects are observed over the course of fluoride addition up to 8 equivalents (where the maximum change occurs) and appear to be dependent on the change in pocket size of the macrocycle upon anion binding. A relatively small pocket, for example in **Eu(3)**, leads to a decrease in luminescence intensity upon interaction with fluoride, because the receptor pocket may increase in size, thus increasing the antenna-Eu³⁺ distance and decreasing the antenna effect. A larger pocket (i.e. **Eu(5)**) yields a significant increase in intensity because the cavity size is significantly decreased upon anion binding, thus increasing the antenna effect. The anion titration experiments of **Eu(3)-Eu(5)** were also monitored at an excitation wavelength of 395 nm, where Eu³⁺ is excited directly (the ligand does not absorb). Interestingly, there is no change in luminescence intensity (outside of what would be expected for dilution) over the course of the titration for **Eu(3)-Eu(5)** when the Eu³⁺ ion is directly excited ($\lambda_{exc} = 395$ nm), indicating that the lanthanide does not participate in anion binding. Luminescence lifetime studies to support this observation have been performed (*vide infra*). In general, these data suggest that a change in conformation of the macrocycle upon anion binding alters the distance between Eu³⁺ and the antennae. Based on the model experiments with **3-5**, we predict anion binding to the thiourea groups in the pocket of the macrocycles **Eu(3)-Eu(5)**. Alternatively, anion binding and/or deprotonation of the thiourea (the -NH directly adjacent to the benzene

moiety is expected to be most acidic)⁴ results in a more electron-rich antennae, which could also alter the efficiency of energy transfer to the Eu³⁺ center.

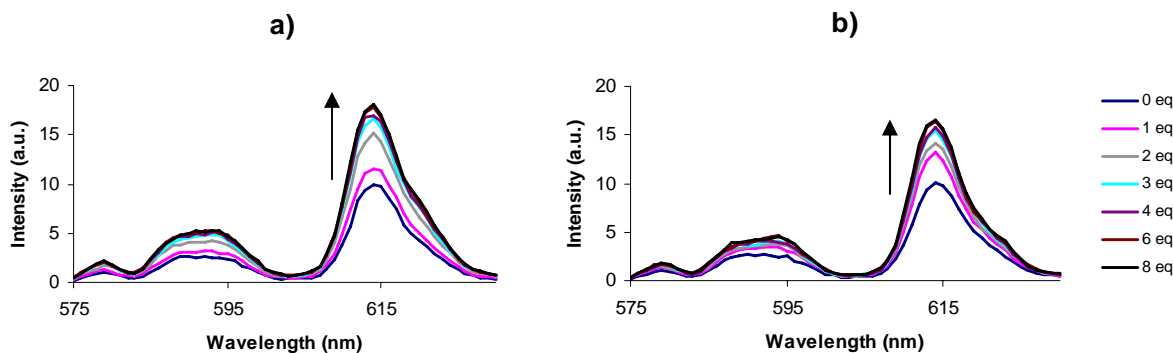


Figure 5. Titration of **Eu(2)** with (a) TBAF and (b) TBAOAc in DMSO as monitored via luminescence (1.0×10^{-5} M, $\lambda_{\text{exc}} = 272$ nm).

Titration of **Eu(2)** with fluoride (TBAF) and acetate (TBAOAc) exhibited similar luminescence responses (Figure 5). The emission (272 nm excitation) of **Eu(2)** at 614 nm was greatly increased with fluoride and acetate (77% and 72%, respectively, with 8 equivalents). This result was higher than expected for the cavity size (the thioureas are linked by a 5-carbon spacer), as **Eu(5)** (8-carbon spacer) revealed a lower intensity increase with the titration of fluoride. Similar to **Eu(3)**-**Eu(5)**, a change in emission intensity was not observed for **Eu(2)** when Eu³⁺ was directly excited at a wavelength of 395 nm during these titrations.

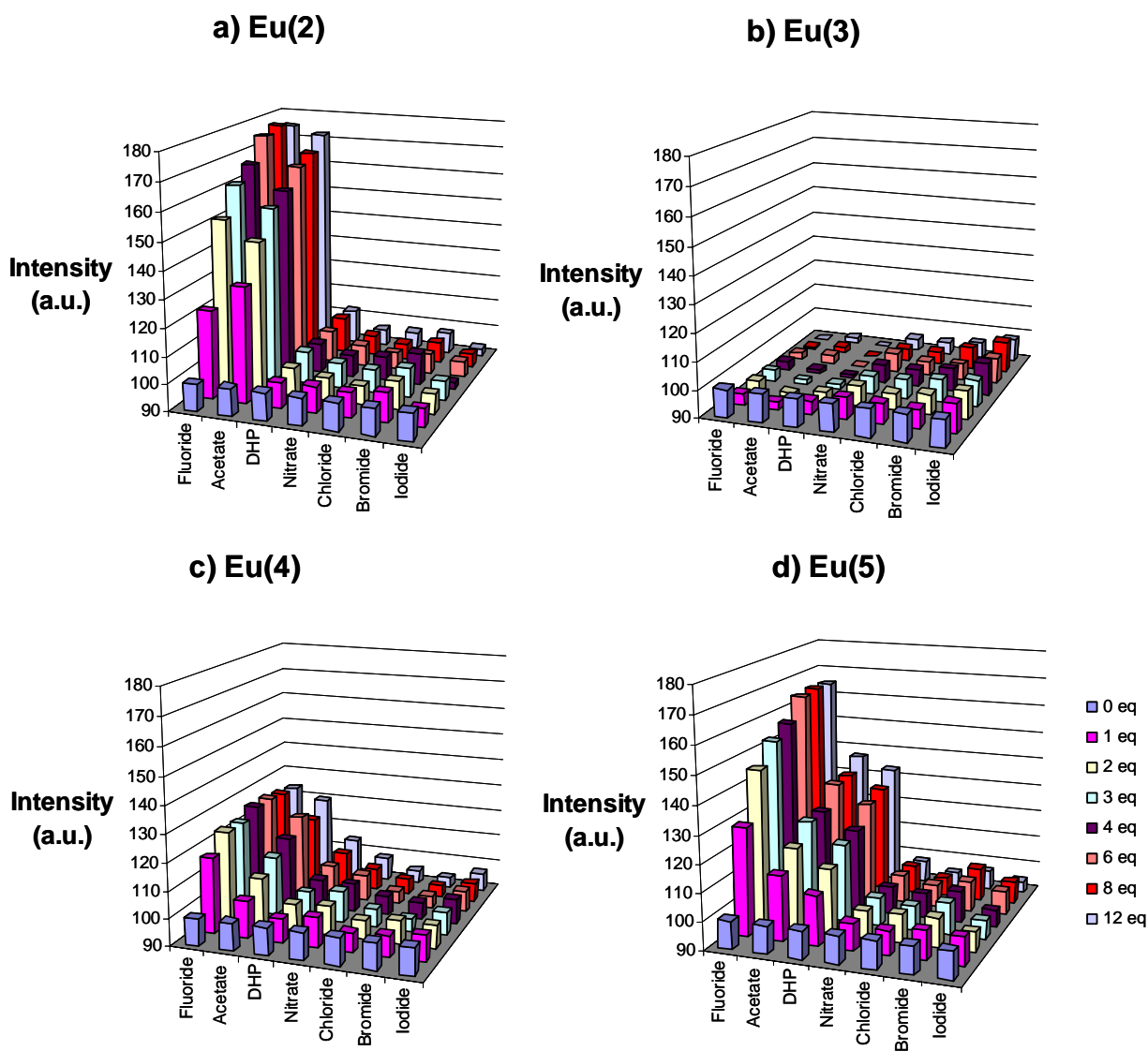


Figure 6. Effect of various anions on the luminescence emission intensity at 614 nm in DMSO of (a) **Eu(2)**, (b) **Eu(3)**, (c) **Eu(4)** and (d) **Eu(5)** ($\lambda_{\text{exc}} = 272$ nm).

The large emission enhancement in the presence of fluoride observed for **Eu(2)** and **Eu(5)** prompted further titration studies with an expanded series of anions to determine the potential selectivity of this macrocycle family. As shown in Figure 6, with all of the macrocycles, significant augmentation of emission occurred in the presence of fluoride and acetate. It should be pointed out that each bar in Figure 6 has an error of less than 5% between

separate experiments. The addition of fluoride elicited a similar increase in luminescence response in **Eu(2)** and **Eu(5)** (77% and 65%, respectively, at 8 equivalents), however, in the presence of acetate the luminescence response was significantly different when comparing **Eu(2)** and **Eu(5)** (increased by 72% and 37%, respectively, at 8 equivalents). The response to dihydrogen phosphate (DHP) also varied between **Eu(2)** and **Eu(5)**, but unlike the observed responses to acetate, a weaker response to DHP was observed upon titration of **Eu(2)** as compared to the higher response of **Eu(5)** (increased by 3% and 33%, respectively, at 8 equivalents). This may indicate that the luminescent signaling in these macrocycles is being affected via different mechanisms depending on the anion, the macrocycle, or both. All remaining anions (nitrate, chloride, bromide, and iodide) did not show a significant effect on the luminescence intensity of the macrocycle solutions. Such a trend in selectivity is common with molecules employing urea or thiourea groups as anion-binding sites, and the effect is associated with the hydrogen bond-accepting abilities and basicities of the anions studied.³⁻⁴ Here, we reveal that sensitized lanthanide luminescence can be exploited as a facile method of anion recognition and sensing.

Examination of the luminescent responses of macrocycles **Eu(3)**-**Eu(5)** to fluoride, acetate and DHP indicates a selectivity trend based on the pocket size of the macrocycle (Figure 6). Macrocycle **Eu(3)**, with the shortest spacer between the two thiourea groups, showed a *decrease* in luminescence intensity of increasing magnitude as the anions increased in size (fluoride < acetate < DHP), as shown in Figure 6b. These results are consistent with our hypothesis that larger anions are able to open the cavity by pushing the antennae farther away from Eu^{3+} in macrocycle **Eu(3)**, which is responsible for the decrease in emission intensity. Similarly, both **Eu(4)** and **Eu(5)** (Figure 6c and 6d, respectively) exhibited an *increase* in

luminescence intensity of decreasing magnitude as the anions increased in size. These results are consistent with our hypothesis that smaller anions are able to pull the antennae closer to Eu^{3+} , yielding an increase in emission intensity. The luminescence intensity of macrocycle **Eu(2)** was observed to increase upon anion addition according to the same general trend observed with macrocycles **Eu(4)** and **Eu(5)** (fluoride > acetate > DHP). However, it was observed that the anion-induced luminescence enhancement of **Eu(2)** was in better agreement with the relative basicities of the anions than to their size, evident in the strong luminescence response to fluoride and acetate but only slight response to DHP. The anion responses of **Eu(2)**-**Eu(5)** were also evaluated according to their I_{272}/I_{395} ratio, and a similar trend was observed. However, due to the large amount of noise in the relatively weak 614 nm emission when $\lambda_{\text{exc}} = 395$ nm, the error was substantially increased. Figure 7 illustrates two proposed mechanisms for the luminescence augmentation observed upon anion interaction for **Eu(2)**, **Eu(4)** and **Eu(5)**: (1) interaction/binding between the anion(s) and the macrocyclic pocket induces a conformation change that shortens the Eu^{3+} -antennae distance, or (2) hydrogen bond donation or deprotonation of the thiourea group results in a change in the electronic structure of the antennae.

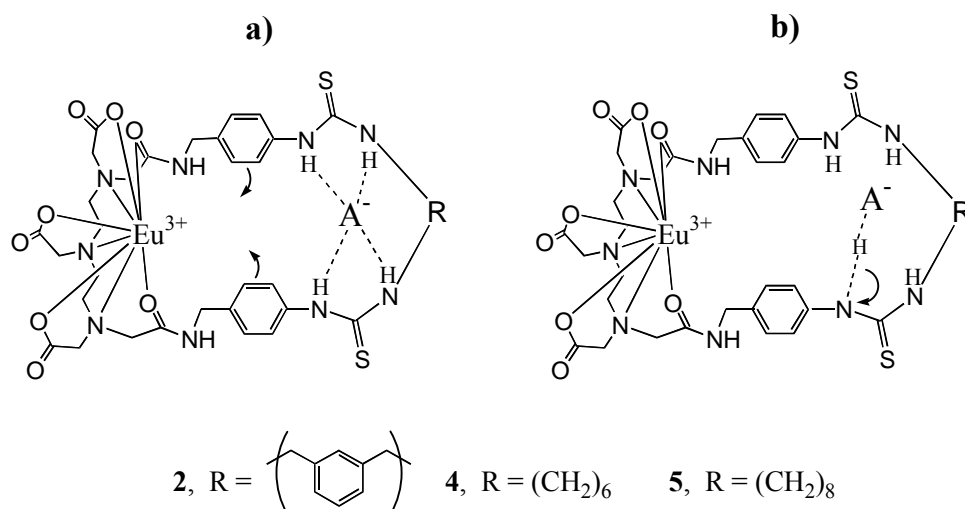


Figure 7. Proposed mechanisms for the luminescence enhancement in **Eu(2)**, **Eu(4)**, and **Eu(5)** upon addition of anion (A^-): (a) anion binding shortens the antennae- Eu^{3+} distance, and (b) deprotonation of the thiourea results in a more electron rich antenna.

Association constants were determined for macrocycle-anion complexes for which both the luminescence enhancement was large (>30%) and a linear dependence of the luminescence enhancement on the concentration was observed, indicating 1:1 (macrocycle: anion) complex formation. Binding constants ($\log K$) for **Eu(2)** and **Eu(5)** with acetate were 4.8 ± 0.1 and 4.5 ± 0.1 , respectively, and **Eu(5)** with DHP was determined to be 4.4 ± 0.1 by the method of Fery-Forgues et al.¹³ The more rigid and preorganized binding pocket of **Eu(2)** gave rise to the stronger binding of acetate as compared to **Eu(5)**. Overall, **Eu(2)** and **Eu(5)** bind the above anions relatively strongly in DMSO, as compared to other neutral receptors⁵⁻⁶ and have *association constants greater than an order of magnitude stronger* than those of the acyclic models **2** and **5**. This augmented binding affinity is attributed to the macrocyclic effect in this preorganized system. The 1:1 complex formation was confirmed using the Job's plot method for **Eu(5)** and acetate. Binding constants for fluoride could not be determined due to the nonlinearity

of the curve obtained when plotting luminescence enhancement versus concentration. The analysis of the fluoride data indicated multiple processes (i.e. deprotonation) occurring during the titration.

To gain further insight into the luminescent response of **Eu(2)**-**Eu(5)** to fluoride and acetate in DMSO, UV-Vis absorbance was measured during the titration, and a significant change in the absorption band at $\lambda_{\text{max}} = 272$ nm was not observed. Thiourea-containing systems have been shown to have dramatic changes in absorption upon anion binding and/or anion-induced deprotonation when the thiourea is appended to aromatic systems.³⁻⁴ Unfortunately, as in the case of the model compounds **2-5**, the heavy solvent absorbance of DMSO below 260 nm interfered with absorbance changes in that region.

Selectivity and Reversibility. The selectivity of **Eu(2)** for fluoride and acetate in the presence of chloride ion (up to 120 equivalents, where $[\text{Cl}^-] = 1.2 \times 10^{-3}$ M) was examined, and the luminescence response was affected only slightly (Figure 8). This feature is extremely valuable for monitoring anion concentrations in environmental and biological samples where chloride is a common interference. Receptors **Eu(3)** and **Eu(5)** exhibited enhanced responses to 8 equivalents of fluoride in the presence of 120 equivalents of chloride, whereas the response of **Eu(4)** was slightly hindered under the same conditions. The acetate titration of macrocycles **Eu(3)**-**Eu(5)** was also unaffected in a similar manner in the presence of 120 equivalents of chloride. Thus, macrocycles **Eu(2)**-**Eu(5)** demonstrated a selectivity for either fluoride or acetate in the presence of a large excess of chloride, where **Eu(2)** was found to be the most selective, particularly for fluoride anions. The large difference in basicities between either fluoride or acetate and chloride is likely the cause of the observed selectivity.³⁻⁵

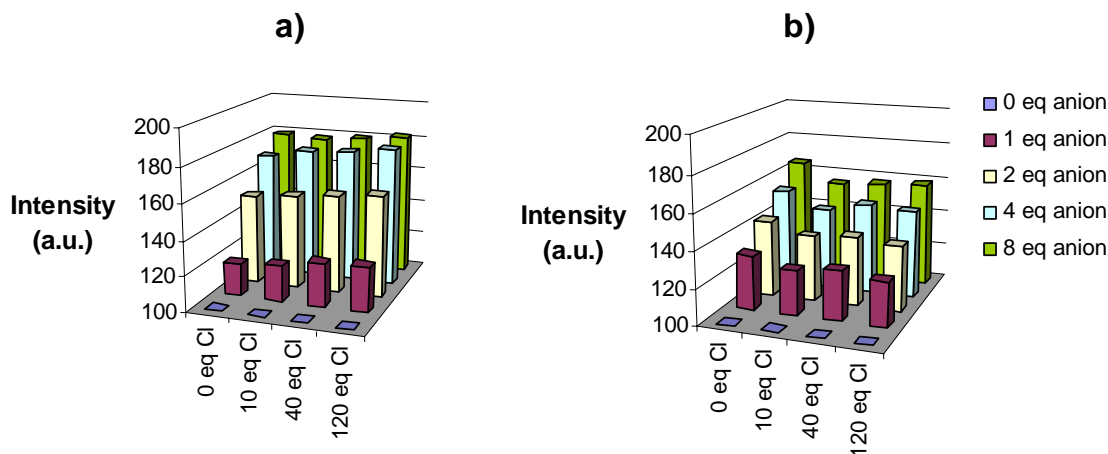


Figure 8. Titration of a 1.0×10^{-5} M solution of **Eu(2)** in DMSO with (a) TBAF and (b) TBAOAc as monitored via luminescence in the presence of increasing amounts of TBACl ($\lambda_{\text{exc}} = 272$ nm, $\lambda_{\text{em}} = 614$ nm, error < 5%).

The effects of fluoride, acetate, and DHP on **Eu(2)**-**Eu(5)** were also found to be reversible upon addition of NH_4Cl , where NH_4^+ functions as a stronger anion binder and pulls the anion out of the macrocycle. Reversibility is highly important in designing molecules for sensing applications, because it would be desirable for the receptor to be recycled, reused, or utilized in a continuous manner. Furthermore, consistent with all of the previous results, when the Eu^{3+} was directly excited at 395 nm, a change in luminescence intensity was not observed ($\lambda_{\text{em}} = 614$ nm) during the titration experiments with the anions previously examined. This behavior is consistent with an interaction between the anion (fluoride, acetate, DHP) and the thiourea moiety, resulting in an augmentation of the antenna effect through a change in conformation and/or electronics of the macrocycle pocket. If the change in luminescence observed at $\lambda_{\text{exc}} = 272$ nm was brought on by interaction of the anion directly with the lanthanide, it is expected that a similar effect would be observed at $\lambda_{\text{exc}} = 395$ nm. An increase in

luminescence is typically observed when water molecules directly bound to the Eu^{3+} ion are displaced by anions coordinating to the metal, and such an increase would be observed at all excitation wavelengths producing a Eu^{3+} emission.^{7c} This effect does not appear to be the cause of the luminescence augmentation in the macromolecules presented here, where water is present in small quantities in the DMSO solvent.

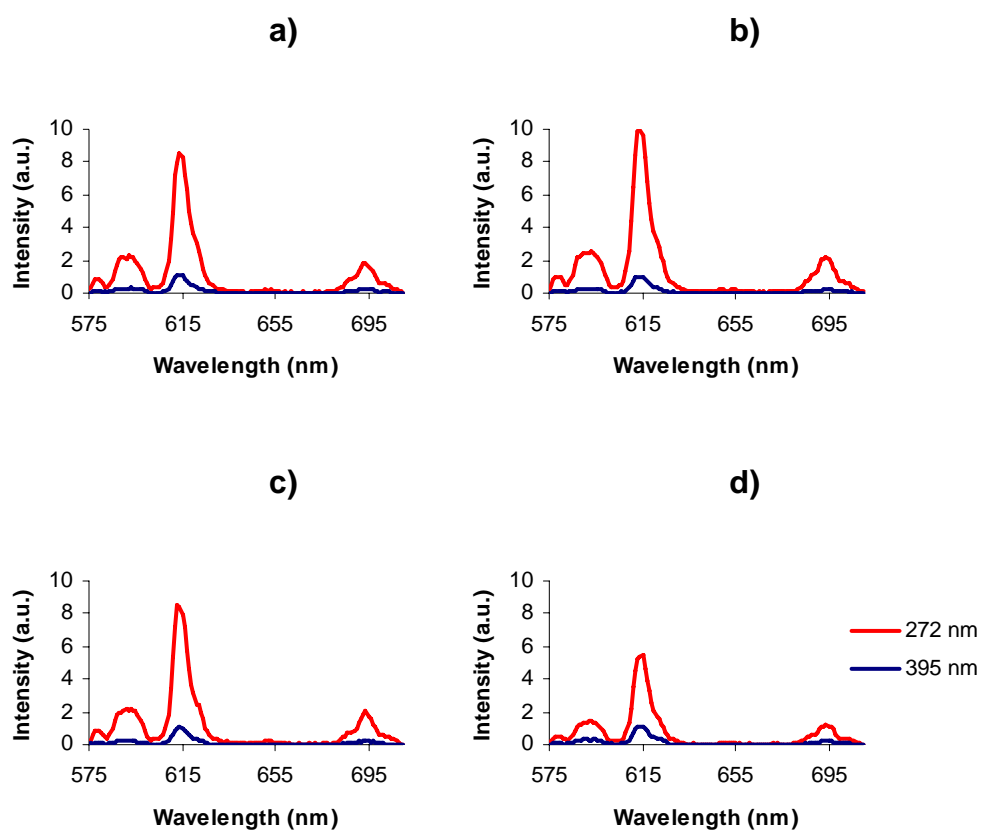


Figure 9. Emission spectra of (a) **Eu(2)**, (b) **Eu(3)**, (c) **Eu(4)**, and (d) **Eu(5)** in DMSO (1.0×10^{-5} M) at excitation wavelengths of 272 and 395 nm.

Table 2. Summary of the emission intensity data at 614 nm for **Eu(2)-Eu(5)**, where “I” is the emission peak intensity at the indicated wavelength, “ I_{272}/I_{395} ” denotes the luminescence enhancement due to the antenna, “# of C” denotes the number of carbons that link the thiourea moieties (length of R in Scheme 1), and “type of linker” describes whether an aryl or alkyl R group is present.

Compound	I_{272}	I_{272}/I_{395}	# of C	Type of linker
Eu(2)	8.55	7.44	5	aryl
Eu(3)	10.00	9.75	4	alkyl
Eu(4)	8.44	7.73	6	alkyl
Eu(5)	5.39	4.66	8	alkyl

Luminescence Emission and Lifetime Studies. Emission spectra were obtained at two different excitation wavelengths, 272 nm and 395 nm, to characterize the luminescence enhancement due to the antennae (I_{272}/I_{395} , Table 2) in the absence of anions. As shown in Figure 9, the Eu^{3+} ion is directly excited at 395 nm, however, the absorption maximum of the macrocycles was at 272 nm and is attributed primarily to the $\pi \rightarrow \pi^*$ transition of the thiourea-functionalized benzene moiety.¹¹ Thus, as shown in Figure 9, the antenna effect is evident, as emission from all macrocycles is enhanced via excitation at 272 nm (ligand absorption).¹¹ It was noticed that the emission intensity and enhancement increased according to a decrease in the macrocycle size, and these data correlated well to the length of the linker between the thioureas (Table 2). As shown in Scheme 1, **Eu(3)-Eu(5)** differ only in the number of carbons in the alkyl chain that links the two thiourea groups, thus the cavity size and degree of flexibility increases with the linker length. However, **Eu(2)** is more rigid due to the *m*-xylyl linker, and the degree of

luminescence enhancement (I_{272}/I_{395}) from the antenna effect is similar to that of the hexyl-linked **Eu(4)** (the spacer length is similar). As discussed previously, there did not appear to be a significant antenna effect from the *m*-xylyl group present in **Eu(2)**, which is likely due to the distance of this linker from the lanthanide ion.¹¹ In general, it was found that emission intensity increased as the linker length decreased throughout the series **Eu(2)**-**Eu(5)**. This result is expected because the degree of energy transfer from the antenna to Eu^{3+} is dependent on the through-space distance between the aromatic antenna and the lanthanide ion.⁹ A shorter linker may hold the antennae in a closer proximity to the Eu^{3+} center, which would subsequently increase luminescence enhancement through the antenna. Thus, the variation in pocket size (and Eu^{3+} to antennae distance) is shown to affect the Eu^{3+} emission intensity. Based on these observations, changes in conformation induced by an anion binding interaction that effect the pocket are expected to alter the emission intensity, as observed in the anion titrations of **Eu(2)**-**Eu(5)** with fluoride, acetate or DHP.¹⁵

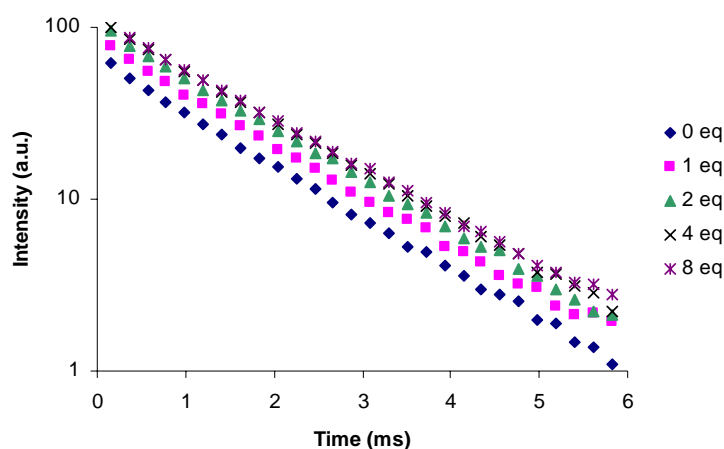


Figure 10. Titration of **Eu(2)** with TBAF in DMSO (1.0×10^{-5} M, $\lambda_{\text{exc}} = 272$ nm, $\lambda_{\text{em}} = 614$) as monitored via luminescence lifetime.

Table 3. Luminescence lifetime data (τ /ms) over the course of the titration of **Eu(2)** with TBAF and TBAOAc in DMSO at $\lambda_{\text{exc}} = 272$ or 395

# eq. TBAX	$\tau_{272 \text{ F}^-}$	$\tau_{395 \text{ F}^-}$	$\tau_{272 \text{ OAc}^-}$	$\tau_{395 \text{ OAc}^-}$
0	1.36 ± 0.02	1.46 ± 0.03	1.30 ± 0.01	1.46 ± 0.02
1	1.41 ± 0.02	1.45 ± 0.03	1.32 ± 0.01	1.37 ± 0.02
2	1.44 ± 0.02	1.46 ± 0.03	1.34 ± 0.01	1.41 ± 0.02
4	1.48 ± 0.02	1.50 ± 0.03	1.34 ± 0.01	1.36 ± 0.02
8	1.49 ± 0.02	1.57 ± 0.04	1.34 ± 0.01	1.38 ± 0.02

The luminescence lifetime of **Eu(2)** was measured upon titration with fluoride ($\lambda_{\text{exc}} = 272$ and 395) to determine whether the increase in luminescence was due to a longer luminescence lifetime (τ), where a luminescence quencher (such as a water molecule or hydroxide) would be removed upon anion binding (Figure 10 and Table 3). Although the luminescence lifetime did slightly increase (8-10%) with addition of fluoride to **Eu(2)**, this small change does not account for the large increase in luminescence intensity observed over the course of the titration, evident in the rise in emission intensity at ~ 0 ms. Additionally, a significant change in the luminescence lifetime of **Eu(2)** was not observed throughout addition of acetate when $\lambda_{\text{exc}} = 272$ nm (Table 3). The luminescence lifetime titration data is consistent with our two proposed mechanisms for the luminescence increase observed with **Eu(2)** and **Eu(5)** as illustrated in Figure 7 in that neither of these events is expected to change τ , which is primarily dependent on the presence of nonradiative pathways for deactivation of the Eu^{3+} excited state.

Hydroxide Studies. The response of **Eu(2)-Eu(5)** to hydroxide was studied using luminescence titration experiments (Figure 11). Hydroxide was chosen to gain insights into whether fluoride was directly coordinating to Eu^{3+} . It was assumed that hydroxide behaves similarly to fluoride because of its small size; however it is a stronger base and deprotonation of the thiourea hydrogens is more likely. An augmentation of emission intensity ($\lambda_{\text{exc}} = 272 \text{ nm}$) was observed exceeding the intensity enhancements observed during the fluoride titrations, and the emission intensity continued to increase until greater than 12 equivalents of hydroxide was added. Despite an initial decrease in the emission intensity of **Eu(3)** (comparable to that observed with fluoride, acetate and DHP), an increase in emission intensity was observed after addition of 6 equivalents of hydroxide. Such behavior indicates that hydroxide affects the luminescence intensity of **Eu(3)** by a different mechanism than the other anions studied, especially after several equivalents. As observed in the response of **Eu(2)-Eu(5)** to all other anions studied, there was no change in the luminescence intensity after direct Eu^{3+} excitation ($\lambda_{\text{exc}} = 395 \text{ nm}$). Furthermore, the luminescence lifetime of the 614 nm emission of **Eu(2)** was measured over the course of the hydroxide titration, and a significant change was not observed. If hydroxide coordinated directly to Eu^{3+} , a detectable decrease in the luminescence lifetime would be expected due to the quenching ability of the O-H bond.^{7c} It does not appear that hydroxide interacts with Eu^{3+} directly, and the large luminescence enhancement is most likely induced by deprotonation of the thiourea in **Eu(2)-Eu(5)**.

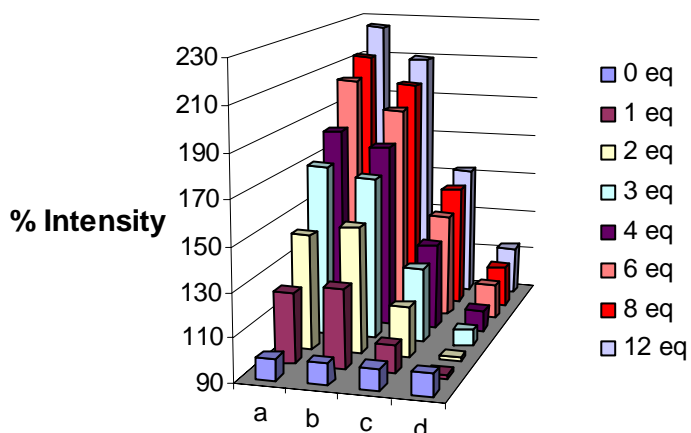


Figure 11. Percentage change (0 eq \equiv 100%) in luminescence intensity upon titration of (a) **Eu(5)**, (b) **Eu(2)**, (c) **Eu(4)** and (d) **Eu(3)**, with TBAOH in DMSO (1.0×10^{-5} M, $\lambda_{\text{exc}} = 272$ nm, $\lambda_{\text{em}} = 614$ nm).

Conclusion. Despite the similarities in structure among all the macrocycles studied, **Eu(2)-Eu(5)** exhibit very different behavior in response to strong hydrogen bond accepting anions (F^- , CH_3COO^- , H_2PO_4^-) when measuring the luminescence at 614 nm after excitation at 272 nm. At this excitation wavelength the antenna absorbs light and transfers energy to Eu^{3+} , resulting in the observed luminescence of the macrocycles. A change in luminescence is *not* observed in the presence of anions when Eu^{3+} is excited directly at 395 nm, and thus the luminescent signaling is dependent on anion binding to the ligand pocket (antenna). The macrocyclic ligands differ only in the alkyl or aryl spacer between the opposing thiourea groups, and these spacers appear to control the anion response, possibly based on pocket size and changes in conformation that allow the movement of the benzene-based antennae upon interaction with some anions. The strong response of **Eu(2)** to fluoride and acetate was not affected by a large excess of chloride anions, making this system promising for further anion

sensing applications in biological systems. **Eu(3)-Eu(5)** also demonstrated a selectivity for either fluoride or acetate in the presence of excess chloride ions, but the luminescent response was only slightly affected.

The collective results presented herein suggest that the anions do not interact with Eu^{3+} directly because similar anion responses would be expected from **Eu(2)-Eu(5)** due to their practically identical DTPA-based chelates as the lanthanide-binding domain within the macrocycle. In addition, although it is well known that O-H oscillators in the first or second coordination sphere (esp. Eu^{3+} and Tb^{3+}) alter the lifetimes of Ln^{3+} emission due to non-radiative energy decay,^{7,9} no significant changes in luminescence lifetime occurred upon titration of the macrocycle solutions with fluoride, acetate or hydroxide. Finally, although only slight changes occurred in the absorbance of **Eu(2)-Eu(5)** upon titration with fluoride or acetate in DMSO (due to possible interference in the absorption of DMSO), a clear shift in the absorbance band was observed with the structurally similar model compound **2** in CH_3CN . Titrations of **2-5** monitored via $^1\text{H-NMR}$ also showed definitive evidence for interaction between the thiourea protons and either fluoride (hydrogen bonding followed by deprotonation) or acetate (hydrogen bonding). This evidence supports our hypothesis that a change in conformation, possibly coupled with a change in the electronic structure of the antennae, is responsible for the changes in the luminescence of **Eu(2)-Eu(5)** upon selective anion interaction. The large binding constants ($>10^4$) determined for acetate and DHP for **Eu(2)** and **Eu(5)** validate the design of the preorganized macrocyclic system in this work. However, the exact bound structure is unknown at this point due to the complexity and extreme difficulties in crystallizing these systems. The diamagnetic La^{3+} analogue to **Eu(2)** was also prepared to examine the anion interactions using $^1\text{H-NMR}$, but the extremely low solubility in DMSO and the presence of water dramatically

reduced the accuracy of the experiment. In addition, the Tb^{3+} analogue to **Eu(2)** was also synthesized and exhibited a similar increase in luminescence upon titration with fluoride. Further experiments are underway to study the mechanism of the luminescent response to anions in these systems.

This unique series of macrocycles, **Eu(2)-Eu(5)**, exhibits differing responses to strong hydrogen bond-accepting anions, especially fluoride and acetate. This is one of the first examples, to our knowledge, of a lanthanide-based system that yields a luminescent response upon anion interaction that does not require the direct coordination of anions to the lanthanide.^{8j,10} Furthermore, because the luminescent signaling occurs only upon excitation through the antenna ($\lambda_{\text{exc}} = 272 \text{ nm}$), and no change is observed at $\lambda_{\text{exc}} = 395 \text{ nm}$, the signal intensity of the latter can function as an internal standard for determining the concentration of the macrocycle, for example, in biological samples. This trait, combined with the selectivities of these macrocycles in the presence of chloride and the time-resolved fluorescence capabilities of the lanthanide metals, gives these systems great potential for further tailoring to be applied in biological studies that contain high background luminescence, such as the cellular environment.

REFERENCES.

- (1) (a) Bianchi, A.; Bowman-James, K.; García-España, E., Eds. *Supramolecular Chemistry of Anions*, Wiley-VCH: New York, 1997. (b) Martínez-Mañez, R.; Sancenón, F. *Chem. Rev.* **2003**, *103*, 4419-4476. (c) Martínez-Mañez, R.; Sancenón, F. *J. Fluoresc.* **2005**, *15*, 267-285. (d) Bondy, C.R.; Loeb, S.J. *Coord. Chem. Rev.* **2003**, *240*, 77-99. (e) Llinares, J.M.; Powell, D.; Bowman-James, K. *Coord. Chem. Rev.* **2003**, *240*, 57-75. (f) Beer, P.D.; Gale, P.A. *Angew. Chem. Int. Ed.* **2001**, *40*, 486-516. (g) Gale, P.A. *Coord. Chem. Rev.* **2003**, *240*, 191-221. (h) Gunnlaugsson, T.; Glynn, M.; Tocci, G.M.; Kruger, P.E.; Pfeffer, F.M. *Coord. Chem. Rev.* **2006**, *250*, 3094-3117.
- (2) Collins, T.F.; Sprando, R.L. In *Reviews in Food and Nutrition Toxicity*; Preedy, V.R., Watson, R.R., Eds.; CRC Press: Baton Rouge, LA, 2005; Vol. 4, pp 105-141.
- (3) (a) Lee, J.Y.; Cho, E.J.; Mukamel, S.; Nam, K.C. *J. Org. Chem.* **2004**, *69*, 943-950. (b) Kim, S.K.; Yoon, J. *Chem. Commun.* **2002**, 770-771. (c) Gunnlaugsson, T.; Davis, A.P.; Hussey, G.M.; Tierney, J.; Glynn, M. *Org. Biomol. Chem.* **2004**, *2*, 1856-1863. (d) Thiagarajan, V.; Ramamurthy, P.; Thirumalai, D.; Ramakrishnan, V.T. *Org. Lett.* **2005**, *7*, 657-660. (e) Kim, S.K.; Bok, J.H.; Bartsch, R.A.; Lee, J.Y.; Kim, J.S. *Org. Lett.* **2005**, *7*, 4839-4842. (f) Cho, E.J.; Moon, J.W.; Ko, S.W.; Lee, J.Y.; Kim, S.K.; Yoon, J.; Nam, K.C. *J. Am. Chem. Soc.* **2003**, *125*, 12376-12377. (g) Cho, E.J.; Ryu, B.J.; Lee, Y.J.; Nam, K.C. *Org. Lett.* **2005**, *7*, 2607-2609. (h) Jose, D.A.; Kumar, D.K.; Ganguly, B.; Das, A. *Org. Lett.* **2004**, *6*, 3445-3448.
- (4) (a) Esteban-Gómez, D.; Fabbriizzi, L.; Licchelli, M.; Monzani, E. *Org. Biomol. Chem.* **2005**, *3*, 1495-1500. (b) Esteban-Gómez, D.; Fabbriizzi, L.; Licchelli, M. *J. Org. Chem.*

- 2005**, *70*, 5717-5720. (c) Boiocchi, M.; Del Boca, L.; Esteban-Gómez, D.; Fabbrizzi, L.; Licchelli, M.; Monzani, E. *Chem. Eur. J.* **2005**, *11*, 3097-3104. (d) Amendola, V.; Esteban-Gómez, D.; Fabbrizzi, L.; Licchelli, M. *Acc. Chem. Res.* **2006**, *39*, 343-353. (e) Evans, L.S.; Gale, P.A.; Light, M.E.; Quesada, R. *Chem. Commun.* **2006**, 965-967.
- (5) (a) Gunnlaugsson, T.; Kruger, P.E.; Jensen, P.; Tierney, J.; Ali, H.D.P.; Hussey, G.M. *J. Org. Chem.* **2005**, *70*, 10875-10878. (b) Kato, R.; Nishizawa, S.; Hayashita, T.; Teramae, N. *Tetrahedron Lett.* **2001**, 5053-5056. (c) Nishiyabu, R.; Anzenbacher, P., Jr. *Org. Lett.* **2006**, *8*, 359-362. (d) Kubo, Y.; Ishihara, S.; Tsukahara, M.; Tokita, S. *J. Chem. Soc., Perkin Trans. 2*, **2002**, 1455-1460. (e) Costero, A. M.; Gaviña, P.; Rodríguez-Muñiz, G. M.; Gil, S. *Tetrahedron*, **2006**, *62*, 8571-8577.
- (6) (a) Fabbrizzi, L.; Foti, F.; Taglietti, A. *Org. Lett.* **2005**, *7*, 2603-2606. (b) Gunnlaugsson, T.; Davis, A.P.; O'Brien, J. E.; Glynn, M. *Org. Lett.* **2002**, *4*, 2449-2452. (c) Gunnlaugsson, T.; Davis, A.P.; O'Brien, J. E.; Glynn, M. *Org. Biomol. Chem.* **2005**, *3*, 48-56. (d) Mei, M.; Wu, S. *New J. Chem.* **2001**, *25*, 471-475. (e) Zeng, Z.; He, Y.; Wu, J.; Wei, L.; Liu, X.; Meng, L.; Yang, X. *Eur. J. Org. Chem.* **2004**, 2888-2893. (f) Nishiyabu, R.; Anzenbacher, P., Jr. *J. Am. Chem. Soc.* **2005**, *127*, 8270. (g) Fitzmaurice, R.J.; Kyne, G.M.; Doheret, D.; Kilburn, J.D. *J. Chem. Soc., Perkin Trans. 1*, **2002**, 841-864.
- (7) (a) Dickins, R.S.; Aime, S.; Batsanov, A.S.; Beeby, A.; Botta, M.; Bruce, J.I.; Howard, J.A.K.; Love, C.S.; Parker, D.; Peacock, R.D.; Puschmann, H. *J. Am. Chem. Soc.* **2002**, *124*, 12697-12705. (b) Parker, D.; Yu, J. *Chem. Commun.* **2005**, 3141-3143. (c) Parker, D. *Coord. Chem. Rev.* **2000**, *205*, 109-130. (d) Montalti, M.; Prodi, L.; Zaccheroni, N.; Carbonnière, L.; Douce, L.; Ziessel, R. *J. Am. Chem. Soc.* **2001**, *123*, 12694-12695. (e)

- Harte, A.J.; Jensen, P.; Plush, S.E.; Kruger, P.E.; Gunnlaugsson, T. *Inorg. Chem.* **2006**, *45*, 9465-9474.
- (8) (a) Anzenbacher, P., Jr.; Try, A.C.; Miyaji, H.; Jursíková, K.; Lynch, V.M.; Marquez, M.; Sessler, J.L. *J. Am. Chem. Soc.* **2000**, *122*, 10268-10272. (b) Anzenbacher, P., Jr.; Jursikova, K.; Sessler, J. *J. Am. Chem. Soc.* **2000**, *122*, 9350. (c) Anzenbacher, P., Jr.; Palacios, M.A.; Jursikova, K.; Marquez, M. *Org. Lett.* **2005**, *7*, 5027-5030. (d) Aldakov, D.; Anzenbacher, P., Jr. *Chem. Commun.* **2003**, 1394-1395. (e) Cho, H.K.; Lee, D.H.; Hong, J. *Chem. Commun.* **2005**, 1690-1692. (f) Kondo, S.; Hiraoka, Y.; Kurumatani, N.; Yano, Y. *Chem. Commun.* **2005**, 1720-1722. (g) Snellink-Ruël, B.H.M.; Antonisse, M.M.G.; Engbersen, J.F.J.; Timmerman, P.; Reinhoudt, D.N. *Eur. J. Org. Chem.*, **2000**, 165-170. (h) Pfeffer, F.M.; Gunnlaugsson, T.; Jensen, P.; Kruger, P.E. *Org. Lett.* **2005**, *7*, 5357-5360. (i) Blanco, J.L.J.; Bootello, P.; Benito, J.M.; Mellet, C.O.; Fernández, J.M.G. *J. Org. Chem.* **2006**, *71*, 5136-5143. (j) dos Santos, C.M.G.; Fernández, P.B.; Plush, S.E.; Leonard, J.P.; Gunnlaugsson, T. *Chem. Commun.*, **2007**, 3389-3391.
- (9) (a) Bünzli, J.-C. G.; Piguet, C. *Chem. Soc. Rev.* **2005**, *34*, 1048-1077. (b) Bünzli, J.-C. G.; Piguet, C. *Chem. Rev.* **2002**, *102*, 1897-1928. (c) Gunnlaugsson, T.; Leonard, J.P. *Chem. Commun.* **2005**, 3114-3131. (d) Terai, T.; Kikuchi, K.; Iwasawa, S.; Kawabe, T.; Hirata, Y.; Urano, Y.; Nagano, T. *J. Am. Chem. Soc.* **2006**, *128*, 6938-6946. (e) Hanaoka, K.; Kikuchi, K.; Kojima, H.; Urano, Y.; Nagano, T. *J. Am. Chem. Soc.* **2004**, *126*, 12470-12476. (f) Pope, S.J.A.; Kenwright, A.M.; Boote, V.A.; Faulkner, S. *Dalton Trans.* **2003**, 3780-3784.
- (10) (a) Poole, R.A.; Kielar, F.; Richardson, S.L.; Stenson, P.A.; Parker, D. *Chem. Commun.* **2006**, 4084-4086. (b) Poole, R.A.; Bobba, G.; Cann, M.J.; Frias, J.; Parker, D.; Peacock, R.D. *Org. Biomol. Chem.* **2005**, *3*, 1013-1024.

- (11) Gulgas, C.G.; Reineke, T.M. *Inorg. Chem.* **2005**, *44*, 9829-9836.
- (12) Hynes, M.J. *J. Chem. Soc., Dalton Trans.* **1993**, 311-312.
- (13) Fery-Forgues, S.; Le Bris, M.; Guetté, J.; Valeur, B. *J. Phys. Chem.* **1988**, *92*, 6233-6237.
- (14) (a) Bühlmann, P.; Nishizawa, S.; Xiao, K.P.; Umezawa, Y. *Tetrahedron* **1997**, *53*, 1647-1654. (b) Nishizawa, S.; Bühlmann, P.; Iwao, M.; Umezawa, Y. *Tetrahedron Lett.* **1995**, *36*, 6483-6486.
- (15) It should be noted that our initial studies on **Eu(2)-Eu(5)** reported slightly different emission spectra than those presented here (they were all very similar), and this was attributed to the presence of bicarbonate in the final product, which likely bound to the macrocycle, altering the cavity size.¹¹ As previously stated, the macrocyclic receptors were carefully purified to remove bicarbonate prior to the luminescence measurements.

Chapter 4. Synthesis and Characterization of Second-Generation Macrocyclic Lanthanide Chelates for Anion Recognition

ABSTRACT: The synthesis, structural characterization, and luminescence of a new series of thiourea-containing Eu^{3+} complexes, **Eu(5)-Eu(7)**, **Eu(10a)** and **Eu(10b)**, are reported. Incorporation of naphthalene, a more efficient antenna for Eu^{3+} , within the macrocyclic structures **Eu(7)** and **Eu(10a)** resulted in 2-3 fold more intense luminescence ($\lambda_{\text{exc}} = 272 \text{ nm}$, $\lambda_{\text{em}} = 614 \text{ nm}$) as compared to the other members of the series. Fluoride ion-induced decreases in emission intensity were observed in DMSO for **Eu(5)-Eu(7)**, maximizing at 30% for **Eu(6)** upon addition of 16 equivalents. Changes in emission intensity for **Eu(5)-Eu(7)** were not observed when $\lambda_{\text{exc}} = 395 \text{ nm}$ over the course of fluoride titration. Additionally, **Eu(10a)** exhibited anion-dependent decreases in Eu^{3+} luminescence intensity in water in preliminary studies. Benzoate and fluoride anions elicited the largest responses relative to the other halide ions and acetate in the aqueous studies.

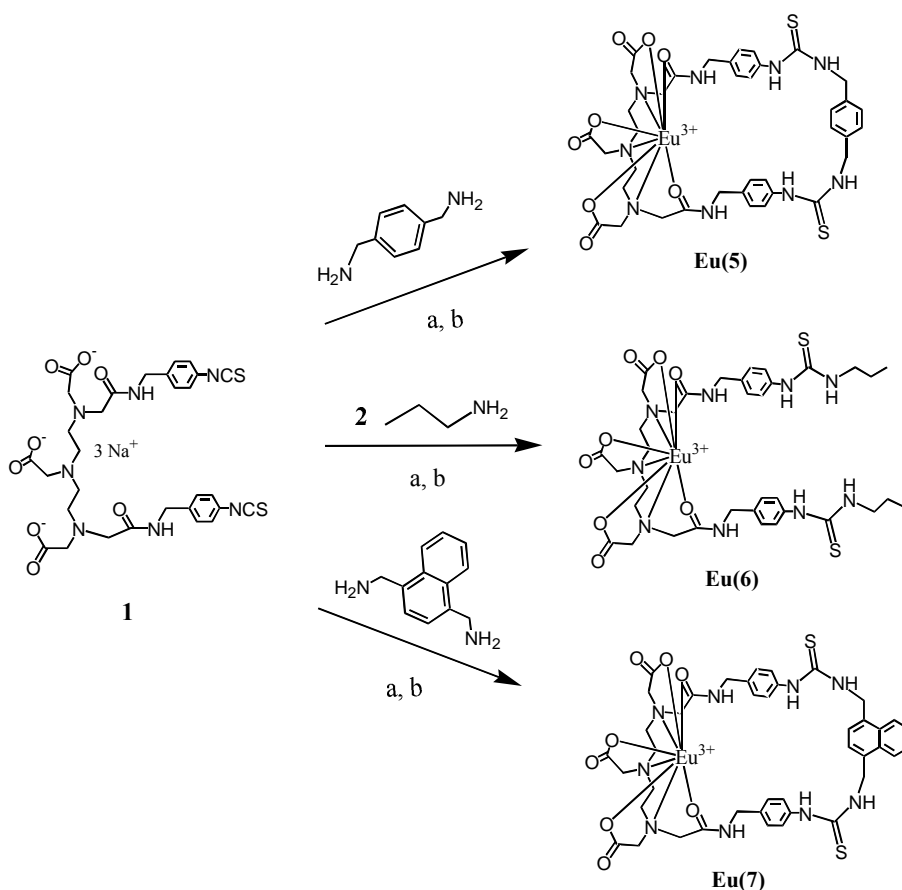
Introduction

The sensing of small inorganic anions in water has proven problematical.¹ However, due to the aqueous nature of most biological, environmental and industrial samples where the accurate determination of anion concentrations is relevant, developing anion sensing systems that function in water or water-containing solvents is central to the field. Anions are larger than isoelectric cations and more diffuse in charge, demanding a variety of complicated receptors for sensing a range of anion geometries.¹ The large free energies of solvation for anions in water

necessitates that sensor molecules have strong binding affinities for their target analyte to compete effectively with the solvent.¹ Macrocyclic lanthanide chelates have shown promise as functional molecular anion sensors.² It is important to expand our initial series of Eu^{3+} -based sensors to develop molecular sensors that are of higher emission intensity, have better solubility properties, and have the potential for stronger binding to small anions, while maintaining selectivity. New complexes can also provide data that impart insights into the mechanism of response for these sensors. The combination of these advancements can lead to molecular sensors capable of function in aqueous environments at low concentrations, which is both ideal and a great challenge. There are currently only a few examples of molecular probes for anions in water, and the majority of these take advantage of metal binding sites for increased binding affinity and selectivity.³⁻⁵ Lanthanides have been utilized in this area as both anion binding sites and as the signaling unit in luminescence-based sensors.⁴ Sensing of simple anions such as halides, carboxylates, and phosphates has been accomplished using fluorescent or colorimetric signaling through the application of sensor arrays on polymer supports based on hydrogen bond donors, as well.⁶ In these systems, selectivity for a given analyte is achieved through the collective response pattern of a large number of nonspecific sensing molecules, as opposed to the specific response of one molecule.⁶ Such an approach is capable of analyzing multicomponent mixtures, but cannot be applied for probing biological processes. A rare example of such a probe (a Eu^{3+} chelate) was created by Parker and Yu for the citrate anion, where subtle changes in the emission bands occurred specifically upon complexation with citrate, allowing for ratiometric determination of citrate concentration in a background of phosphates, lactate, chloride, and bicarbonate.^{4c} However, much work is necessary for developing molecular probes for other anions ubiquitous in biology, such as amino acid carboxylates or phosphates. Towards this end,

a new series of Eu^{3+} complexes, **Eu(5)**-**Eu(7)**, **Eu(10a)** and **Eu(10b)**, are reported. The synthesis, characterization and luminescence properties of **Eu(5)**-**Eu(7)**, an extension of our previously reported series, are discussed.² Additionally, two second-generation macrocycles, **Eu(10a)** and **Eu(11a)** have been synthesized with pendant aromatic groups, for potential applications in aqueous solutions. The synthesis, Eu^{3+} luminescence, and preliminary anion recognition data in water are reported.

Scheme 1. Synthesis of **Eu(5)**-**Eu(7)**.



(a) $\text{MeOH}/\text{H}_2\text{O}$, Na_2CO_3 (b) $\text{EuCl}_3 \cdot \text{H}_2\text{O}$, H_2O

Experimental

General. All reagents used in the synthesis, if not specified, were obtained from either Aldrich Chemical Co. (Milwaukee, WI) or Acros Organics (Morris Plains, NJ) and were used without further purification. The mass spectra were obtained from an IonSpec HiResESI mass spectrometer in positive ion mode. NMR spectra were collected on a Bruker AV-400 MHz spectrometer. Luminescence studies were performed using a Varian Cary Eclipse Fluorescence Spectrophotometer. Dimethyl sulfoxide (DMSO) used in the absorption and luminescence experiments was spectrophotometric grade. Dialysis membranes [500 molecular weight-cutoff (MCWO)] were manufactured by Spectrum Laboratories, Inc. (Rancho Dominguez, CA). Compound **1**,² 1-(4-(1-aminomethyl)-naphthyl)methylamine,⁷ and *N,N''-bis-trifluoroamidodiethylenetriamine*⁸ were synthesized according to published procedures.

Synthesis.

***N,N''-bis-trifluoroamido-N'-(1-naphthyl)methyldiethylenetriamine (8a)*.** *N,N''-bis-trifluoroamidodiethylenetriamine* (5.72 g, 19.4 mmol) was dissolved in 10 mL of CH₂Cl₂ and 1-bromomethylnaphthalene (2.19 g, 9.90 mmol) in 8 mL of CH₂Cl₂ was added dropwise at RT. The solution was refluxed for 14 hours and the solvent was mostly removed. The product was purified by flash column chromatography (50:48:2, hexane/CH₂Cl₂/MeOH) and isolated as a yellow solid. Yield: 0.700 g, 8.30%. ESI-MS: Calculated *m/z*: 436.15 [(**8a**)H⁺]. Found *m/z*: 436.07. ¹H-NMR (400 MHz, CDCl₃): δ_H 7.80-8.12 (m, 3H), 7.39-7.52 (m, 4H), 6.57 (br s, 2H), 4.04 (s, 2H), 3.43 (q, 4H), 2.76 (t, 4H). ¹³C-NMR (100 MHz, CDCl₃): δ_C 157.6 (q), 134.0, 133.3, 131.9, 128.9, 128.1, 126.6, 126.1, 125.1, 123.2, 111.3-120.0 (q), 57.8, 52.8, 37.5.

N,N''-bis-trifluoroamido-N'-(1-pyryl)methyldiethylenetriamine (8b). N,N''-bis-trifluoroamidodiethylenetriamine (1.63 g, 5.53 mmol) was dissolved in 6 mL of CHCl₃ and 1-bromomethylpyrene (0.830 g, 2.80 mmol) in 8 mL of CHCl₃ was added dropwise at RT. The solution was refluxed for 14 hours and the solvent was mostly removed. The product was purified by flash column chromatography (98:2, CHCl₃/MeOH) and isolated as an off-white solid. Yield: 0.235 g, 16.5%. ESI-MS: Calculated *m/z*: 510.16 [(8b)H⁺]. Found *m/z*: 510.16. ¹H-NMR (400 MHz, CDCl₃): δ_H 8.08-8.35 (m, 7H), 7.93 (d, 2H), 6.64 (br s, 2H), 4.32 (s, 2H), 3.48 (q, 4H), 2.84 (t, 4H).

N'-(1-naphthyl)methyldiethylenetriamine (9a). Compound 8a (0.305 g, 0.700 mmol) was dissolved in 10 mL MeOH and K₂CO₃ (0.970 g, 7.00 mmol) in 4 mL H₂O was added. The reaction stirred at RT for 6 hours. The solvent was removed, 4 mL H₂O (pH = 12) was added, and the product was extracted with CH₂Cl₂ (4 x 4 mL) and dried with MgSO₄. Removal of solvent gave a brown oil which solidified upon standing. Yield: 0.067 g, 39.4%. ESI-MS: Calculated *m/z*: 244.18 [(9a)H⁺]. Found *m/z*: 244.16. ¹H-NMR (400 MHz, CDCl₃): δ_H 8.24 (d, 1H), 7.83 (d, 1H), 7.78 (d, 1H), 7.40-7.51 (m, 4H), 4.02 (s, 2H), 2.73 (t, 4H), 2.60 (t, 4H), 1.73 (br s, 4H). ¹³C-NMR (100 MHz, CDCl₃): δ_C 135.1, 133.9, 132.3, 128.6, 128.0, 127.5, 126.0, 125.7, 125.2, 124.2, 58.4, 57.7, 39.8.

N'-(1-pyryl)methyldiethylenetriamine (9b). Compound 8b (0.125 g, 0.246 mmol) was dissolved in 10 mL MeOH and K₂CO₃ (0.339 g, 2.46 mmol) in 2 mL H₂O was added. The reaction stirred at RT for 2 days. The solvent was removed, 3 mL H₂O (pH = 12) was added, and the product was extracted with CHCl₃ (4 x 3 mL) and dried with MgSO₄. Removal of solvent gave a brown solid. Yield: 0.030 g, 38.5%. ESI-MS: Calculated *m/z*: 318.20 [(9b)H⁺].

Found m/z : 318.19. $^1\text{H-NMR}$ (400 MHz, CDCl_3): δ_{H} 8.37 (d, 1H), 8.00-8.21 (m, 9H), 4.31 (s, 2H), 2.79 (t, 4H), 2.66 (t, 4H), 1.45 (br s, 4H).

General Procedure for Macrocycle Synthesis.

***p*-Xylyl Macrocycle (5).** Compound **1** (0.167 g, 0.218 mmol) and Na_2CO_3 (0.060 g, 0.566 mmol) were dissolved in 20 mL of 1:1 MeOH/ H_2O . A solution of *p*-xylylenediamine (0.035 g, 0.254 mmol) was prepared in 20 mL of MeOH. The two solutions were then added dropwise to a vigorously-stirred solution of MeOH (20 mL) in equal amounts by pipet to a three-neck reaction flask over 1 hr. The reaction was left to stir for 20 hrs, after which the solvent was evaporated down to ~5 mL. Hydrochloric acid (0.5 M) was then slowly added until pH = 3, where a white precipitate had formed. The solution was then filtered and dried under vacuum to isolate the precipitate, **5**, as a monosodium salt. Yield: 0.176 g, 98.3 %. ESI-MS: Calculated m/z : 820.29 [(**5**)-H] $^+$. Found m/z : 820.33. $^1\text{H-NMR}$ (400 MHz, D_2O): δ 7.01-7.38 (m, 12H), 4.38 (s, 4H), 3.25 (s, 4H), 3.15 (s, 4H), 2.98 (s, 2H), 2.57 (br d, 8H).

“Opened” Macrocycle (6). Compound **1** (0.167 g, 0.218 mmol), Na_2CO_3 (0.060 g, 0.566 mmol), and propylamine (0.030 g, 0.508 mmol) were reacted as described above for **5**. Compound **6** was isolated as an off-white powder. Yield: 0.155 g, 88.4%. ESI-MS: Calculated m/z : 802.34 [(**6**)-H] $^+$. Found m/z : 802.34. $^1\text{H-NMR}$ (400 MHz, D_2O): δ 7.34 (d, 4H), 7.22 (d, 4H), 4.41 (s, 4H), 3.47 (br s, 4H), 3.27 (s, 4H), 3.18 (s, 4H), 3.04 (s, 2H), 2.61 (br d, 8H), 1.56 (br d, 4H), 0.89 (br s, 6H).

Naphthyl Macrocycle (7). Compound **1** (0.046 g, 0.060 mmol), Na_2CO_3 (0.033 g, 0.31 mmol), and 1-(4-(1-aminomethyl)-naphthyl)methylamine (0.017 g, 0.066 mmol) were reacted as described above for **5**. Compound **7** was isolated as an orange powder. Yield: 0.035 g, 67%.

ESI-MS: Calculated m/z : 870.31 [(7)-H]⁻. Found m/z : 870.35. ¹H-NMR (400 MHz, D₂O): δ 7.78 (br s, 2H), 7.44 (br s, 2H), 7.01-7.31 (m, 10H), 4.87 (s, 4H, hidden under HOD resonance), 4.35 (br s, 4H), 3.24 (s, 2H), 3.16 (s, 4H), 3.08 (s, 4H), 2.54 (br d, 8H).

Naphthyl Lariate Macrocycle (10a). Compound **1** (0.189 g, 0.247 mmol), Na₂CO₃ (0.065 g, 0.61 mmol), and compound **9a** (0.060 g, 0.247 mmol) were reacted as described above for **5**.

Compound **10a** was isolated as an off-white powder. Yield: 0.185 g, 74.3%. ESI-MS:

Calculated m/z : 927.36 [(10a)-H]⁻. Found m/z : 927.37. Anal. Calcd for C₄₅H₅₆N₁₀O₈S₂Na · HCl · H₂O: C, 54.34; H, 5.94; N, 13.51. Found: C, 54.23; H, 5.76; N, 14.05. ¹H-NMR (400 MHz, D₂O): δ 7.85-8.00 (m, 3H), 6.98-7.51 (m, 12H), 4.30 (s, 4H), 3.95 (s, 2H), 3.46 (s, 4H), 3.17 (d, 8H), 2.99 (s, 2H), 2.40-2.74 (m, 12H).

Pyryl Lariate Macrocycle (10b). Compound **1** (0.070 g, 0.092 mmol), Na₂CO₃ (0.036 g, 0.34 mmol), and compound **9a** (0.029 g, 0.092 mmol) were reacted as described above for **5**.

Compound **10b** was isolated as a light brown powder. Yield: 0.085 g, 86%. ESI-MS:

Calculated m/z : 1001.380 [(10b)-H]⁻. Found m/z : 1001.384. ¹H-NMR (400 MHz, D₂O): δ 6.7-8.2 (m, 17H), 4.10-4.41 (m, 6H), 3.81 (s, 2H), 2.9-3.7 (m, 12H), 2.1-2.8 (m, 12H).

General procedure for Eu complex formation with macrocycles.

Eu(5). Macrocycle **5** (0.056 g, 0.064 mmol) was dissolved in an aqueous NaOH solution (10 mL; 2.7×10^{-2} M) and Eu(Cl)₃ (0.017 g, 0.067 mmol) in H₂O (10 mL) was added dropwise over 30 minutes. This mixture was stirred at 45 °C for 5 hours. The solution was evaporated down to ~5 mL under reduced pressure and then transferred into a 500 MWCO cellulose membrane for dialysis (24 hours; 3 x 4L H₂O exchange). The water was evaporated and the remaining solid

dried under vacuum to yield an off-white powder. Yield: 0.061 g, 98%. ESI-MS: Calculated m/z : 972.20 [(**Eu(5)**)H]⁺. Found m/z : 972.24.

Eu(6). Macrocycle **6** (0.055 g, 0.064 mmol) and Eu(Cl)₃ (0.017 g, 0.067 mmol) were reacted as described above for **Eu(5)**, yielding an off-white powder. Yield: 0.051 g, 84%. ESI-MS: Calculated m/z : 954.0 [(**Eu(6)**)H]⁺. Found m/z : 954.0.

Eu(7). Macrocycle **7** (0.028 g, 0.030 mmol) and Eu(Cl)₃ (0.0085 g, 0.033 mmol) were reacted as described above for **Eu(5)**, yielding an off-white powder. Yield: 0.027 g, 88%. ESI-MS: Calculated m/z : 1022.22 [(**Eu(7)**)H]⁺. Found m/z : 1022.31.

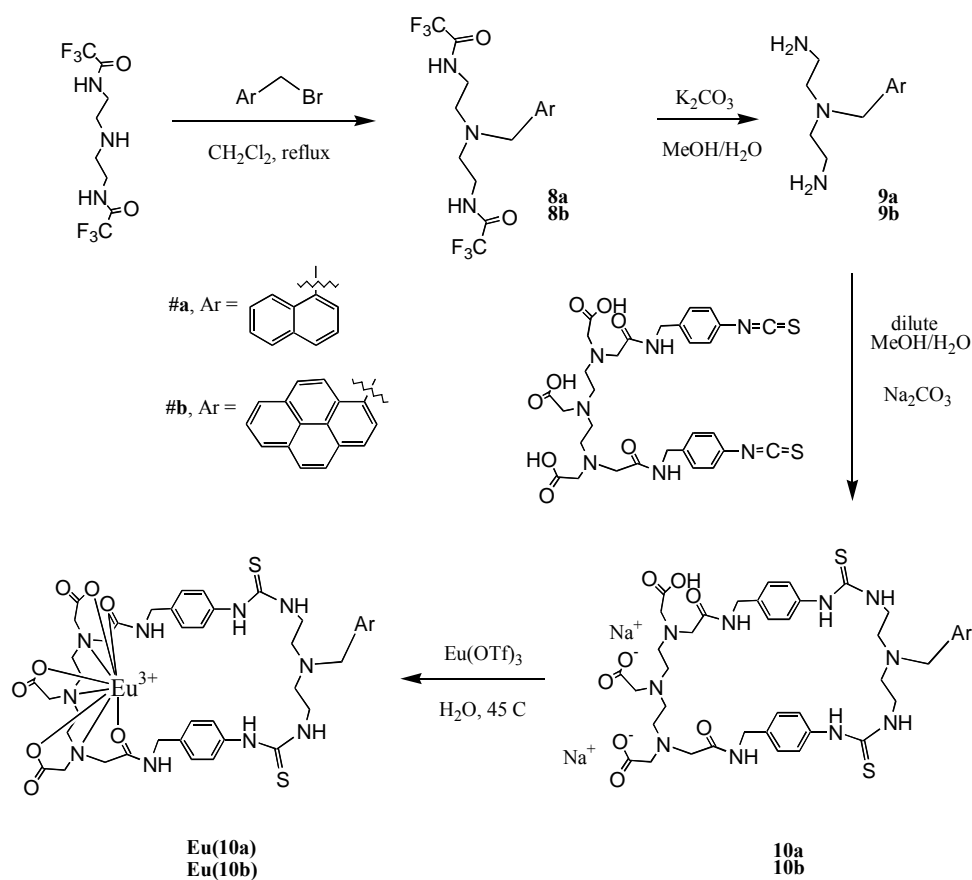
Eu(10a). Macrocycle **10a** (0.040 g, 0.039 mmol) and Eu(OTf)₃ (0.025 g, 0.042 mmol) were reacted as described above for **Eu(5)**, yielding an off-white powder. Yield: 0.035 g, 73%. ESI-MS: Calculated m/z : 1079.28 [(**Eu(10a)**)H]⁺. Found m/z : 1079.33.

Eu(10b). Macrocycle **10b** (0.059 g, 0.059 mmol) and Eu(Cl)₃ (0.017 g, 0.067 mmol) were reacted as described above for **Eu(5)**, yielding an off-white powder. Yield: 0.054 g, 79%. ESI-MS: Calculated m/z : 1153.29 [(**Eu(10b)**)H]⁺. Found m/z : 1153.32.

Luminescence Studies. Excitation and emission spectra of **Eu(5)**-**Eu(7)**, **Eu(10a)**, and **Eu(10b)** (DMSO or H₂O, 1.0 x 10⁻⁵ M) were obtained in phosphorescence mode with a total decay time of 0.01 s, a delay time of 0.10 ms, and a gate time of 5.0 ms. Excitation and emission slit widths were set at 5 and 10 nm, respectively. The excitation wavelengths (λ_{exc}) used in the emission studies were either 272 nm or 395 nm. The emission wavelength (λ_{em}) for the excitation studies was 614 nm. The fluoride anion titration studies were performed at the above instrument settings and each aliquot of anion solution was made such that 10.0 μ L = 1 equivalent (eq) of anion, where “one equivalent” of anion means that the anion and receptor are present in equal molar

amounts (1:1 molar ratio). The aliquots were added to a cuvette originally containing 3.00 mL of macrocycle solution in DMSO (1.0×10^{-5} M). All anions were used as their tetrabutylammonium (TBA) salts, except where specifically noted.

Scheme 2. Synthesis of **Eu(10a)** and **Eu(10b)**.



Results and Discussion

Synthesis. Compounds **5-7**, **10a**, and **10b** were synthesized from compound **1** as a common precursor in an analogous fashion to those previously reported (Schemes 1 and 2).² The

most diagnostic resonance in the ^1H -NMR spectrum is that of the methylene protons adjacent to the thiourea. These broadened resonances appear in the 4.3-4.9 ppm region, and can be obscured by the HOD resonance in some instances. These polyaminocarboxylate ligands are also easily characterized by ESI-MS in negative ion mode, where the presence of excess starting material or unwanted side products containing the DTPA unit can be easily detected. Chelation of Eu^{3+} is accomplished by addition of either the trichloride or tritriplate salt in aqueous solution followed by exhaustive dialysis in H_2O to remove salts. ESI-MS and luminescence spectroscopy were used to characterize the final products. Yields of both the cyclization and Eu^{3+} chelation steps were high, in accord with the synthesis of previous compounds of this series, in the range of 75-98%.

The synthesis of **Eu(10a)** and **Eu(10b)** required the synthesis of new triamines **9a** and **9b**, respectively (Scheme 2). *N,N'*-bis-trifluoroamidodiethylenetriamine⁸ was reacted with either 1-bromomethylnaphthalene or 1-bromomethylpyrene (**8a** or **8b**, respectively) to functionalize the reactive central amine with a pendant chromophore. Products were purified by flash column chromatography and characterized by ^1H and ^{13}C -NMR and ESI-MS. The most notable diagnostic resonance of the trifluoroacetyl protecting group in the ^{13}C -NMR was a quartet (signal splitting by ^{19}F) centered at 115.7 ppm for **8a**. Protonated molecular ion peaks were observed at 436.07 and 510.16 m/z for **8a** and **8b**, respectively, in the ESI-MS despite a significant occurrence of bond cleavage β to the aromatic group in both cases. Removal of the trifluoroacetyl protecting groups from **8a** and **8b** was accomplished using K_2CO_3 in $\text{MeOH}/\text{H}_2\text{O}$, affording **9a** and **9b**, respectively. Although the reaction was complete (TLC and ^1H -NMR), difficulties in the extraction of the product due to solubility fluctuations resulted in low yields. The ^1H -NMR signal due to the methylene unit adjacent to the strongly electron withdrawing

trifluoroamido group was significantly shifted upfield (~ 0.8 ppm) in both cases upon deprotection. The ESI-MS displayed peaks for the protonated molecular ion at 244.16 and 318.19 m/z for **9a** and **9b**, respectively, amidst several other peaks attributed to reactions involving carbocations generated from bond cleavage β to the aromatic group. The free amines were then reacted with compound **1** as described above to synthesize macrocycles **10a** and **10b**.

Luminescence Emission Studies. Compounds **Eu(5)** and **Eu(6)** were synthesized to provide further insights into the mechanism of response of our initial series of macrocycles.² Due to the selective response of a *m*-xylyl-bridged macrocycle described in chapter 3, **Eu(5)** was designed to study the role of a different xylyl bridging unit. **Eu(6)** was designed as an “opened” macrocycle to test the hypothesis that changes in conformation induced by anion binding pull the benzene antennas closer to the Eu^{3+} center which results in a luminescence increase (*vide infra*). Additionally, a naphthalene-containing bridging group was incorporated into **Eu(7)** to function as stronger antenna for enhanced Eu^{3+} luminescence. The emission spectra of **Eu(5)** - **Eu(7)** are shown in Figure 1. The use of the ratio I_{272}/I_{395} as a metric for the antenna effect was introduced in Chapter 3. **Eu(5)**, with a *p*-xylyl linker and $I_{272}/I_{395} = 6.4$, has a slightly weaker antenna effect than the *m*-xylyl analog ($I_{272}/I_{395} = 7.4$) which is consistent with an increase in length of the spacer between the two antennae, which holds them farther from the Eu^{3+} center. The antenna effect observed for **Eu(6)** is weaker still, but surprisingly is stronger than that observed for the largest macrocycle of the initial series (with an octyl linker). These data are consistent with **Eu(6)** adopting a different conformation than its more highly restricted macrocyclic analogs due to its open or linear structure. It is possible that the thiourea units hydrogen bond to the oxygen atoms of the DTPA unit in **Eu(6)**, where this event would be much less likely in the macrocyclic structures. **Eu(7)** contains a naphthyl linker and exhibits by far the most pronounced antenna

effect, where $I_{272}/I_{395} = 31.0$. Naphthalene is a well-known sensitizer of Eu^{3+} , primarily due to its triplet excited states lying at a more appropriate energy level for energy transfer to Eu^{3+} to occur.⁹

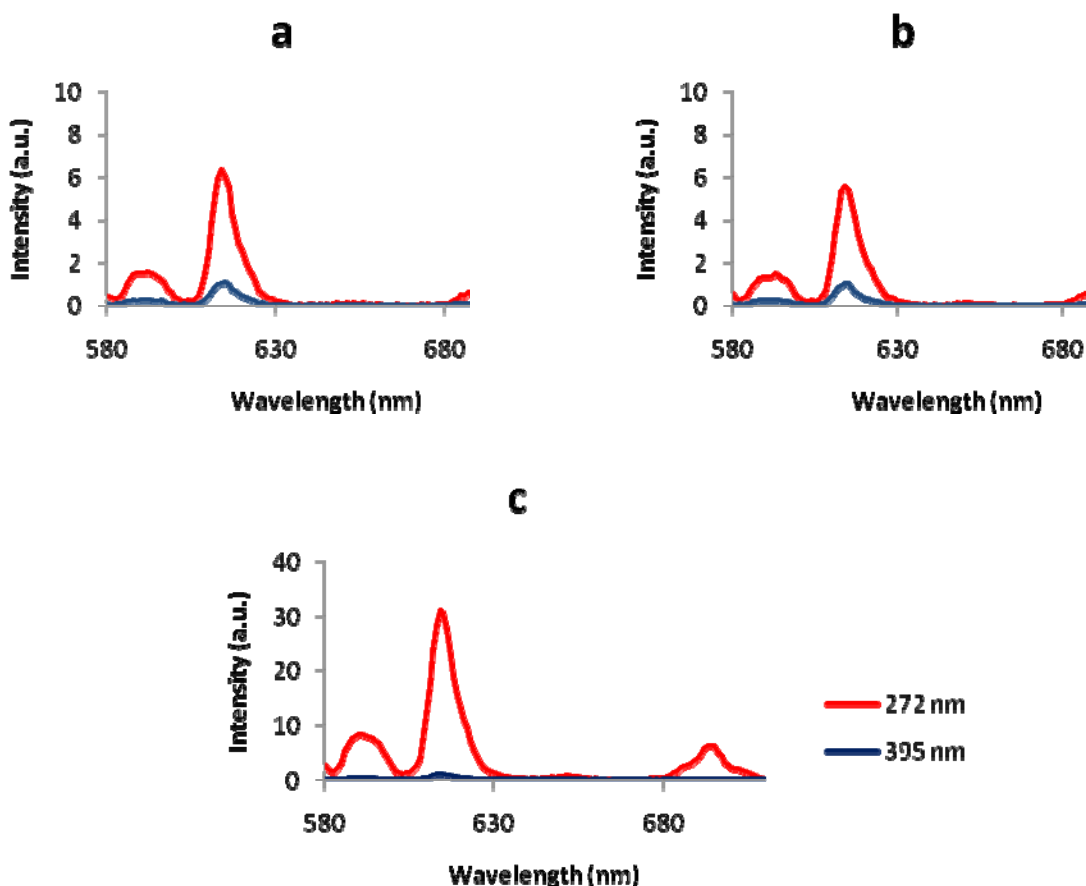


Figure 1. Emission spectra of (a) **Eu(5)**, (b) **Eu(6)**, and (c) **Eu(7)** in DMSO (1.0×10^{-5} M) at excitation wavelengths of 272 and 395 nm.

Eu(10a) and **Eu(10b)** were synthesized as second-generation macrocycles for anion-sensing applications in aqueous environments. Upon protonation in water, the basic tertiary amine in the pocket of each macrocycle allows for higher water solubility, as well as stronger binding to anions based on electrostatic attraction. Hence, the luminescence spectra for **Eu(10a)**

and **Eu(10b)** were obtained in both DMSO and H₂O, displayed in figures 2 and 3, respectively. In DMSO, **Eu(10a)** showed the larger antenna effect ($I_{272}/I_{395} = 21.1$), consistent with the naphthyl group functioning as an antenna. Because the naphthyl group in **Eu(10a)** is capable of rotating out into solution, increasing its distance to Eu³⁺, this effect is not as large as that observed for **Eu(7)** (which also has a substituted naphthalene group as part of its structure in a fixed position as part of the macrocyclic ring). Subtle electronic effects (i.e., triplet energy levels) may also play a role in the energy transfer efficiencies of **Eu(7)** and **Eu(10a)**. Pyrene is not an efficient sensitizer for Eu³⁺, and a smaller antenna effect is observed in DMSO for **Eu(10b)** ($I_{272}/I_{395} = 10.6$), most likely originating from the functionalized benzene arms of the macrocycle.

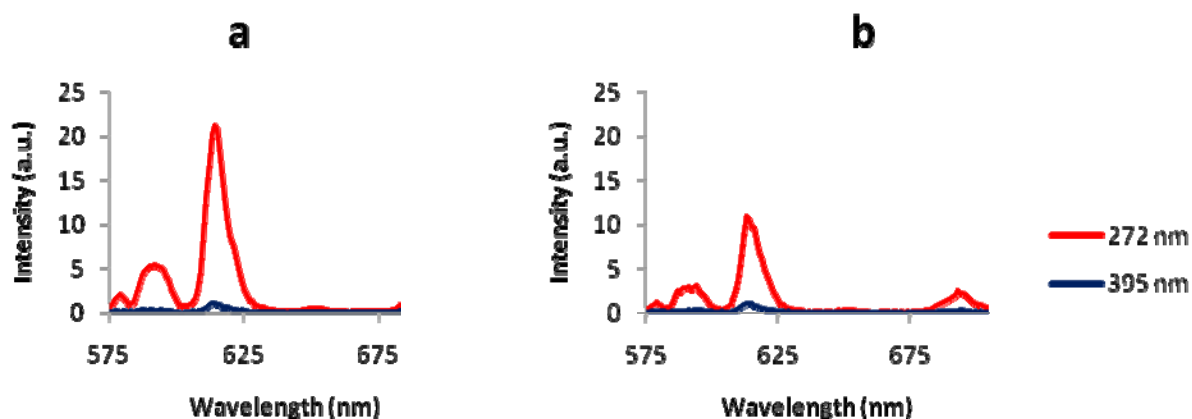


Figure 2. Emission spectra of (a) **Eu(10a)** and (b) **Eu(10b)**, in DMSO (1.0×10^{-5} M) at excitation wavelengths of 272 and 395 nm.

The luminescence of **Eu(10a)** in H₂O (Figure 3) was much brighter in intensity than previously studied macrocycles and the antenna effect was quite large ($I_{272}/I_{395} = 44.2$). Such an augmentation of luminescence could be an indication of a hydrophobic effect, driving the

naphthyl group into the pocket of the macrocycle to shield its surface from disrupting the favorable interactions between nearby water molecules. The distance to Eu^{3+} is expected to be shortened if the naphthyl group resides inside the pocket, increasing its ability to function as an antenna. For sensing applications, this phenomenon can potentially be exploited by anions that are able to force the antenna out of the pocket and further away from Eu^{3+} , resulting in a decreased signal. The luminescence observed for **Eu(10b)** was rather weak at $\lambda_{\text{exc}} = 395$ nm, and a reliable measurement was not obtained. However, the luminescence at $\lambda_{\text{exc}} = 272$ nm was significant (Figure 3), but much weaker than that observed for **Eu(10a)**, consistent with the results in DMSO. Additionally, fluorescence measurements were obtained of **Eu(10b)** and characteristic emission bands from the pyrene moiety were observed, centered at 376 nm and 395 nm. A broad excimer emission centered at 475 nm was also observed, and was significantly more intense in H_2O than in DMSO, most likely due to hydrophobic aggregation of the pyrene units in solution.

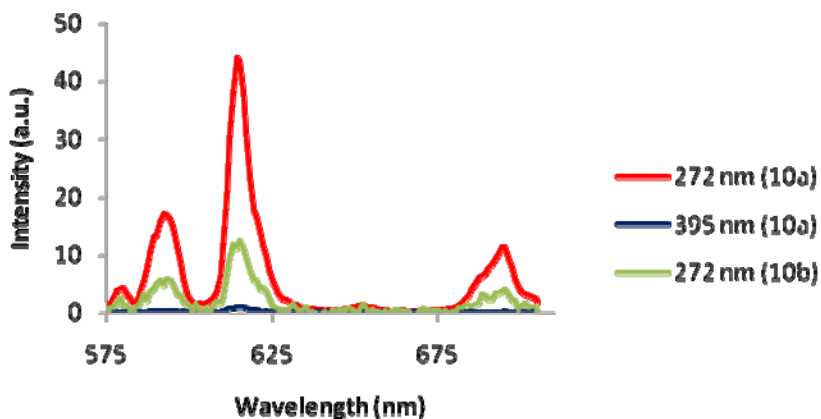


Figure 3. Emission spectra of **Eu(10a)** (red and blue lines) and **Eu(10b)** (green line) in H_2O (1.0×10^{-5} M) at indicated excitation wavelengths.

Anion Response. The macrocycles **Eu(5)**-**Eu(7)** were titrated with DMSO solutions of TBAF and the Eu^{3+} luminescence was monitored to determine their ability to function as anion sensors (Figure 4). **Eu(5)**, the *p*-xylyl bridged macrocycle, exhibited a decrease in luminescence of 25% at 16 equivalents of TBAF. This result was in stark contrast to that obtained with the *m*-xylyl analog (described in Chapter 3), which showed a large increase in luminescence under similar conditions. The titration results for **Eu(6)** were also unexpected, and a decrease in emission of 30% was observed. The non-cyclic nature of **Eu(6)** was hypothesized to result in an increase in luminescence if the thiourea arms cooperatively bound fluoride, requiring that the benzene antennae would be held closer to the Eu^{3+} center in such a conformation. However, as indicated by the significant antenna effect observed for **Eu(6)** prior to anion addition, it is possible that a change in conformation occurs upon anion binding that *increases* the Eu^{3+} -antenna distance, accounting for the observed *decrease* in emission. Other mechanisms for the observed decrease are possible, but mechanistic studies were not performed for **Eu(6)**.

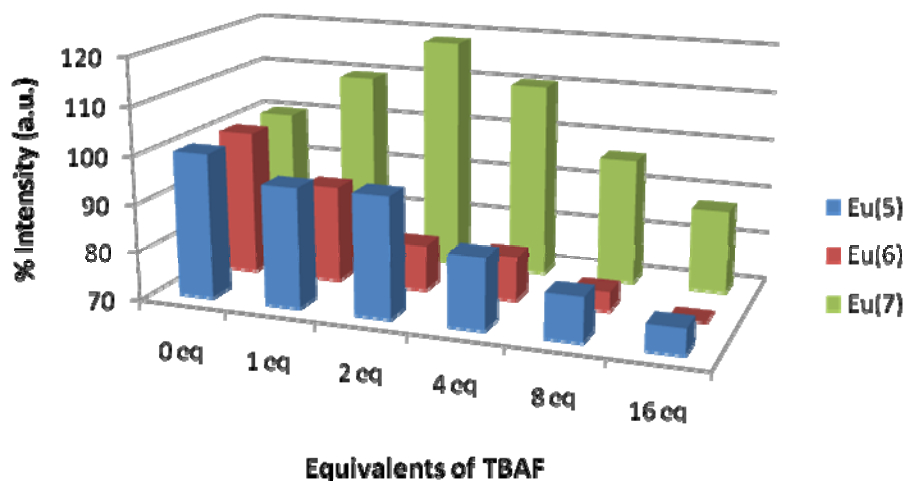


Figure 4. Effect of fluoride ion on the % luminescence intensity of **Eu(5)**-**Eu(7)** ($\lambda_{\text{exc}} = 272$ nm, $\lambda_{\text{em}} = 614$ nm, emission intensity @ 0 eq \equiv 100%).

An increase in Eu^{3+} luminescence (of 18% after two equivalents) was only observed for **Eu(7)** in this series of compounds, possibly due to conformation changes of the type discussed in Chapter 3 for the first series of compounds studied. However, addition of more than two equivalents of fluoride resulted in a decrease in luminescence of 13% (at 16 equivalents of TBAF) from the initial intensity. It is well known that fluoride is capable of removing thiourea protons when present in excess of two equivalents due to the formation of the stable bifluoride ion, HF_2^- , which correlates well to the onset of luminescence quenching. Photoinduced electron transfer (PET) quenching has been reported for naphthalene chromophores separated from thiourea moieties by a methylene spacer, especially upon deprotonation of the thiourea, which increases the likelihood of electron donation from sulfur.¹⁰ Hence, it is possible that PET quenching of the excited state of the naphthalene antenna is responsible for the observed decrease in luminescence for **Eu(7)**. In addition, as discovered previously with macrocycles of

this type, titration of **Eu(5)**-**Eu(7)** with fluoride resulted in insignificant luminescence changes when monitored at an excitation wavelength of 395 nm (direct Eu^{3+} excitation).

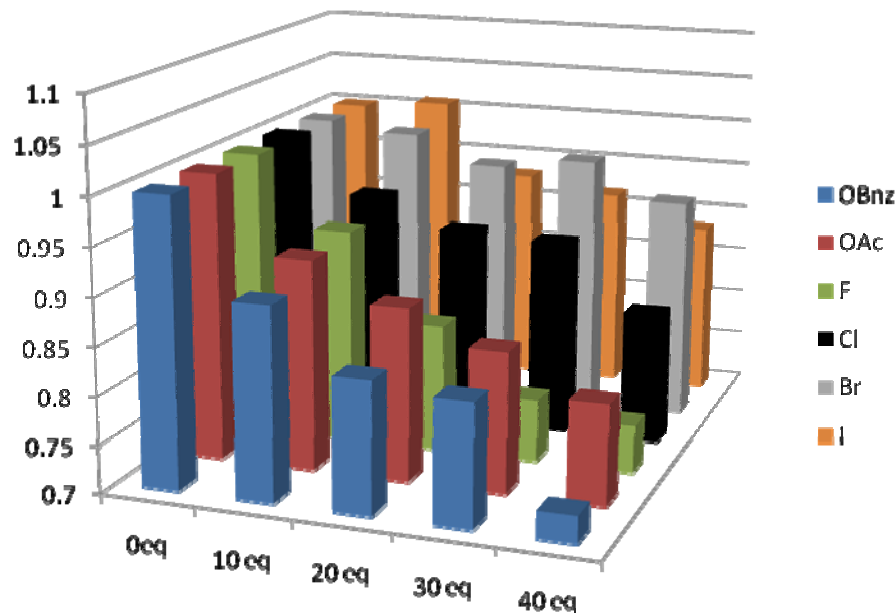


Figure 5. Effect of the Na^+ salts of different anions on the luminescence intensity of **Eu(10a)** in H_2O (1.0×10^{-5} M, $\lambda_{\text{exc}} = 272$ nm, $\lambda_{\text{em}} = 615$ nm).

Prior to the synthesis of **Eu(10a)**, preliminary studies of the response to anions (of macrocycles described in this work) performed in aqueous solution displayed no activity. However, the high water solubility and luminescence intensity of **Eu(10a)** made it a suitable candidate for studies in water with various anions. Figure 5 shows the preliminary results of titration experiments with a series of anions and **Eu(10a)**. A decrease in luminescence intensity was observed for all anions studied. However, the degree of luminescence quenching varied depending on the anion, with the largest decreases observed upon titration with fluoride and benzoate. The overall luminescence intensity correlates well with the basicities of the anions studied, but does not appear to be due to changes in pH of the solution. The pH of the solution

was monitored during the course of each titration and was fairly constant ($\text{pH} = 6.3 \pm 0.2$) except in the case of benzoate, where the solution was slightly more basic ($\text{pH} = 6.7 \pm 0.1$). Although fluctuations in luminescence intensity were observed with **Eu(10a)** when measured over a wide pH range (3-11), no significant change was observed in the region where the anion studies were performed. These preliminary results from titration experiments in water with **Eu(10a)** show a luminescence decrease dependent on the anion, but selectivity is minimal and may be the result incorporating a positive charge onto this receptor. Further studies are required to gain information regarding the exact nature of the observed response.

Conclusion. Five new Eu^{3+} complexes were synthesized and characterized as potential luminescent, anion sensing molecules. Synthesis of each Eu^{3+} complex from a common precursor, compound **1**, expanded the generality of this synthetic pathway, and for **Eu(10a)** and **Eu(10b)**, included functional groups linking the thioureas together that incorporate tertiary amines with pendant aromatic groups. The first series, **Eu(5)-Eu(7)**, was an expansion of complexes described in Chapters 2 and 3, designed to provide further insight into the mechanism of the observed anion response. Most notably, the luminescence response of **Eu(6)** to fluoride indicated that a macrocyclic design may be important for restricting the position and orientation of the antenna-thiourea arms, which effects the energy transfer efficiency to Eu^{3+} . **Eu(7)**, employing a naphthalene functionality in the bridging group, was also found to be more highly luminescent than previously studied complexes of this series, most likely due to an antenna effect from the substituted naphthyl group. **Eu(10a)** showed a luminescent response to anions in aqueous solution in preliminary studies. Despite the minimal selectivity observed, the results indicate the possibility of this class of molecules functioning as sensors for anions in water. **Eu(10b)** was designed with a pendant pyrene moiety to bind the molecule to a carbon nanotube

scaffold (in collaboration with Dr. Liming Dai at the University of Dayton) for sensing applications involving DNA and these studies are ongoing. Additionally, the pyrene emission may serve as an alternative signal for ratiometric sensing capabilities.

REFERENCES

- (1) (a) Martínez-Máñez, R.; Sancenón, F. *Chem. Rev.* **2003**, *103*, 4419-4476. (b) Bianchi, A.; Bowman-James, K.; García-España, E., Eds. *Supramolecular Chemistry of Anions*, Wiley-VCH: New York, 1997.
- (2) Gulgas, C.G.; Reineke, T.M. *Inorg. Chem.* **2005**, *44*, 9829-9836.
- (3) (a) Blanco, J.L.J.; Bootello, P.; Benito, J.M.; Mellet, C.O.; Fernández, J.M.G. *J. Org. Chem.* **2006**, *71*, 5136-5143. (b) Gunnlaugsson, T.; Kruger, P.E.; Jensen, P.; Tierney, J.; Ali, H.D.P.; Hussey, G.M. *J. Org. Chem.* **2005**, *70*, 10875-10878. (c) Kato, R.; Nishizawa, S.; Hayashita, T.; Teramae, N. *Tetrahedron Lett.* **2001**, 5053-5056.
- (4) (a) Parker, D. *Chem. Soc. Rev.* **2004**, *33*, 156-165. (b) Dickins, R.S.; Aime, S.; Batsanov, A.S.; Beeby, A.; Botta, M.; Bruce, J.I.; Howard, J.A.K.; Love, C.S.; Parker, D.; Peacock, R.D.; Puschmann, H. *J. Am. Chem. Soc.* **2002**, *124*, 12697-12705. (c) Parker, D.; Yu, J. *Chem. Commun.* **2005**, 3141-3143. (d) Parker, D. *Coord. Chem. Rev.* **2000**, *205*, 109-130. (e) Harte, A.J.; Jensen, P.; Plush, S.E.; Kruger, P.E.; Gunnlaugsson, T. *Inorg. Chem.* **2006**, *45*, 9465-9474. (f) Charbonnière, L.J.; Schurhammer, R.; Mameri, S.; Wipff, G.; Ziessel, R. F. *Inorg. Chem.* **2005**, *44*, 7151-7160.
- (5) (a) Cho, H.K.; Lee, D.H.; Hong, J. *Chem. Commun.* **2005**, 1690-1692. (b) Fabbrizzi, L.; Foti, F.; Taglietti, A. *Org. Lett.* **2005**, *7*, 2603-2606.
- (6) (a) Palacios, M.A.; Nishiyabu, R.; Marquez, M.; Anzenbacher, Jr., P. *J. Am. Chem. Soc.* **2007**, *129*, 7538-7544. (b) Nishiyabu, R.; Anzenbacher Jr., P. *J. Am. Chem. Soc.* **2005**, *127*, 8270-8271. (c) Anzenbacher Jr, P.; Jursikova, K.; Aldakov, D.; Marquez, M.; Pohl, R. *Tetrahedron* **2004**, *60*, 11163-11168. (d) Descalzo, A.B.; Rurack, K.; Weisshoff, H.; Martínez-

Máñez, R.; Marcos, M.D.; Amorós, P.; Hoffmann, K.; Soto, J. *J. Am. Chem. Soc.* **2005**, *127*, 184-200.

(7) Choi, S.; Mammen, M.; Whitesides, G.M. *J. Am. Chem. Soc.* **1997**, *119*, 4103-4111.

(8) Hay, M.P.; Prujin, F.B.; Gamage, S.A.; Liyanage, H.D.S.; Kovacs, M.S.; Patterson, A.V.; Wilson, W.R.; Brown, J.M.; Denny, W.A. *J. Med. Chem.* **2004**, *47*, 475-488.

(9) (a) Beeby, A.; Parker, D.; Williams, J.A.G. *J. Chem. Soc., Perkin Trans. 2* **1996**, 1565-1578.

(b) Skinner, P.J.; Beeby, A.; Dickins, R.S.; Parker, D.; Aime, S.; Botta, M. *J. Chem. Soc., Perkin Trans. 2* **2000**, 1329-1338.

(10) (a) Gunnlaugsson, T.; Glynn, M.; Tocci, G.M.; Kruger, P.E.; Pfeffer, F.M. *Coord. Chem. Rev.* **2006**, *250*, 3094-3117.

(b) Kubo, Y.; Ishihara, S.; Tsukahara, M.; Tokita, S. *J. Chem. Soc., Perkin Trans. 2* **2002**, 1455-1460. (c) Mei, M.; Wu, S. *New J. Chem.* **25**, 471-475.

Chapter 5. Synthesis, Characterization and Relaxivity of a New Gd^{3+}

Chelate for Imaging the Dopamine Transporter

ABSTRACT: Magnetic resonance imaging (MRI) has evolved to demand targeted agents for specific studies of biological processes and conditions. A novel cocaine-conjugated, water-soluble polyaminocarboxylate contrast agent, **Gd(1)**, was synthesized and structurally characterized for application as a dopamine transporter targeting MRI-CA. The analogous Eu^{3+} complex, **Eu(1)** was also synthesized and was determined to have 2 coordinated water molecules in aqueous solution by luminescence lifetime studies. A relaxivity of $7.1 \text{ mM}^{-1}\text{s}^{-1}$ was measured for **Gd(1)** at 400 MHz and 310 K.

Introduction

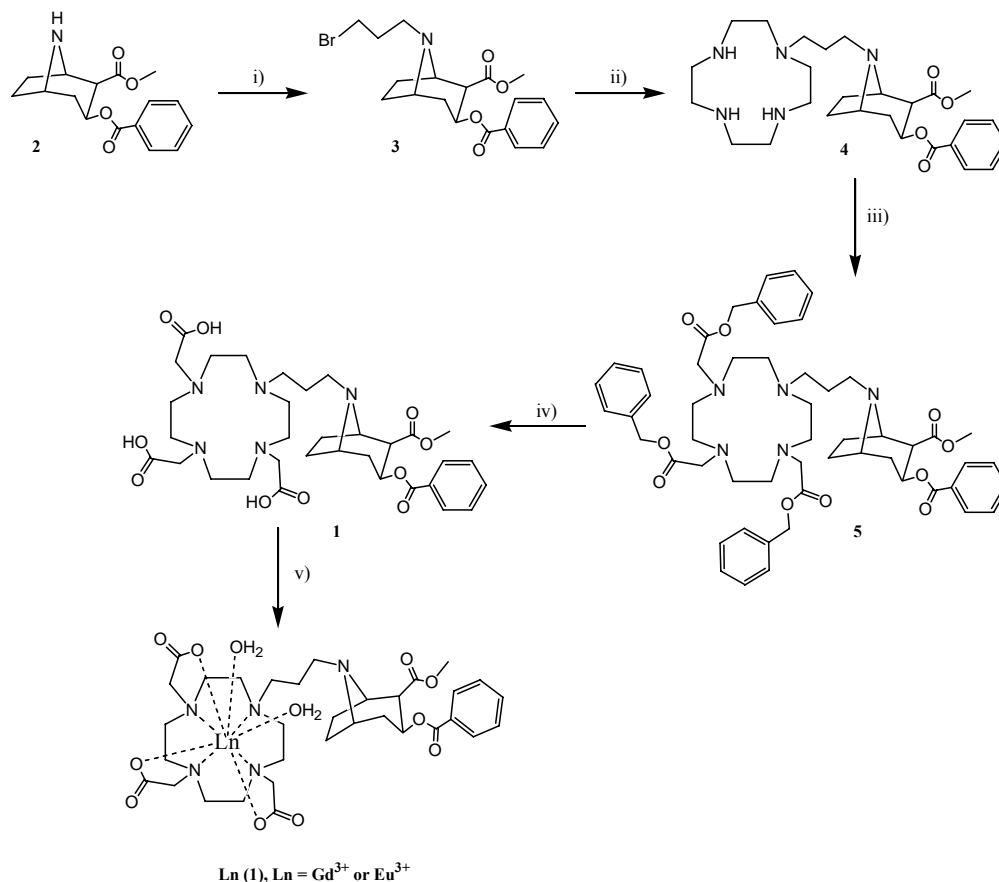
Magnetic resonance imaging (MRI) is one of the most widely utilized diagnostic tools in medicine, primarily due to the non-invasive nature of the technique.¹⁻⁴ The use of a paramagnetic contrast agents (CA) to enhance the resolution of the MRI scan is routine. Typical CAs approved for clinical use are based on either diethylenetriaminepentaacetic acid (DTPA) or 1,4,7,10-tetraazacyclododecane-1,4,7,10-tetraacetic acid (DOTA) ligand architectures for strong binding of the highly paramagnetic Gd^{3+} ion.¹⁻² The Gd^{3+} ion enhances the relaxation rate of excited protons within close proximity by both inner-sphere and outer-sphere mechanisms. Three parameters are most commonly manipulated to enhance the relaxivities (r_1) of Gd^{3+} -based MRI-CAs: rotational correlation time (τ_r), water-exchange rate (τ_m) and the number of coordinated water molecules to Gd^{3+} (q).¹⁻⁶ CAs of larger molecular weight have longer values of τ_r in general, attributed to the slower molecular rotation in solution, which can increase the

relaxivity of the CA. Specifically, small CAs bearing targeting ligands for large biomolecules have been developed and show augmentations of τ_r and relaxivity upon binding to the target.^{1,5-6} When the small CA is bound to a large molecule, it assumes a rotation similar to that of the latter, which is generally much slower.¹ Rates of water-exchange vary immensely among known CAs, with τ_m particularly slowed by nearby amide (-NH) bonds, which can stabilize the coordinated water molecule through hydrogen-bonding interactions.^{1,3} Slow τ_m rates have adverse effects on relaxivity where, in the case of some Gd^{3+} complexes with tetraamide derivatives of polyaminocarboxylate ligands, the coordinated water molecule is effectively exchange inert.^{1,3} Larger values for q are obtained by reducing the number of potential donor atoms of the chelating ligand which, although significantly increasing relaxivity, can result in decreases in kinetic stability of the complex.^{1,7} Current clinically approved MRI-CAs have one inner-sphere water molecule in solution ($q = 1$), primarily for concerns related to the toxicity problems associated with the release of the Gd^{3+} ion from the chelate structure, which is similar in size to Ca^{2+} .

The need for MRI-CAs of relatively high relaxivity for the study and diagnosis of specific diseases is substantial.¹⁻⁴ MRI-CAs designed to target the blood pool,² liver³ and breast cancer^{4c} are a few examples. The field of MRI is also progressing toward the molecular imaging of receptor and enzyme activity.^{1,4} Molecular imaging relying on fluorescence methods suffers from low tissue penetration, and positron emission tomography (PET) requires radioactive compounds as labels with relatively short half-lives.^{1,4,8-10} MRI technology is revered for its deep tissue penetration, and CAs targeted to specific receptors may allow molecular imaging based on MRI.^{1,4} However, there is currently only one example of a MRI-CA developed for imaging the brain, employing the spiperone moiety as a targeting moiety for the dopamine D2

receptor.^{4a} The CA was found to retain some of the affinity of the spiperone group in binding studies with isolated mouse striatal tissue, despite the large change in overall structure of adding a Gd³⁺ chelate.^{4a} Dopamine transporter imaging has implications in the study of neurological diseases, esp. Parkinson's disease.⁸⁻¹⁰ Previously, images of the brain for studying the dopamine transporter have been augmented by the use of radioactive single photon emission computed tomography (SPECT) agents based on ^{99m}Tc, requiring a chelating ligand appended to a targeting moiety.⁸⁻¹⁰ The evolution of targeting groups for the dopamine transporter has resulted in numerous ligands of very high affinities, typically based on the structure of cocaine.¹⁰⁻¹² In the design of the targeted metal complex, it is important that the complex be overall neutral, have a minimal number of hydrogen-bond donors and acceptors, and be of relatively small molecular size to be capable of crossing the blood-brain barrier.¹³ We have applied these principles to the design of a Gd³⁺-based MRI-CA, and herein we report the synthesis, characterization and relaxivity of **Gd(1)** as a prototype CA for imaging the dopamine transporter.

Scheme 1. Synthesis of Gd(1) and Eu(1).^a



^a (i) 3-bromopropyltriflate, CH₂Cl₂; (ii) cyclen, CHCl₃, 45° C; (iii) benzyl 2-bromoacetate, DMF, Na₂CO₃; (iv) H₂, 10% Pd/C, MeOH; (v) LnCl₃ · xH₂O, MeOH, NaOMe.

Experimental

General. All reagents used in the synthesis, if not specified, were obtained from Aldrich Chemical Co. (Milwaukee, WI) and were used without further purification. Norcocaine, **2**,¹⁴ and 3-bromopropyl triflate¹⁵ were synthesized according to published procedures. The mass spectra were obtained from an IonSpec HiResESI mass spectrometer in positive ion mode. NMR spectra were collected on a Bruker AV-400 MHz spectrometer. Relaxivity measurements were performed using a Bruker AMX-400 MHz spectrometer. Determination of the %Eu and %Gd

content was performed using a Perkin-Elmer ELAN 6000 Inductively-Coupled Plasma Mass Spectrometer. Luminescence studies were performed using a Varian Cary Eclipse Fluorescence Spectrophotometer. Thin-layer chromatography (TLC) was performed using TLC plastic sheets (silica gel 60 F₂₅₄) from Merck (Darmstadt, Germany). Dialysis membranes [500 molecular weight-cutoff (MCWO)] were manufactured by Spectrum Laboratories, Inc. (Rancho Dominguez, CA).

Synthesis.

***N*-(3-bromopropyl)norcocaine (3).** 3-Bromopropyl triflate (0.506 g, 1.86 mmol) was dissolved in 10 mL CH₂Cl₂ and stirred at 0°C. Norcocaine, **2** (0.549 g, 1.86 mmol) in 10 mL CH₂Cl₂ was then added dropwise using an addition funnel. The reaction mixture stirred for 20 min. at 0°C, and was then brought to RT and stirred for 5 hrs. Following removal of solvent, 10 mL saturated NaHCO₃ soln. was added to the flask and a brown oil formed, which was extracted with 3 x 8 mL CH₂Cl₂ and dried with MgSO₄. Removal of solvent afforded a yellow oil as the product. Yield: 0.750 g, 98.1%. ESI-MS: Calculated *m/z*: 410.097 [(**3**)H⁺]. Found *m/z*: 410.081. ¹H-NMR (400 MHz, CDCl₃): δ_H (ppm) 8.03 (d, 2H), 7.56 (t, 1H), 7.44 (t, 2H), 5.25 (m, 1H), 3.73 (s, 3H), 3.54 (m, 3H), 3.34 (br s, 1H), 3.05 (br s, 1H), 2.41 (m, 4H), 1.76-2.04 (m, 6H). ¹³C-NMR (100 MHz, CDCl₃): δ_C (ppm) 170.6, 166.2, 133.0, 130.4, 129.8, 128.3, 67.2, 63.3, 60.4, 51.4, 50.6, 50.3, 35.7, 32.2, 31.1, 26.0, 25.7.

***N*-(3-(1,4,7,10-tetraazacyclododecan-1-yl)propyl)norcocaine (4).** Cyclen (0.830 g, 4.83 mmol) was dissolved in 10 mL CHCl₃ and stirred at RT. Compound **3** (0.750 g, 1.82 mmol) was dissolved in 5 mL CHCl₃ and added dropwise to the solution of cyclen. The reaction temperature was raised to 45°C and the reaction mixture was stirred for 24 hrs. Removal of

solvent and purification by flash column chromatography (silica gel, gradient from 80:20 CHCl₃/MeOH to 60:38:2 CHCl₃/MeOH/H₂O) yielded **4** as a yellow solid following drying *in vacuo*. Yield: 0.750 g, 82.0%. ESI-MS: Calculated *m/z*: 502.339 [(**4**)H⁺]. Found *m/z*: 502.340. ¹H-NMR (400 MHz, CDCl₃): δ_H (ppm) 8.03 (d, 2H), 7.54 (t, 1H), 7.42 (t, 2H), 5.25 (m, 1H), 3.72 (s, 1H), 3.71 (s, 3H), 3.37 (br s, 1H), 3.02 (br s, 1H), 2.29-2.80 (m, 20H), 1.50-2.15 (m, 8H). ¹³C-NMR (100 MHz, CDCl₃): δ_C (ppm) 170.5, 165.9, 132.7, 130.2, 129.5, 128.1, 67.2, 62.1, 60.0, 51.7, 51.3, 51.1, 50.1, 49.3, 46.8, 46.0, 44.9, 35.6, 26.7, 26.0, 25.2.

Compound 5. Compound **4** (0.655 g, 1.30 mmol) and Na₂CO₃ (0.555 g, 5.24 mmol) were placed in a flask and 10 mL of anhydrous DMF was added to the mixture. Benzyl bromoacetate (1.00 g, 4.37 mmol) in 5 mL DMF was added dropwise to the mixture at 0°C. The reaction solution was then heated to 80°C and stirred for 48 hrs. Removal of solvent gave a brown oil which was taken up in 4 mL dilute aq. NaOH soln., extracted with CH₂Cl₂ (3 x 4 mL) and dried with MgSO₄. Most of the solvent was then removed, and purification by flash column chromatography (silica gel, gradient from 99:1 CH₂Cl₂/MeOH to 95:5 CH₂Cl₂/MeOH) yielded **5** as an off-white solid following drying *in vacuo*. Yield: 0.534 g, 43.5%. ESI-MS: Calculated *m/z*: 946.497 [(**5**)H⁺]. Found *m/z*: 946.486. ¹H-NMR (400 MHz, CDCl₃): δ_H (ppm) 7.98 (dd, 2H), 7.51 (dt, 1H), 7.38 (m, 2H), 7.29 (m, 15H), 5.04-5.21 (m, 7H), 3.68 (s, 1H), 3.66 (s, 3H), 3.65 (s, 2H), 3.54 (s, 4H), 2.10-3.30 (m, 22H), 1.47-2.05 (m, 8H). ¹³C-NMR (100 MHz, CDCl₃): δ_C (ppm) 171.0, 170.9, 170.8, 166.0, 135.4, 135.3, 135.1, 133.0, 130.2, 129.7, 129.6, 128.7, 128.5, 128.3, 128.2, 67.4, 67.3, 67.2, 66.6, 66.5, 62.1, 60.0, 56.1, 55.5, 55.3, 54.7, 53.2, 53.0, 51.4, 51.2, 50.0, 48.0, 35.7, 26.0, 25.7, 22.6.

Ligand 1. Compound **5** (0.157 g, 0.166 mmol) and 10% Pd/C (0.075 g) were placed in a flask and methanol was added (7 mL) under a N₂ atmosphere, dissolving **5** and forming a black, turbid

solution upon stirring. This solution was degassed by bubbling N₂ through the solution for 30 min. H₂ was then bubbled into the mixture using a needle outlet. After 35 min. the outlet was removed, and the solution stirred under H₂. After 14 hrs, the reaction appeared complete by TLC, however, the mixture was allowed to stir for a total of 20 hrs to ensure complete conversion. The solution was then vacuum filtered through celite, the solvent removed, and vacuum dried yielding the desired compound as a white powder. Yield: 0.109 g, 97.0%. ESI-MS: Calculated *m/z*: 676.356 [(1)H⁺]. Found *m/z*: 676.286. ¹H-NMR (400 MHz, CD₃OD): δ_H (ppm) 7.91 (d, 2H), 7.55 (t, 1H), 7.43 (t, 2H), 5.51 (m, 1H), 4.27 (s, 1H), 4.08 (s, 1H), 3.78 (s, 1H), 3.73 (s, 3H), 3.53 (s, 6H), 2.60-3.48 (m, 20H), 1.70-2.50 (m, 8H). ¹³C-NMR (100 MHz, CD₃OD): δ_C (ppm) 176.2, 174.7, 174.2, 166.7, 134.7, 130.6, 130.5, 129.7, 65.9, 64.6, 61.7, 60.7, 54.5, 53.5, 52.8, 51.4, 51.3, 50.6, 49.9, 47.9, 47.1, 34.3, 24.9, 24.4, 23.6.

Gd(1). Ligand **1** (0.050 g, 0.074 mmol) and NaOMe (0.011 g, 0.21 mmol) were dissolved in 3 mL of MeOH and a solution of GdCl₃·6H₂O (0.029 g, 0.078 mmol) in 2 mL MeOH was added dropwise over 5 minutes. This mixture was heated to 45°C and stirred for 4 hrs. The solvent was removed to give an off-white solid, which was then dissolved in 5 mL of H₂O and transferred into a 500 MWCO cellulose membrane for dialysis (24 hours; 3 x 4L H₂O exchange). The water was evaporated and the remaining solid dried under vacuum to yield an off-white powder. Yield: 0.061 g, 95.2%. ESI-MS: Calculated *m/z*: 831.257 [**Gd(1)**H⁺]. Found *m/z*: 831.260. ICP-MS: Calculated Gd content for C₃₃H₄₆GdN₅O₁₀ · HCl · 4H₂O: 16.76%. Found: 16.77%

Eu(1). Ligand **1** (0.0103 g, 0.0153 mmol) and NaOMe (0.0023 g, 0.043 mmol) in 2 mL of MeOH and a solution of EuCl₃·H₂O (0.0045 g, 0.016 mmol) in 2 mL MeOH were reacted as described above for **Gd(1)**. The product was isolated following dialysis and drying under

vacuum as an off-white powder. Yield: 0.013 g, 93%. ESI-MS: Calculated m/z : 826.253 [Eu(1)H⁺]. Found m/z : 826.277. ICP-MS: Calculated Eu content for C₃₃H₄₆EuN₅O₁₀ · HCl · 3H₂O: 16.60%. Found: 16.62%.

Luminescence Studies.

Excitation and emission spectra of **Eu(1)** (DMSO, 1.0 x 10⁻⁴ M) were obtained in phosphorescence mode with a total decay time of 0.01 s, a delay time of 0.10 ms, and a gate time of 5.0 ms. Excitation and emission slit widths were both set at 10 nm. The excitation wavelengths (λ_{exc}) used in the emission studies were either 273 nm or 395 nm. The emission wavelength (λ_{em}) for the excitation studies was 614 nm. Determination of the luminescence lifetime (τ) of **Eu(1)** was performed in both H₂O and D₂O (1.0 x 10⁻⁴ M) with a delay time of 0.05 ms, a gate time of 0.2 ms, $\lambda_{\text{exc}} = 273$ nm, and $\lambda_{\text{em}} = 614$ nm. Excitation and emission slit widths were 10 nm. Calculations of q used the equation $q = 1.11[k_{\text{H}_2\text{O}} - k_{\text{D}_2\text{O}} - 0.31 + 0.075n_{\text{O}=\text{CNH}}]$ where k is the rate of luminescence decay and $n_{\text{O}=\text{CNH}}$ is the number of amide N-H oscillators in which the amide carbonyl oxygen is coordinated to Eu³⁺.¹⁶

Relaxivity Measurement.

Solutions of **Gd(1)** were prepared in H₂O at concentrations of 1 mM, 2 mM, 3 mM, 4 mM and 5 mM. The longitudinal relaxation time (T_1) for each concentration was measured using an inversion recovery pulse sequence (180° - τ - 90° - acquire) on a Bruker AMX-400 MHz spectrometer at 310K. Each inversion recovery experiment was performed in duplicate and yielded 2D spectra which were processed using NUTS software and fit to a three-parameter model. Relaxivity (R_1) was obtained from a linear least squares determination of the slope of $1/T_1$ vs. [Gd].

Results and Discussion

Synthesis and Characterization. The synthesis of **Gd(1)** is shown in Scheme 1. Norcocaine was reacted with 3-bromopropyl triflate in CH_2Cl_2 , with substitution occurring exclusively at the carbon bearing the triflate moiety, affording compound **3** in nearly quantitative yield. Characteristic peaks of approximately equal size indicating bromine were observed in the ESI-MS for the 3H^+ peak (410 and 412 m/z). Intramolecular nucleophilic substitution of bromine with the bridgehead nitrogen of the ecgonine ring system to form a new four-membered ring was also observed in the ESI-MS at 330 m/z, but was not observed in solution under mild conditions. Compound **3** was then reacted with a 3-fold excess of cyclen in CHCl_3 at 45°C to avoid the synthesis of unwanted, more highly substituted cyclen products. Compound **4** was isolated in 82% yield after purification by flash column chromatography ($\text{CHCl}_3/\text{MeOH}$). Addition of a slightly more than 3 equivalents of benzyl 2-bromoacetate to compound **4** in DMF in the presence of Na_2CO_3 afforded **5** as a yellow oil. Purification by flash chromatography ($\text{CH}_2\text{Cl}_2/\text{MeOH}$) yielded **5** as an off-white solid in a 43% yield. Quaternization of the amines on the cyclen backbone was not observed by $^1\text{H-NMR}$ or ESI-MS, with the major peak occurring at 946.5 m/z for 5H^+ . Hydrogenolysis of **5** with 10% Pd/C in MeOH to remove the benzyl esters¹⁷ afforded ligand **1** as a white powder in nearly quantitative yield following filtration of the catalyst and removal of solvent. The $^1\text{H-NMR}$ spectrum exhibited drastic changes in the aromatic region through the disappearance of the resonances due to the protons of the benzyl esters, as shown in Figure 1. Resonances at 5.1-5.2 ppm assigned to the methylene unit of the benzyl ester vanished from the spectrum as well and the partially obscured, characteristic ecgonine resonance at 5.2 ppm shifted downfield to 5.5 ppm upon conversion of **5** to **1** (Figure 1). Additionally, the structural integrity of the cocaine moiety, containing two ester

functionalities, remained entirely intact. The ESI-MS of ligand **1** revealed a major peak at 676.3 m/z for 1H^+ , consistent with the proposed structure. Tricarboxylate cyclen-based lanthanide chelates are routinely synthesized from routes employing t-butyl esters, which are generally removed using acid. The synthetic route shown in Scheme 1 is advantageous for preparing lanthanide chelates that contain acid-sensitive functional groups because the hydrogenolysis step is mild.

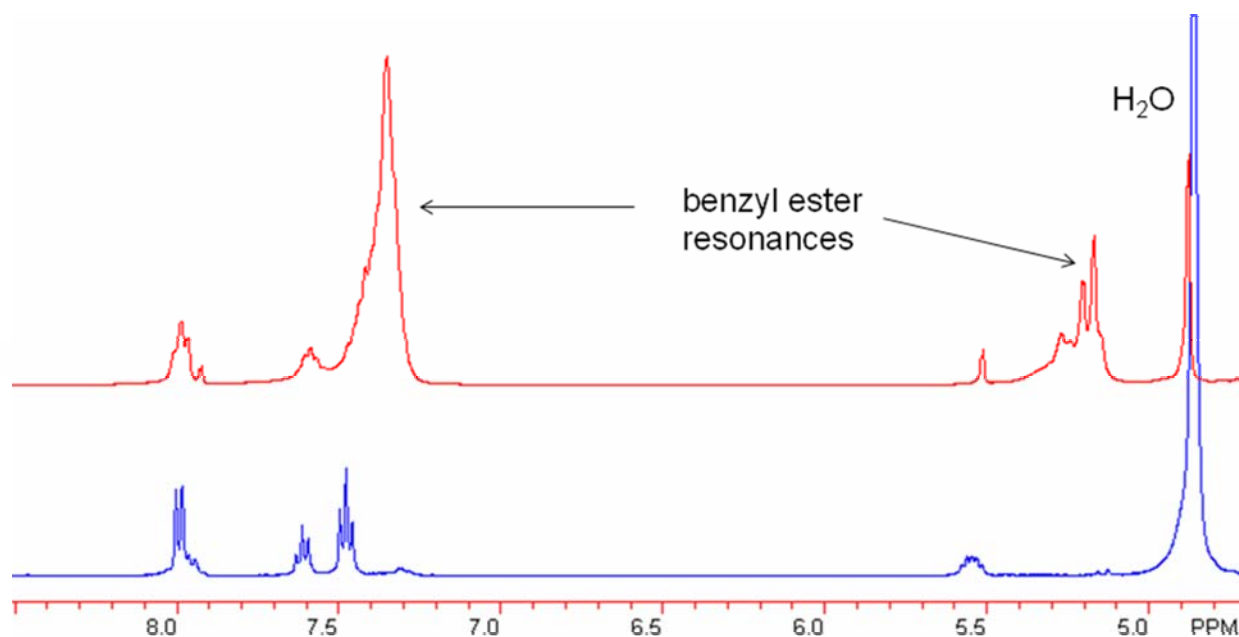


Figure 1. ^1H -NMR spectra of compounds **5** (top) and **1** (bottom) in CD_3OD , illustrating the selectivity of the hydrogenolysis reaction in removing the benzyl esters.

Synthesis of the final complexes **Gd(1)** and **Eu(1)** in high yield was accomplished by addition of the appropriate lanthanide chloride salt to ligand **1** and three equivalents of NaOMe in MeOH at 45°C followed by extensive dialysis in water to remove NaCl. Removal of water gave the HCl salts of **Gd(1)** and **Eu(1)** as white to off-white crystalline powders, characterized by ESI-MS and ICP-MS. Peaks were observed in the ESI-MS consistent with the isotopic

distribution of the respective lanthanide, with the major peak for **Gd(1)**H⁺ at 831.3 m/z and for **Eu(1)**H⁺ at 826.3 m/z. ICP-MS determination of % Ln content was consistent with molecular formulae of **Gd(1)**·HCl·4H₂O and **Eu(1)**·HCl·3H₂O for each product. Both complexes were stable in aqueous solution up to at least 14 days, and no hydrolysis was observed.

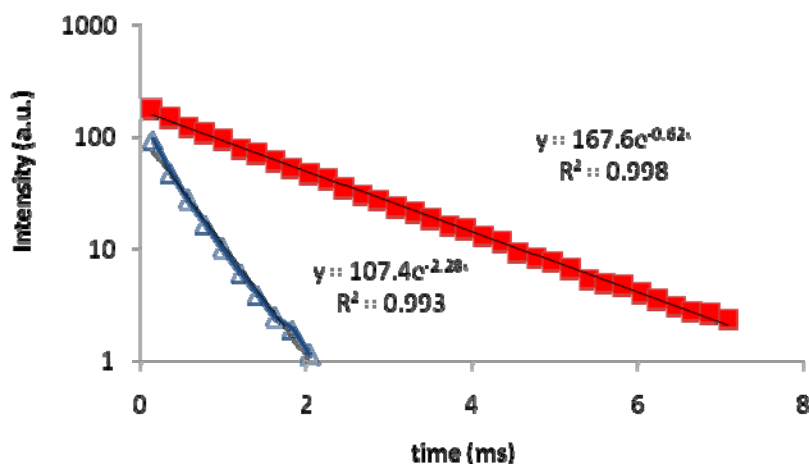


Figure 2. Decay of the luminescence emission ($\lambda_{\text{exc}} = 273 \text{ nm}$; $\lambda_{\text{em}} = 614 \text{ nm}$) of a 1.0×10^{-4} M solution of **Eu(1)** in H₂O (open triangle) and D₂O (closed square).

The possibility of the presence of more than one coordinated water molecule ($q > 1$) in **Gd(1)** and **Eu(1)** was indicated from the ICP-MS analysis. However, the precise amount of coordinated water molecules can be estimated from the luminescence lifetime of **Eu(1)** in H₂O and D₂O solutions of the complex using Horrocks' method.¹⁶ For purposes of approximation, the value of q obtained for **Eu(1)** can be extended to **Gd(1)** because of their very similar coordination chemistries and size. The lifetime data for **Eu(1)** is illustrated in Figure 2, and $q = 2.1 \pm 0.2$. Excitation of the complex was most efficient at 273 nm, indicating an antenna effect from the benzoate functionality of the ligand. Typically, europium and gadolinium complexes of

DOTA-based ligands are nine-coordinate, and the heptadentate nature of ligand **1** is consistent with a q of approximately 2 for **Eu(1)**. It is assumed that **Gd(1)** will have a similar q , resulting in an increased relaxivity for the complex, which is important for medical applications, especially in cases where the concentration of the CA in the area of interest is low.

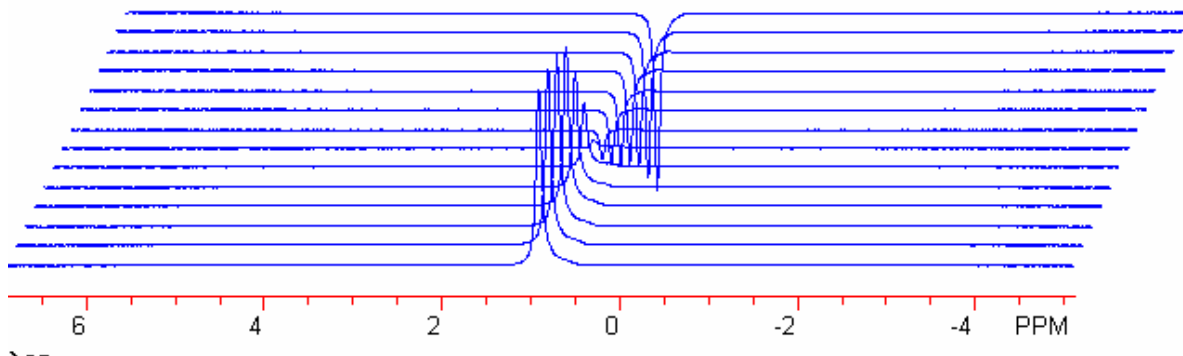


Figure 3. Stacked plot at 14 time points of the H₂O resonance of a solution of **Gd(1)** (4.0×10^{-3} M) during relaxation.

The relaxivity of **Gd(1)** was determined through performing inversion recovery experiments at five different concentrations. A stacked plot of 14 different time points during the experiment is shown in Figure 3. R_1 for **Gd(1)** (400 MHz, 310 K) was found to be $7.1 \text{ mM}^{-1} \text{ s}^{-1}$, obtained from a plot of T_1^{-1} vs. $[\text{Gd(1)}]$ using the slope of the best fit curve for a linear relationship (Figure 4). Under the same experimental conditions, $[\text{Gd(DTPA)}]^{-2}$, one of the most commonly-used CA in the clinic, exhibited a relaxivity of $3.8 \text{ mM}^{-1} \text{ s}^{-1}$.¹⁸ The enhanced relaxivity of **Gd(1)** is consistent with an increase in the number of coordinated water molecules to approximately $q = 2$, allowing **Gd(1)** to more efficiently catalyze the relaxation of nearby waters through coordination to the metal center.

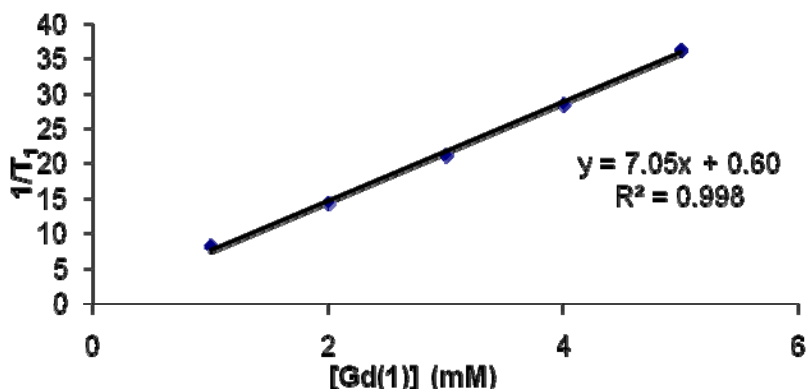


Figure 4. Plot of T_1^{-1} vs. $[\text{Gd}(\mathbf{1})]$ (400 MHz, 310 K) where the relaxivity (R_1) is given by the slope of the best fit curve.

The synthesis of **Gd(1)** is a step towards developing MRI-CAs capable of enhancing MR images of the brain, specifically related to the dopamine transporter. The relatively high molecular relaxivity, small size, and lack of hydrogen-bond donating groups within the structure of **Gd(1)** make it an attractive candidate for further studies. Preliminary binding studies with **Gd(1)** and dopamine transporter proteins have shown a binding affinity similar to cocaine, and thus the specificity of the targeting group has been preserved upon attachment to the CA. The binding affinity can likely be improved through structural modification of the cocaine-based targeting group.⁷⁻¹⁰ Dopamine receptor binding studies in the literature have revealed that replacement of the benzoate ester on the ecgonine ring structure with any of a number of various halogen substituted benzene rings can augment binding affinity by several orders of magnitude, partially dependent on the animal tissue used.¹² Additionally, to increase the sensitivity of the CA, binding of **Gd(1)** to the dopamine transporter protein could result in drastic increases in molecular relaxivity due to a slowed molecular rotation and increase in τ_r , leading to higher

contrast in the region of interest.⁴ Accumulation of receptor-bound CAs on the dopamine transporter protein would largely increase the local contrast and distinguish the site from the background, signaling an active receptor. In conclusion, **Gd(1)** was synthesized and characterized as a potential targeted MRI-CA for the dopamine transporter with a molecular relaxivity of $7.1 \text{ mM}^{-1} \text{ s}^{-1}$ at 400 MHz and 310 K. The synthetic pathway described here is versatile in its approach and tolerates many different functional groups, including acid-sensitive esters, by utilizing the Pd-catalyzed hydrogenolysis deprotection step in the synthesis of ligand **1**. This pathway is currently being explored for the synthesis of a series of targeted complexes based on the cocaine structure for imaging the dopamine receptor. The effect of the Gd^{3+} chelate on the binding affinity of the targeting moiety and the effect of binding to the receptor protein on the relaxivity of the chelate are to be addressed.

REFERENCES.

- (1) (a) Caravan, P.; Ellison, J.J.; McMurry, T.J.; Lauffer, R.B. *Chem. Rev.* **1999**, *99*, 2293-2352. (b) Caravan, P. *Chem. Soc. Rev.* **2006**, *35*, 512-523. (c) Woods, M.; Botta, M.; Avedano, S.; Wang, J.; Sherry, A.D. *Dalton Trans.* **2005**, 3829-3837. (d) Raymond, K.N.; Pierre, V.C. *Bioconjugate Chem.* **2005**, *16*, 3-8.
- (2) (a) Clarkson, R.B. *Top. Curr. Chem.* **2002**, *221*, 201-235. (b) Saeed, M.; Wendland, M.F.; Higgins, C.B. *J. Magn. Reson. Imaging* **2000**, *12*, 890-898. (c) Kroft, L.J.M.; de Roos, A. *J. Magn. Reson. Imaging* **1999**, *10*, 395-403.
- (3) (a) Lewin, M.; Clément, O.; Belguise-Valladier, P.; Tran, L.; Cuénod, C.; Siauve, N.; Frija, G. *Invest. Radiol.* **2001**, *36*, 9-14. (b) Mahfouz, A.E.; Hamm, B.; Taupitz, M. *Eur. Radiol.* **1997**, *7*, 507-513. (c) Yan, G.; Liu, M.; Li, L. *Radiography* **2005**, *11*, 117-122.
- (4) (a) Zigelboim, I.; Offen, D.; Melamed, E.; Panet, H.; Rehavi, M.; Cohen, Y. *J. Incl. Phenom. Macrocycl. Chem.* **2007**, *59*, 323-329. (b) Artemov, D. *J. Cell. Biochem.* **2003**, *90*, 518-524. (c) Gunanathan, C.; Pais, A.; Furman-Haran, E.; Seger, D.; Eyal, E.; Mukhopadhyay, S.; Yehoshoa, B.; Leitus, G.; Cohen, H.; Vilan, A.; Degani, H.; Milstein, D. *Bioconjugate Chem.* **2007**, *18*, 1361-1365. (d) Barrett, T.; Brechbiel, M.; Bernardo, M.; Choyke, P.L. *J. Magn. Reson. Imaging* **2007**, *26*, 235-249. (e) Morawski, A.M.; Winter, P.M.; Crowder, K.C.; Caruthers, S.D.; Fuhrhop, R.W.; Scott, M.J.; Robertson, J.D.; Abendschein, D.R.; Lanza, G.M.; Wickline, S.A. *Magn. Reson. Med.* **2004**, *51*, 280-286. (f) Sosnovik, D.E.; Weissleder, R. *Curr. Opin. Biotechnol.* **2007**, *18*, 4-10. (g) Morawski, A.M.; Lanza, G.A.; Wickline, S.A. *Curr. Opin. Biotechnol.* **2005**, *16*, 89-92.

- (5) Lee, J.; Zylka, M.J.; Anderson, D.J.; Burdette, J.E.; Woodruff, T.K.; Meade, T.J. *J. Am. Chem. Soc.* **2005**, *127*, 13164-13166.
- (6) Mishra, A.; Pfeuffer, J.; Mishra, R.; Engelmann, J.; Mishra, A.K.; Ugurbil, K.; Logothetis, N.K. *Bioconjugate Chem.* **2006**, *17*, 773-780.
- (7) Kumar, K.; Chang, C.A.; Francesconi, L.C.; Dischino, D.D.; Malley, M.F.; Gougoutas, J.Z.; Tweedle, M.F. *Inorg. Chem.* **1994**, *33*, 3567-3575.
- (8) Meltzer, P.C.; Liang, A.Y.; Brownell, A.-L.; Elmaleh, D.R.; Madras, B.K. *J. Med. Chem.* **1993**, *36*, 855-862.
- (9) Meltzer, P.C.; Blundell, P.; Jones, A.G.; Mahmood, A.; Garada, B.; Zimmerman, R.E.; Davison, A.; Holman, B.L.; Madras, B.K. *J. Med. Chem.* **1997**, *40*, 1835-1844.
- (10) Meltzer, P.C.; Blundell, P.; Zona, T.; Yang, L.; Huang, H.; Bonab, A.A.; Livni, E.; Fischman, A.; Madras, B.K. *J. Med. Chem.* **2003**, *46*, 3483-3496.
- (11) Milius, R.A.; Saha, J.K.; Madras, B.K.; Neumeyer, J.L. *J. Med. Chem.* **1991**, *34*, 1728-1731.
- (12) (a) Singh, S. *Chem. Rev.* **2000**, *100*, 925-1024. (b) Drewes, B.; Sihver, W.; Willbold, S.; Olsson, R.A.; Coenen, H.H. *Nucl. Med. Biol.* **2007**, *34*, 531-539.
- (13) Lipinski, C.A.; Lombardo, F.; Dominy, B.W.; Feeney, P.J. *Adv. Drug Delivery Rev.* **1997**, *23*, 3-25.
- (14) Zhou, J.; Zhang, A.; Kläss, T.; Johnson, K.M.; Wang, C.Z.; Ye, Y.P.; Kozikowski, A.P. *J. Med. Chem.* **2003**, *46*, 1997-2007.

- (15) Chi, D.Y.; Kilbourn, M.R.; Katzenellenbogen, J.A.; Welch, M.J. *J. Org. Chem.* **1987**, *52*, 658-664.
- (16) Supkowski, R. M. Horrocks, Jr., W. D. *Inorg. Chim. Acta* **2002**, *340*, 44-48.
- (17) Kim, K.S.; Kim, J.H.; Lee, Y.J.; Lee, Y.J.; Park, J. *J. Am. Chem. Soc.* **2001**, *123*, 8477-8481.
- (18) Labadie, C.; Lee, J.-H.; Véték, G.; Springer, C.S. *J. Magn. Reson., Ser. B* **1994**, *105*, 99-112.

Chapter 6. Conclusions

The design and synthesis of novel macrocyclic lanthanide chelates for sensing and imaging purposes was the focus of this doctoral thesis. Lanthanide ions in the field of anion sensing were, until recently, restricted to signaling roles dependent on direct coordination to the metal.¹⁻² The goal of my research in this area was to design Eu^{3+} chelates that respond to anions not by means of metal ion coordination, but through interactions with a binding pocket that indirectly affect the Eu^{3+} luminescence.³⁻⁴ This approach opens the door to implementing known anion binding functional groups into supramolecular schemes for creating selectivities unachievable through lanthanide ion coordination, particularly small inorganic anions or monocarboxylates. The literature is rich with anion sensing molecules utilizing hydrogen-bond donor groups such as amides,⁵⁻⁶ pyrroles,⁷ and (thio)ureas⁸ to achieve selectivities based on geometry and the nature of the hydrogen bonding groups. The work described in this doctoral thesis, where a *bis*-thiourea system was attached to a Eu^{3+} chelate to form a macrocycle capable of luminescence sensing, with binding constants for acetate and dihydrogen phosphate over an order of magnitude higher than the *bis*-thiourea system alone, is progress toward the development of functional lanthanide probes for anions in competitive DMSO or aqueous solution. The incorporation of lanthanide ions into other organic systems may reveal further advancements. For anion recognition in biological environments, it is critical to develop specificity to take advantage of the time-resolved luminescence capabilities of the lanthanide metal ions.^{2b,c}

For biological studies, lanthanides have long been applied in the form of Gd^{3+} -containing MRI-CAs.⁹ Our interests were in the development of a new MRI-CA targeted to the dopamine

transporter protein for molecular imaging of the brain and dopamine transporter activity.

Currently, only one MRI-CA specifically for brain imaging applications has been described.¹⁰

My approach was to synthesize a neutral Gd^{3+} chelate with a lipophilic linker and cocaine-based targeting group for selective binding to the dopamine transporter as a proof-of-concept. The synthetic route was designed to be general for the synthesis of a library of compounds to identify candidates capable of crossing the blood-brain barrier and binding to the dopamine receptor.

Successful accumulation of CA in the brain is important for advanced neurological studies, where more sensitive MRI is necessary.⁹⁻¹¹

Current Results and Directions

I have synthesized a series of novel macrocycles incorporating a DTPA *bis*-amide chelate, two sensitizing benzene antennae, and two thiourea hydrogen-bond donors for binding and luminescent signaling of anions in DMSO solution.³ These macrocycles can be synthesized in high yields and purity from a common precursor, and a series of similar complexes can be realized in a short amount of time for identifying structure-activity relationships. Successful recognition of acetate and DHP was shown with macrocycles of this series through the formation of 1:1 complexes with relatively high binding constants in DMSO ($\log K = 4-5$), even in the presence of large excesses of chloride ion. These binding constants are among the strongest for thio(urea)-based anion sensors in DMSO,⁸ and are comparable to highly preorganized calix[4]pyrrole sensors.^{7d-f} My research has shown that anion coordination to the Eu^{3+} ion is not responsible for the luminescence changes observed in this series of macrocycles upon titration with fluoride, acetate or DHP.⁴ Importantly, the luminescent signaling is only observed when the chelates are excited at 272 nm, where energy is absorbed primarily through the ligand, as indicated through UV-Vis absorbance studies of the chelates and organic model systems. Direct

excitation of Eu^{3+} at 395 nm leads to no change in luminescence upon titration with solutions of different anions. Our hypothesis is that a change in conformation is primarily responsible for the observed luminescence changes, whereby the movement of the benzene antennae affects the energy transfer efficiency to Eu^{3+} . This particular mechanism and approach to anion sensing has not been reported in the literature with lanthanide ions, and there is great potential for anion sensors of novel selectivities through application of this method. Second-generation macrocyclic chelates were also synthesized with pendant naphthalene and pyrene groups for application in aqueous solutions, expanding the series to include macrocycles capable of acquiring a positive charge.

Future directions in this research include designing systems that include more binding sites for higher affinities and shape selectivity, depending on the anion of interest. Specifically, alteration of the chelate structure to provide a binding site at the lanthanide metal center may result in higher binding affinities while maintaining the selectivity of the binding pocket. These systems may be more practical in designing molecular probes for complex mixtures such as blood or urine. Additionally, incorporation of lanthanide antennae with lower energy absorptions is important for studies of biological systems, due to the absorbance of UV light by tissues.^{1e} The initial series was created as a proof-of-concept for designing advanced macrocycles tailored to specific anions. These macrocycles show promise as selective sensors for amino acid carboxylates or for the study of phosphorylated anions and phosphorylation reactions.

Additionally, the synthesis of a new dopamine transporter-targeted MRI chelate is a step towards developing MRI-CA capable of enhancing MR images of the brain and imaging dopamine transporter activity. The relatively high molecular relaxivity ($7.1 \text{ mM}^{-1}\text{s}^{-1}$), small size,

and lack of hydrogen-bond donating groups within its structure make it an attractive candidate for further studies, where crossing the blood-brain barrier is necessary.¹² Preliminary binding studies with dopamine transporter proteins have shown a small binding affinity, but similar to that of cocaine, which can likely be improved through structural modification of the cocaine-based targeting group.⁵ It is important that the Gd^{3+} chelate does not interfere with the binding of the targeting moiety, and competitive inhibition studies are necessary to determine such effects. Preparation of a series of Gd^{3+} chelates with various targeting moieties and linker lengths is important for determining the feasibility of the overall chelate design, as well as obtaining relaxivity of the complex when bound to the dopamine transporter protein. The use of longer, more lipophilic linkers (hexyl or octyl chains) may improve the chelate's ability to cross the blood-brain barrier and bind to the dopamine receptor, and the linker can also influence the relaxivity of the CA.¹⁰ However, for large enhancements of the binding affinity to the dopamine receptor, modifications to the cocaine structure are necessary.¹¹ Replacement of the benzoate ester on cocaine with substituted aromatics has been shown to enhance binding affinity to the dopamine receptor by several orders of magnitude.¹¹ The synthetic scheme developed in this doctoral research lends itself well to such adjustments, and should contribute to the rapid synthesis of new targeted MRI-CAs for the dopamine receptor. Ultimately, animal studies are necessary for identifying whether this design is capable of penetrating the brain for enhanced images and studies of neurological conditions involving the dopamine transporter.

REFERENCES

- (1) (a) Parker, D. *Coord. Chem. Rev.* **2000**, *205*, 109-130. (b) Parker, D. *Chem. Soc. Rev.* **2004**, *33*, 156-165. (c) Bünzli, J.-C. G.; Piguet, C. *Chem. Soc. Rev.* **2005**, *34*, 1048-1077. (d) Bünzli, J.-C. G.; Piguet, C. *Chem. Rev.* **2002**, *102*, 1897-1928. (e) Pandya, S.; Yu, J.; Parker, D. *Dalton Trans.* **2006**, 2757-2766.
- (2) (a) dos Santos, C.M.G.; Fernández, P.B.; Plush, S.E.; Leonard, J.P.; Gunnlaugsson, T. *Chem. Commun.*, **2007**, 3389-3391. (b) Poole, R.A.; Kielar, F.; Richardson, S.L.; Stenson, P.A.; Parker, D. *Chem. Commun.* **2006**, 4084-4086. (c) Parker, D.; Yu, J. *Chem. Commun.* **2005**, 3141-3143.
- (3) Gulgas, C.G.; Reineke, T.M. *Inorg. Chem.* **2005**, *44*, 9829-9836.
- (4) Gulgas, C.G.; Reineke, T.M. *Inorg. Chem.* **2007**, *in revision*.
- (5) (a) Martínez-Máñez, R.; Sancenón, F. *Chem. Rev.* **2003**, *103*, 4419-4476. (b) Martínez-Máñez, R.; Sancenón, F. *J. Fluoresc.* **2005**, *15*, 267-285.
- (6) (a) Bondy, C.R.; Loeb, S.J. *Coord. Chem. Rev.* **2003**, *240*, 77-99. (b) Choi, K.; Hamilton, A.D. *Coord. Chem. Rev.* **2003**, *240*, 101-110. (c) Choi, K.; Hamilton, A.D. *J. Am. Chem. Soc.* **2001**, *123*, 2456-2457.
- (7) (a) Camiolo, S.; Gale, P. A. *Chem. Commun.* **2000**, 1129-1130. (b) Gale, P.A.; Anzenbacher Jr., P.; Sessler, J.L. *Coord. Chem. Rev.* **2001**, *222*, 57-102. (c) Pohl, R.; Aldakov, D.; Kubát, P.; Jursíková, K.; Marquez, M.; Anzenbacher Jr., P. *Chem. Commun.* **2004**, 1282-1283. (d) Nishiyabu, R.; Anzenbacher Jr., P. *J. Am. Chem. Soc.* **2005**, *127*, 8270-8271. (e) Palacios,

- M.A.; Nishiyabu, R.; Marquez, M.; Anzenbacher Jr. P. *J. Am. Chem. Soc.* **2007**, *129*, 7538-7544. (f) Nishiyabu, R.; Anzenbacher Jr., P. *Org. Lett.* **2006**, *8*, 359-362.
- (8) (a) Gunnlaugsson, T.; Davis, A.P.; Hussey, G.M.; Tierney, J.; Glynn, M. *Org. Biomol. Chem.* **2004**, *2*, 1856-1863. (b) Gunnlaugsson, T.; Glynn, M.; Tocci, G.M.; Kruger, P.E.; Pfeffer, F.M. *Coord. Chem. Rev.* **2006**, *250*, 3094-3117. (c) Cho, E.J.; Moon, J.W.; Ko, S.W.; Lee, J.Y.; Kim, S.K.; Yoon, J.; Nam, K.C. *J. Am. Chem. Soc.* **2003**, *125*, 12376-12377. (d) Jose, D.A.; Kumar, D.K.; Ganguly, B.; Das, A. *Org. Lett.* **2004**, *6*, 3445-3448. (e) Gunnlaugsson, T.; Davis, A.P.; O'Brien, J. E.; Glynn, M. *Org. Biomol. Chem.* **2005**, *3*, 48-56. (f) Sasaki, S.; Mizuno, M.; Naemura, K.; Tobe, Y. *J. Org. Chem.* **2000**, *65*, 275-283. (g) Hisaki, I.; Sasaki, S.; Hirose, K.; Tobe, Y. *Eur. J. Org. Chem.* **2007**, 607-615. (h) Hay, B.P.; Firman, T.K.; Moyer, B.A. *J. Am. Chem. Soc.* **2005**, *127*, 1810-1819.
- (9) (a) Caravan, P.; Ellison, J.J.; McMurry, T.J.; Lauffer, R.B. *Chem. Rev.* **1999**, *99*, 2293-2352. (b) Caravan, P. *Chem. Soc. Rev.* **2006**, *35*, 512-523. (c) Woods, M.; Botta, M.; Avedano, S.; Wang, J.; Sherry, A.D. *Dalton Trans.* **2005**, 3829-3837.
- (10) Zigelboim, I.; Offen, D.; Melamed, E.; Panet, H.; Rehavi, M.; Cohen, Y. *J. Incl. Phenom. Macrocycl. Chem.* **2007**, *59*, 323-329.
- (11) (a) Meltzer, P.C.; Blundell, P.; Jones, A.G.; Mahmood, A.; Garada, B.; Zimmerman, R.E.; Davison, A.; Holman, B.L.; Madras, B.K. *J. Med. Chem.* **1997**, *40*, 1835-1844. (b) Meltzer, P.C.; Blundell, P.; Zona, T.; Yang, L.; Huang, H.; Bonab, A.A.; Livni, E.; Fischman, A.; Madras, B.K. *J. Med. Chem.* **2003**, *46*, 3483-3496.
- (12) Lipinski, C.A.; Lombardo, F.; Dominy, B.W.; Feeney, P.J. *Adv. Drug Delivery Rev.* **1997**, *23*, 3-25.